Department of Precision and Microsystems Engineering

TITLE: Cryo Sample Transfer Solution of Correlated Light and Electron Microscopy

NAME: Xuanmin He

Report no : 2019.020
Coach : mr. ir. Sander den Hoedt
Professor : Assoc. Prof. ir. J.W. (Jo) Spronck
Specialisation : MSD
Type of report : Master thesis
Date : 15/7/2019

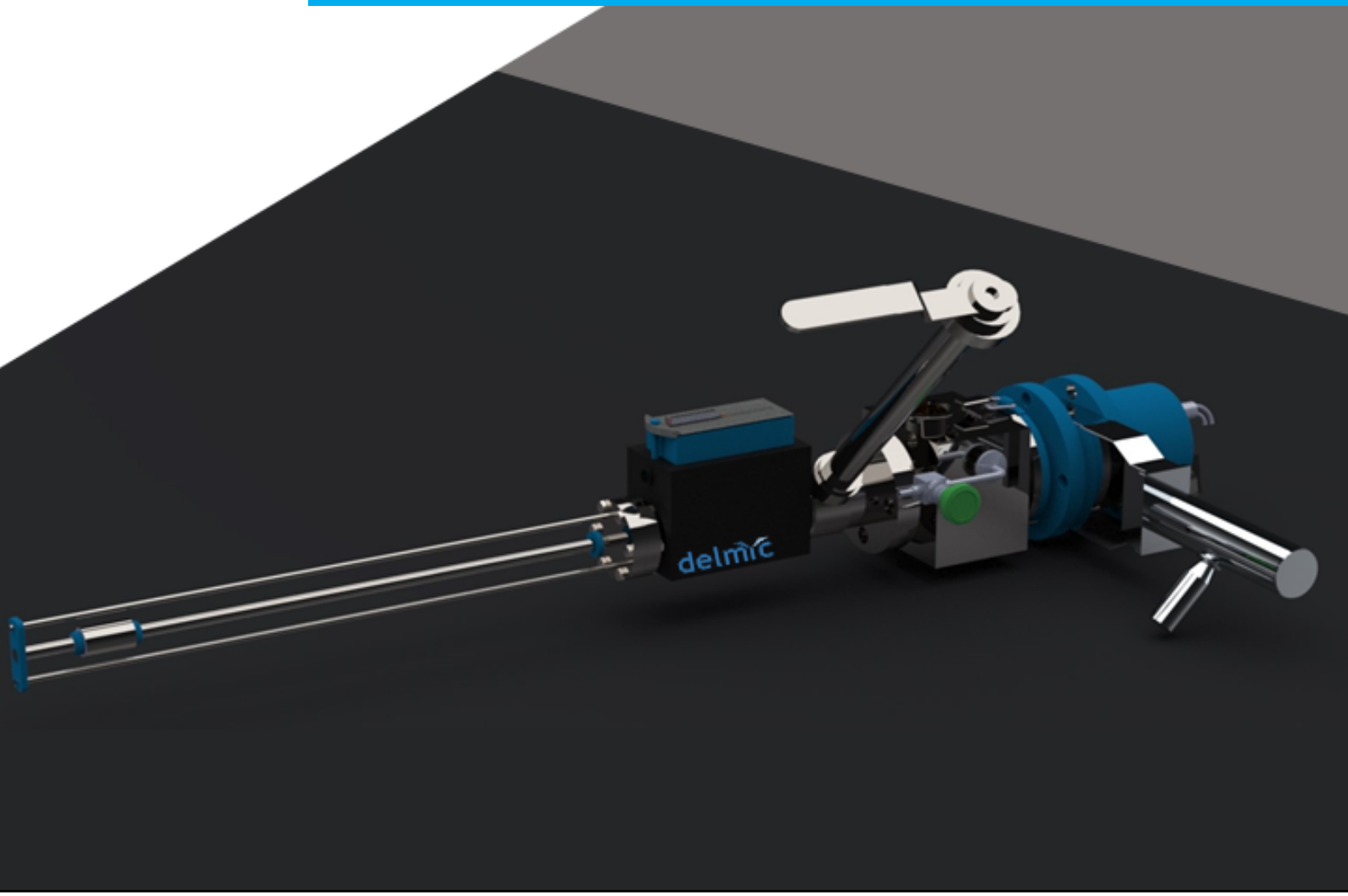

TU Delft Delft University of Technology

Challenge the future

Master Thesis

Cryo Sample Transfer Solution of Correlated Light and Electron Microscopy

by

Xuanmin He

to obtain the degree of Master of Science
at the Delft University of Technology,
to be defended on 29th of July, 2019 at 9:45 AM.

Student number:	4694627	
Project duration:	September 3, 2018 – July 29, 2019	
Thesis committee:	Assoc. Prof. ir. J.W. (Jo) Spronck,	TU Delft, supervisor
	mr. ir. Sander den Hoedt,	Delmic, supervisor
	Dr. S.H. Hossein Nia Kani,	TU Delft, Assistant Professor
	Dr. M.K. Ghatkesar	TU Delft, Assistant Professor

An electronic version of this thesis is available at http://repository.tudelft.nl/.

TU Delft

Acknowledgements

I was offered a unique thesis internship at Delmic B.V. that allowed me to set foot in the world of electron microscopy and be part of an era of discovery and technology for the company and the Delft University of Technology (TU Delft).

During the eleven months of research and development at Delmic, I received daily support and guidance from my company supervisor mr. ir. Sander den Hoedt and my faculty supervisor Assoc. Prof. ir. J.W. (Jo) Spronck. Their mutual interest in developing my engineering skills and improving my career potentials created an effective feedback loop that encouraged me to become a specialist in the field of mechanical engineering.

I doubt I would have achieved as much and progressed as well in my academic or personal life without the support from my supervisors, colleagues, family, and friends. Therefore, I would like to express my gratitude.

To Mr. den Hoedt, for seeing my potential and entrusting me with this project, thank you for guiding me with friendliness and patience. Through our daily discussions over the design iterations, you provided excellent guidance and contributed to the fulfillment of my project.

To my faculty supervisor, Mr. Spronck, thank you for your brilliant ideas, career suggestions, and ensuring this project remained on track throughout the process. I appreciate your helpful advice during our Monday meetings and your hilarious and intuitive approach when discussing problems with me!

To my table-mates and colleagues from Delmic, Bas Bikker and Shubhonil Chatterjee, thank you for you time and encouragement. Working with you was a great pleasure. I thoroughly enjoyed the STUP meeting every morning discussing our project updates, problems. Having two bright minds to use as soundboards for issues and questions was invaluable. Our daily discussion that ran from work and thesis to daily life provided me emotional support and frequently cheered me up.

To Mr. Thomas van der Heijden , Mr. Daan Boltje, Mr. Wouter Roelofsen and all my colleagues in Delmic, thank you for creating such a lovely, supporting environment for my first experience at a company and in a team. Getting to know each of you has granted me the possibility to expand my circle of friends and get to know a lot more about the world during the lunch talks and hackathons.

To my parents and my friends Lukas Steiner, Ekaterina Sokolovskaya and Erika Srebnicki, words fall short in expressing my gratitude to you for all the love, care, and mental support you have offered me.

Thank you all for what you have done for me, I wish all of you success and joy in your life!

Executive summary

Xuanmin He
Delft, July 2019

This paper presents a design project on a sample transfer system for a cryo correlated light and electron microscopy (cryo-CLEM) workflow, which is a graduation project commissioned and supervised by Delmic B.V. and Delft University of Technology's 3mE faculty. Current transfer processes of cryo-CLEM are disadvantaged due to their reliance on heavy manual operation and lack of dedicated and integrated transfer devices found in the market. To improve the low yield of the current sample transfer workflow, a user-oriented, pragmatic strategy was used to generate a solution space and create the final concept of a new transfer system. The new workflow is designed and proposed to improve the yield, imaging quality, and user experience of cryo-CLEM.

The goal of this project is to design a sample transfer system which protects the delicate cryo samples used in the CLEM workflow. The cryo samples frequently receive damage caused by heating and contamination during the process of being transferred from the sample preparation device (Vitrobot), to the imaging chambers of the Focused Ion Beam Scanning Scanning Electron Microscopes (FIB/SEM), and Transmission Electron Microscopes (TEM).

Cryo-immobilized samples (at a temperature lower than −165°C), exhibit a large temperature gradient with its surroundings (27°C), when being transferred in the current workflow. This results in the attraction of water molecules and other particles from their surroundings. Drastic heating, which can be as fast as 2.912°C/s then causes a transition to form ice on the samples. The contaminants, such as cubic ice accumulated on sample surfaces, have a very negative influence on the imaging results of FIB/SEM and TEM: almost 90% of the samples transferred in this workflow end up being wasted.

An integrated sample transfer system which fits the interfaces of CLEM devices and protects the samples from heating and contamination in transfer has been designed to conquer the problems, ensure better imaging results, and increase the process yield. The literature research which covers relevant research contributions in areas such as electron microscopy, cryogenics, sample transfer systems, and vacuum technologies is carried out to theoretically support the design. Based on the analysis of the literature, a set of research questions is proposed for designing as well as choosing each component. The main research question asks what the cheapest, easiest, most damage-free workflow for cryo sample transfer systems is.

Answering these questions ultimately pushes forward the overall design of the system: a plunging bath designed for sample preparation, a shield to shield the samples from heating and contamination, a vacuum box for vacuum generation and connection, a Delmicup to transfer and shield the samples, and a cooling rod to actively cool the samples. A feedthrough pushing rod is selected to replace most of the human handling, a cryogen circulation & draining circuit for cryo cooling and a pumping system are integrated to reach cryo high-vacuum condition. The thermal simulations have proved the effectiveness of the passive and active cooling of the new workflow and the improvements over the old workflow. The mechanical simulations have shown the system's structural strength. The vacuum calculation suggests the pumping efficiency and time of the system. The new transfer system provides a faster, easier, more contamination-free, more temperature-stable, more user-friendly workflow that can increase the yield of sample transfer from 10% to 90%.

There is also room for improvements due to the limit in time and equipment of this project, since the workflow could be more automated in the following aspects: the clipping mechanism, most of the manual steps and system control. Experiments of sample contamination buildup and its influence on imaging results should also be carried out in both old and new workflow in the future to compare the difference and quantify the improvements.

keywords: plunge freezing, thermal modelling, sample transfer, design, contamination, devitrification, FIB/SEM, TEM

Contents

1

Introduction

The Nobel Prize in Chemistry went to Professor Jacques Dubochet, Professor Joachim Frank, and Professor Richard Henderson in the year 2017 for their great contribution to the development of cryo-electron microscopy, pushing science to a new era of observing the tiny world. Since the invention of the electron microscope, the resolution of ultra-small structures has been improved from 200nm to 0.1nm, a brand new dimension of physics revealed itself and is attributed to the success of the discovery of new cells and viruses, the diagnosis of unknown diseases, the mapping of human genomes and the manufacturing of semiconductors. Started from 60 years ago, cryo-EM established and developed its own right in the field of life science and pharmaceuticals. However, back in the days when bio-samples were physically or chemically immobilized, scientists were not able to see the life-like state of cells for they are structurally damaged[29] due to dehydration. With cryo-fixation techniques, bio-samples are seen distortion-free, in better resolution, and with shorter preparation time. Even the visualization of delicate or unstable structures can be realized.

Despite all the advantages, many challenges of cryo sample imaging remain unsolved or need to be improved. One of them lies in the transfer process of the sample: samples are plunge frozen with a high speed to guarantee that the water within living cells is vitrified at a cooling rate of at least 10^{6}°C/s to form vitreous ice, which is also called amorphous ice. Vitreous ice is transparent to electron beams and has almost same density as water at room temperature. Therefore the cells are not expanded or distorted[14] by the density change, and high resolution images of hydrated cells can be obtained. The temperature of the samples are frozen to around -196.15°C and need to be kept well below -165°C and stable, otherwise the vitreous ice within the solution will transform into cubic ice or hexagonal ice and hence influences imaging results[15]. When the researcher transfers cryo samples to storage or inserts them to the imaging chamber with tools, the thermal exposure or the particles from the surroundings will cause heating and contamination to the samples. For example, water vapour can crystallize and accumulate on the sample surface. These cryo deposits then absorb or scatter the electron beams unwantedly[35]. In the Correlative light-electron microscopy (CLEM) workflow, the same sample is imaged first in a focused ion beam scanning electron microscope (FIB/SEM) or/and a fluorescence microscope, then transferred to and imaged in a transmission electron microscope (TEM). During the tedious and slow transfer workflow, sample damage caused by contamination and heating will result in a sample damage rate of 90% .

To prevent or mitigate this problem, several attempts have been made by some researchers and institutions. Many products aiming at keeping the samples in a contamination-free environment have been developed for Electron microscopes. But an integrated cryo sample transfer system which is compatible to the current cryo-CLEM system has not been developed yet. Therefore, this project aims at creating a better, cleaner, faster sample transfer workflow for cryo-CLEM. The project will be based on disentangling the problems surrounding the creation of a sample transfer system, and translating them into the design guidance.

This chapter covers the introduction of the current workflow, the relevant background

information, the benchmarking of the current industrial solutions to similar problems in this field, and the methodology used in generating the solution in this project. This will help define the problems in the current workflow and propose a better workflow.

1.1. EM technology

Electron microscopes are designed to conquer the limitation in imaging resolution of only 200nm due to the limit of diffraction of light in optic microscopes. A beam of accelerated electrons is used to illuminate the sample and obtain images of very high resolution. After the invention of electromagnetic lenses by Hans Busch in 1926, two engineers at Berlin Technische Hochschule, Max Knoll and Ernst Ruska, invented the electron microscope in 1931[55]. In 1933, Ruska built the first EM that has a resolution exceeding the best light microscope. By the 1940s, the resolution of EM, has reached 2nm[51].

1.2. Cryo-CLEM

Correlative light-electron microscopy (CLEM) is the combination of using fluorescence microscopy and electron microscopy to image bio-samples. The optical microscope (a fluorescence microscope for most of the cases) is used to find the region of interest, and the electron microscope obtains high resolution images of this region. In the CLEM system that we are working on, samples are imaged by a focused ion beam SEM (FIB/SEM) and a TEM. Above this, the FIB/SEM utilizes the interaction of electrons with molecules on the surface of the sample lamella created by the focused ion beam to recreate the image, while the TEM has the electrons transmit through 50–100nm thick cross-sections of samples and can reach a resolution of a few Angstroms[7]

In CLEM imaging, the bio-materials should be visualized in near-life condition for better research results. However, bio-materials are very sensitive to direct radiation exposure by electrons (Chung, 2017[11]). Their low weight elemental composition also results in poor electron scattering capability. Additionally, they can get dehydrated easily when exposed to the high vacuum condition within the imaging chamber[11].

These problems lead to the development of sample fixation techniques, to kill or immobilize bio-samples before imaging them, which is also called immobilization. Fixation techniques are divided into chemical fixations and physical fixations. In chemical fixation techniques, bio-samples are immersed in chemical fixatives which can kill and stabilize the cell contents. While physical fixation means microwaving or cryopreserving samples to inactivate cellular activities[30].

Traditional fixation techniques like chemical fixations and most physical fixations can cause structural collapse or distortion to the bio-molecules[11], this results in the quality of imaging not be guaranteed.

However, the cryo fixation techniques minimize the cell damage that can be introduced by traditional fixation techniques. Bio-samples are fixed by being frozen rapidly with cryogen. The water within bio-materials is turned into amorphous ice by this rapid temperature drop. Amorphous ice is a non-crystallized form of water that shares similar density with it so that the structure supported by water in hydrated cells does not expand or distort. The life-like structure of the sample is thereby preserved to obtain better images.

1.2.1. FIB/SEM

Scanning electron microscopy uses low-mass electrons to interact with the sample, it collects the secondary electrons (See Figure 1.1) to generate images of the sample surface and composition of sub-nanometer resolution.

While a focused ion beam shares almost same operational principle with SEM, it uses a beam of ions rather than electrons which have a comparably high-mass property to interact with samples. The beam 'cuts' or modifies the sample directly[60] to form thin layer of sample slices called 'lamella', the precision can be sub-millimeters or even nanometers.

Both SEM and FIB can be used to form images while SEM causes less damage to samples compared to FIB. In low beam current, FIB reaches a resolution of 5nm[50] and will remove material from the sample when larger currents are applied. SEM, on the other hand,

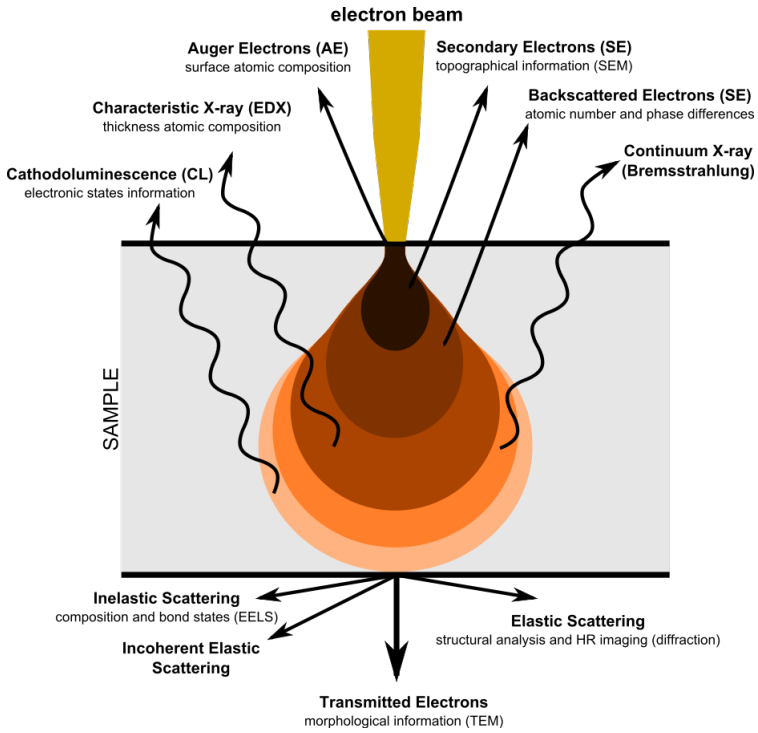

Figure 1.1: Types of electrons[1]

reaches sub nanometer with minor damages to samples. Combined with the FIB in the same chamber, FIB/SEM would be much more powerful because it takes advantage of the benefit of both. Also, as SEM requires a conducting surface in the sample, FIB can be of great help when imaging highly insulating samples by imaging with positive secondary ions.

1.2.2. TEM

Transmission electron microscopy forms images by collecting the transmitted electrons (See Figure 1.1, the transmitted electrons go through the sample) through the ultra-thin layer of samples (around 100nm on average). The imaging result is largely dependent on the electron transparency and thickness of the sample. TEM offers good inspection of inner structure of samples such as crystal structure, stress state information, and morphology[46]. Its resolution can reach a few Angstroms.

1.2.3. Cryo sample

A cryo sample is the combination of a sample carrier and the targeted bio-molecules immobilized by cryo fixation techniques carried by the carrier. The bio-molecules include single particles, cell cultures, and multicellular organisms or tissues[37].

Current cryo fixation techniques include vitrification, cryo protectants fixation, high-pressure freezing and sublimation. The cryo protectants retard the onset of crystallization of water, the high pressure hinders the ice expansion to suppress crystallization, and the sublimation removes the ice crystals on the sample surface to obtain high quality samples[4]. Each of these techniques has its advantages and disadvantages. Due to its ease of operation, good sample quality, and low toxicity or artifacts to cells, vitrification is utilized by the CLEM workflow in this project.

AutoGrids are used as the sample carrier to carry bio materials which will later be plunge frozen in the vitrification process. An AutoGrid is a gold or copper grid wrapped or strengthened by copper AutoGrid rings and can spread the sample solution into an ultra-thin layer on the tiny holes of the grid surface to accommodate with cryo fixation, and FIB/SEM, TEM

[1]Image courtesy: Chauhan, Ankur, 2018, Johns Hopkins University in the paper 'Deformation and damage mechanisms of ODS steels under high-temperature cyclic loading'

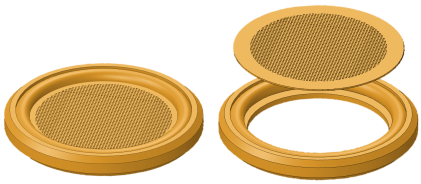

(a) AutoGrid model

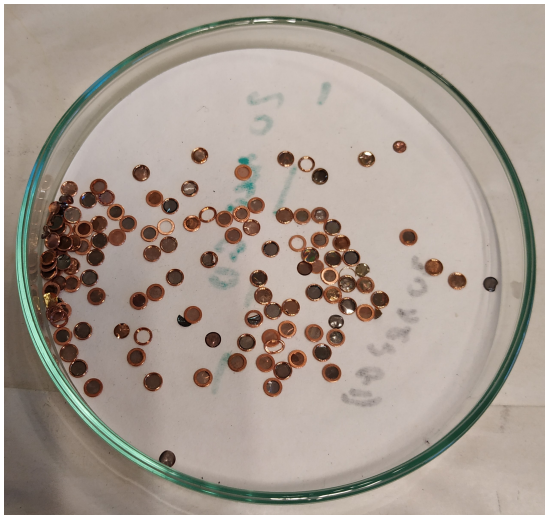

(b) AutoGrids in NeCEN lab[2]

Figure 1.2: AutoGrids

imaging of CLEM workflow. CLEM imaging will generate the overall information on the inner structure, stress state information, morphology, surface condition and composition of the sample carried by AutoGrids.

According to 'Cryo-focused Ion Beam Sample Preparation for Imaging Vitreous Cells by Cryo-electron Tomography' by Miroslava Schaffer et al., to prepare cryo samples, the first step is to pipette around 2.5μL liquid sample solution to the grid, get rid of the extra solution by blotting, then plunge freeze the grid, clip it into the AutoGrid, then transfer and store or image the AutoGrid[57].

AutoGrid and grid

The AutoGrid consists of three parts (see figure 1.2(a)): the grid, the C ring and the AutoGrid ring. The grid designed for cryo microscopy is a thin circular plate of 3mm in diameter and 0.025mm in thickness with holey pattern in the center, the pattern and size vary according to different samples that vary in shape, size and behaviors. In this study, we focus specifically on AutoGrids of the above-mentioned size. The grid is usually made of copper, nickel, or gold to ensure good thermal conductivity and mechanical behavior against drastic temperature change in cryo freezing and human handling. The grid carries the sample solution and the regular holey pattern aims for expanding the solution over the holes to be ultra-thin layers. Microscopically, the thin layer in a single hole will have the shape of a concave lens. The holey pattern will make it easier to distinguish the objects and their locations[19].

The structure of the AutoGrid is designed to strengthen the mechanical and thermal behavior of the delicate grid by wrapping it with an outer copper ring like a wall and clipping it with a C ring to fix it to the outer ring tightly.

Amorphous ice

Back in 1935, E. F. Burton and W. F. Oliver wrote in their article 'The crystal structure of ice at low temperatures[9],' that water condensed and frozen rapidly on the surface of an apparatus under -110.15°C is vitreous, which is also called amorphous ice. Amorphous ice is the non-equilibrium state of water at extremely low temperatures, it forms a glass rather than crystallizing into other forms such as cubic ice[2][3]. Actually, four main forms of water in the cryogenic condition prevail in existence: cubic ice, Ic; low density amorphous, LDA; high density amorphous, HDA; and a naturally occurring form of ice, hexagonal ice, which includes 12 crystalline and 3 amorphous, Ih [42]. Most importantly, amorphous ice shares the greatest structural, molecular arrangement and thermodynamic state similarities with

[2]Image courtesy: FEI AutoGrids images taken under the permission of NeCEN lab of Leiden University

liquid water[3]. When cooled to go through the transition of glassy water, the nucleation of crystal water is avoided by the fast heat transfer. The amorphous ice formed in this way is transparent to electrons while the other forms of non-glassy water undergo heterogeneous nucleation, which may cause local heating of the sample and induce catalytic-like formation of crystals sized at 100nm to 1μm[15]. These segregation compartments impedes accurate SEM imaging of the macromolecular hydrogel structure[3]. The similar densities of the amorphous ice and water at room temperature (0.997g/cm^3), also guarantees the preservation of the hydrated state by preventing the distortion or deformation of cells in cryo temperatures. See the table by Thomas Loerting and Nicolas Giovambattista, the density of the four forms of water in different temperatures are:

Table 1.1: The densities of water in different forms:[3]

Form	Density (g/cm^3)	Temperature range (°C)
Ih	0.92	>-113.15
Ic	0.93	-137.15 -113.15
LDA	0.94	-258.15 -137.15
HAD	1.17	< -258.15

Many conditions such as temperature and pressure change can lead to transitions between different amorphous states[45] or change the amorphous state completely, which are irreversible. In 2014, David T. Limmer and David Chandler created the phase diagram of amorphous ice and found the devitrification temperature of ice to be -137°C and to form a vitrified sample, while the cooling rate should be faster than 10^6°C/s [40]. In practice, to obtain stable imaging qualities, the temperature should be further lowered to -165°C for cryo samples. The temperature of the frozen samples should be kept strictly below it. The fluctuation of temperature should be avoided to prevent the potential transition in certain conditions.

Vitrification and vitrobot

The physical fixation technique that creates cryo samples with amorphous ice within and around the bio-molecules with high cooling rate is called vitrification. The process of plunging the grid with bio molecules into the cryogen at a fast speed to form amorphous ice in the hydrated sample is called plunge-freeze. The cooling process is often carried out with a robotic plunging machine with fast up-and-down motion with an ethane bath. The plunging arm is attached with a tweezer to hold the grid tightly. To make sure the ice layer is as thin as possible to provide better contrast in imaging, blotting the sample with filter paper to remove extra water (around 80% of the liquid) is also important.

Some new prototypes in the market are using a tiny droplet of sample solution to 'write' a thin layer of sample line on the grid, so that the blotting can be skipped.

The robotic plunging machine is called vitrobot (also called 'plunge freezer', 'cryo plunger', see figure 1.4). It can adjust the humidity, temperature, plunge speed, blotting force/time to plunge freeze samples with different 'recipes'. FEI vitrobot and Gatan cryo plunger are currently the most widely used vitrobots, that all have a tall shape for the up-down accelerating motion. There are also new prototypes in the market that abandon the traditional shape by narrowing down the exit of the AutoGrid to replace the blotting process, combining an incubator with the sample storage chamber, and using a jet of liquid ethane to fast freeze the AutoGrids[1].

The cryogen used for vitrification needs a large heat capacity, good thermal contact, and a rapid cooling rate[4]. The literature values for cooling rate and heat capacity of the three most generally used cryogens: nitrogen, ethane and propane are studies by Serp, Silvester, Shimoni and Müller [52][62][61] which show that LN2 (liquid nitrogen), is not an ideal cryogen for fast freezing. Ethane, propane, on the other hand, can be handy in forming amorphous ice in samples due to large thermal capacities. The ethane bath for plunge freezing is designed

[3]Table courtesy: by Thomas Loerting and Nicolas Giovambattista in their paper 'Amorphous ices: experiments and numerical simulations' in the Journal of Physics: Condensed Matter in 2006 Department of Chemical Engineering, Princeton University, stacks.iop.org/JPhysCM/18/R919

Figure 1.3: FEI Vitrobot Mark IV, image by Stony Brook University[4]

in such a way that the small cylindrical ethane chamber in the middle of the container is surrounded by an outside cylinder filled with LN2, this ensures that the ethane gas can be cooled and liquefied by the surrounding LN2 when being purged into the small chamber[59]. The workflow of vitrification with a vitrobot is as follows: start the vitrobot, grip a new grid with the tweezer and fasten the grip by pushing the clamping ring. Attach the tweezer to the vitrobot which is later raised up, and wait for sample pippetting. Pipette 3.5μl of sample solution to the grid, set the blotting time, force and humidity of the vitrobot. Now the grid is ready to be plunged into the ethane bath.

1.2.4. Cassette and other accessories

The TEM in the transfer workflow is the new Thermo Scientific™ Krios™ G3i Cryo Transmission Electron Microscope by Thermo Fisher Scientific. 12 AutoGrids are transferred by a stainless-steel cartridge called cassette (see figure 1.5). An Autoloader is designed for picking up the cassette and taking out AutoGrids automatically to the imaging chamber with high throughput and good sample protection.

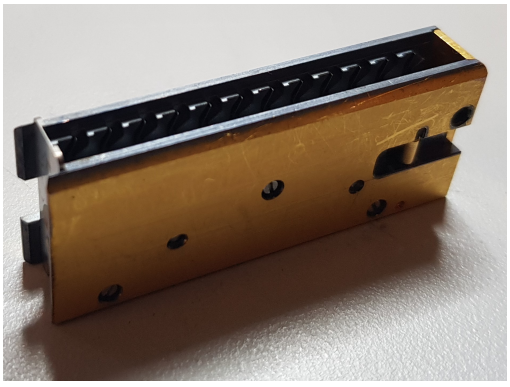

Figure 1.4: Cassette by ThermoFisher Scientific, image by Dr. Sebastian Tacke[5]

[4] Image courtesy: FEI Vitrobot Mark IV photo by Stony Brook University in 2019", https://www.stonybrook.edu/commcms/cryo/equipment/

[5] Image courtesy: cassette image taken under the permission of NeCEN lab of Leiden University

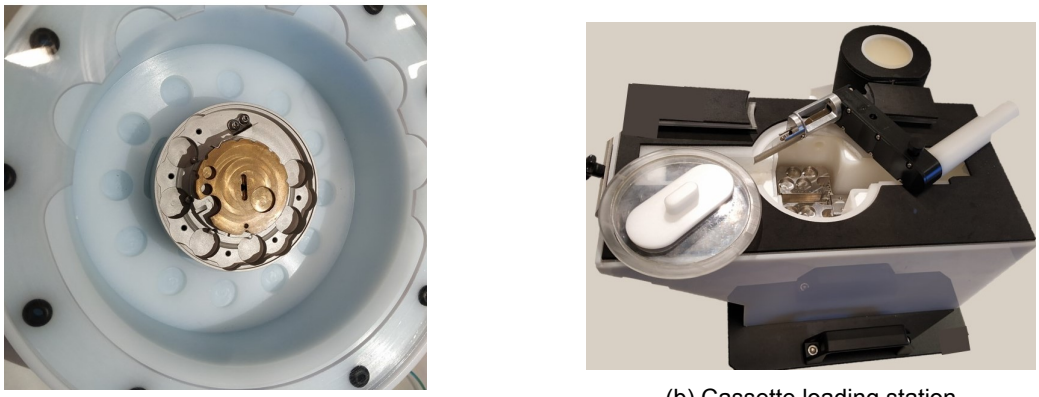

(a) Loading box clipping station

(b) Cassette loading station

Figure 1.5: Loading boxes in NeCEN lab[6]

The cassette is a 9.58×18.40×47.64mm^3 block and has an opening on one side that allows the loading and unloading of the AutoGrids. Its large thermal mass acts like a heat sink that shields the samples from being heated. The current way of cooling down the cassette is by immersing the cassette into a special designed loading box filled with LN2. Samples are loaded into the cassette in the loading box , then the cassette is transferred into a LN2 transfer cup called Nanocup. Before TEM imaging, the Nanocup is transferred and attached to the interface of the Autoloader where the cassette is later picked up and loaded to the TEM.

1.2.5. Current Workflow

The CLEM sample imaging follows strict rules and procedures to reduce the contamination build-up and reach better imaging results.

The current workflow is listed as follows (see figure 1.6). First prepare the ethane bath: pour LN2 in the outer chamber, put in the tweezer, grid box and other cryo operating tools into the LN2 to cool them down. When the LN2 stops boiling, vent the inner chamber with an ethane gas hose, the ethane will liquefy in to liquid within the chamber. Pick up one grid using the tweezer and attach the tweezer to the plunge freezer. Pipette 2.5μl sample solution to the grid (see figure 1.6(1)). Adjust the humidity, blotting time and force, the plunge freezer then blot, and plunge freeze the grid into the liquid ethane bath (see figure 1.6(2)). Relieve the grid by pushing the clamping ring of the tweezer.

What follows is the first transfer: A plastic tube (cryotube) filled with liquid nitrogen is used to transfer the plunge-frozen grids to a another loading box (see figure 1.6 (3)) filled with liquid nitrogen. Use the clipping tool to clip the grid with the C-ring to the AutoGrid ring within the clipping station (see figure 1.5(a)) in the loading box (the clipping tool is a long pen-shaped hollow cylinder that can be fed with C rings, one end of it is the push button and the C ring can be loaded in and pushed out from the other end of the cylinder where the opening is narrowed down to fit the C ring to the AutoGrid ring. The AutoGrid ring and the grid is aligned and sat within the loading station, which is a small cylinder stage with a cylindrical slot to align the grid, the AutoGrid ring and the clipping tool).

Then load two clipped AutoGrids to a shuttle (a stainless steel block of 1.6x2x0.8cm^3, it has two tilted slots where two AutoGrids can be loaded in and a thread at the bottom for attaching with the feedthrough rod (see figure 1.6 (4)) sitting in the middle of the loading box. Attach the transfer unit (which is actually a cylindrical chamber that has a small sealable vacuum tube in the middle to create a local vacuum environment for the shuttle. It also has a long vacuum feedthrough rod that can pick up the shuttle and later insert it to the imaging chamber when the transfer unit is attached to the FIB/SEM chamber (see figure 1.6 (5)) to the top of the loading box. The rod picks up the shuttle in the loading box and rises it up to the small tube. The loading box then drains the liquid ethane and pump the space to rough

[6]Image courtesy: loading box image taken under the permission of NeCEN lab of Leiden University

Figure 1.6: Current workflow

vacuum using a slushy pump. Close the rotary vacuum seal of the vacuum tube and detach the transfer unit from the loading box.

Now the transfer unit can be moved freely to the targeted chamber, which in this case, is a FIB/SEM chamber (see figure 1.6 (6)). An airlock enables the vacuum transfer of the shuttle to the imaging chamber and the rod will send the shuttle to the cryo stage of the imaging chamber. The sample is then cut into lamellas and imaged (see figure 1.6 (7)).

After imaging, reattach the feedthrough rod with the shuttle, retreat the rod, close the vacuum tube, detach the transfer unit. Then bring the transfer unit back to the loading box (see figure 1.6 (8)). Put the AutoGrids back to the LN2. If 12 samples are required to be imaged in CLEM, the same procedure will be repeated six times. The next step is to bring the twelve samples to the loading box of cassette with a cryotube.

The loading box for cassette (see figure 1.5 (b) and figure 1.6 (9)), has a slot for the cassette and multiple slots of grid boxes of AutoGrids and is used for loading AutoGrids to the cassette within LN2 and loading the cassette to the Nanocup (see figure 1.6 (10)). When the cassette is fully loaded with AutoGrids, take out the cassette and put it into the Nanocup filled with liquid nitrogen. Attach the Nanocup to the Autoloader (see figure 1.6 (11)). The Autoloader will then automatically manipulate the cassette; a finger will then take the AutoGrid to the imaging stage for imaging and load the AutoGrids back to the cassette after this process.

1.3. Overview of Cryo Sample Transfer System

Sample transfer devices that can create cryo temperature and vacuum condition for microscopy have a rather short history. But cryo sample storage or pick & place devices are not rare in the manufactural, biological, or pharmaceutical industries.

For example, a device (see figure 1.7), that can store 96 protein crystal samples and mount them to a synchrotron beamline under cryo temperature gives an brief idea of an overall transfer solution to a similar condition. This device was developed by the Stanford Synchrotron Radiation Laboratory in 2002, but devices like this are still far away from the versatile system

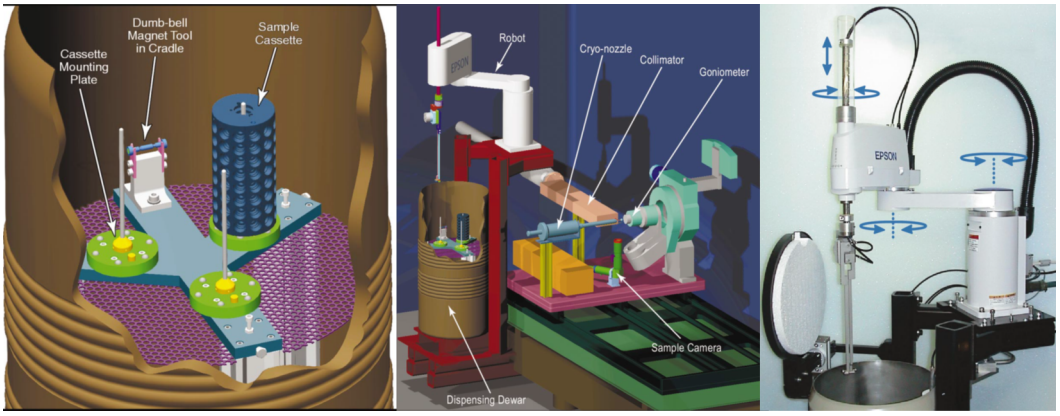

Figure 1.7: An automated system to mount cryo-cooled protein crystals on a synchrotron beamline[7]

which can tackle the problems faced in the delicate microscopic system.

The trials of cryo sample protection devices starts from providing protection during imaging process in light microscopes.

In 2009, the Leiden University Medical center developed a station to tackle the contamination and cooling problems during imaging for a Leitz fluorescence microscope (see figure 1.8).

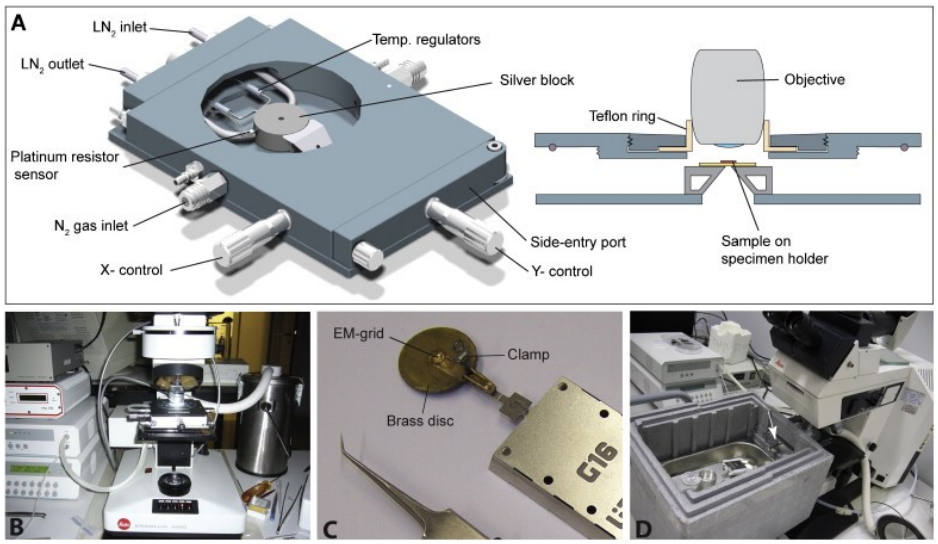

Figure 1.8: Sample protection device for fluorescence microscope by Leiden University[8]

Within this station, a silver block is used as the heat sink which is cooled by automated liquid nitrogen and dry nitrogen gas circulation. The grid is clamped to a brass disc which acts like a cold trap and shield. The operation is not carried out in vacuum condition and the station is directly inserted under the objective lens. A Teflon ring lid seals the gap between the station and the lens to create a local air blockage. Sample preparation is done under liquid nitrogen in a Styrofoam box to prevent frost built up. The station can also manipulate the sample in x,y, and tilt motion. A 60% drop of humidity is reported using this setup, but the insertion process of this station can introduce contamination. Also, a Teflon ring is not ideal for creating clean environments[68].

In 2010, the California Institute of Technology published a sample anti-contamination device for cryo-imaging in the book 'Correlated light and electron cryo-microscopy[8]'. This

[7]Image courtesy: an automated system to mount cryo-cooled protein crystals on a synchrotron beamline by Stanford Synchrotron Radiation Laboratory in 2002

[8]Image courtesy: Leiden University Medical Center, 2019

device is also designed for imaging cryo samples in a light microscope. A liquid nitrogen storage tank is integrated to surround the sample holder and release nitrogen gas to create negative cooling. The sample stage is surrounded by a box with a lid made of thermalplastic material to maintain local air isolation. The glass covers, though, does not provide sufficient air blockage as gas leakage between gaps can be inferred.

Similar devices assembled by the European Molecular Biology Laboratory in 2014 are also attached directly to the objective lens of a cryo-FM except for the liquid nitrogen and dry nitrogen cooling box. A dry ice cooling chamber is attached to the stage-lens interface to prevent potential vibrations due to boiling of liquid nitrogen[58]. The N2 gas circulation within the chamber improved the surrounding of the sample hence contamination can be largely reduced. A silver block is used as the imaging stage. Aircraft grease is used instead of lubricants, for lubrication, to prevent contamination. However it has the same problem as the previous products–contamination in non-vacuum condition can build up greatly.

Later vacuum pumps started to be integrated to such devices. Two pumps are attached to the objective lens in the HOPE stage in 2017 in China: a turbomolecular pump and a pre-pump can pump the chamber down to 10^{-6}mbar[39].

GATAN UK developed the ALTO sample transfer series for SEM and combined ion beam systems[43]. Liquid nitrogen and nitrogen gas circulation bath are used for cooling, a heater is used for quick ice sublimation. A turbo molecular pump is integrated for creating vacuum. This device can also do sample cutting or sputtering owing to the two windows design. The grid can be fed through the transfer chamber to the imaging chamber connected by the bellow valve. This is indeed a mature cryo-sample transferring system with most of the functions integrated.

The Quorum PP3010T Cryo-SEM Preparation system is by far the most functionalized sample transfer device. Developed in 2015, PP3010T is able to actively cool, fracture, coat, store cryo samples in high vacuum condition (turbo molecular pump). It can also detect film thickness, sublimate ice layer, record the operation process automatically with the control of a touch pad[18].

Figure 1.9: PP3010T Cryo-SEM Preparation System by Quorum, UK [9]

In 2016, Universität Münster in Germany designed a solution for reducing contamination for cryo-microscopy. Within the bakeable beryllium bronze transport box, a temperature controlled cryo-stage can store eight samples a time and is protected by a movable anti-contaminator. A brass sample cartridge can shield and attach the sample to the shaft which can later feed the sample into the targeted chamber. This device is compatible for standard EM grids or high pressure freezer carrier and is equipped with a scroll pump and a turbo-molecular pump which can create an environment of 10^{-7}-10^{-8}mbar. LN2 passive cooling is also used in this chamber to store samples[65].

[9]Image courtesy: PP3010T Cryo-SEM Preparation System, Quorum UK 2015

The Laboratory for Biological Geochemistry in Switzerland developed a passive sample transfer system that can store the sample under -120°C, $3x10^{-7}$mbar for 2 hours in the year 2017. It consists of a high vacuum chamber that acts as the sample carrier with LN2, a manipulator to move the sample, a flange that is compatible to many imaging modalities[66]. This chamber still uses passive cooling with a liquid nitrogen level warning insert.

Figure 1.10: Leica VCT500[10]

Leica Microsystems GmbH(DE) has been developing highly compacted sample transfer systems that can optimise the workflow. The Leica VCT100, VCT500 series have active cooling systems and a new valve concept to keep the sample in vacuum and low temperature at all times. All peripheral equipment is avoided which makes this device portable and highly dynamic for operators. It allows direct feeding of samples to the imaging stage with less leakage at the connections and costs about 150k-500k euros[69].

1.4. Delmic

This project, together with two other projects under the cryo transfer graduation project, is an internship combined graduation project commissioned by Delmic B.V. The company has its aim at creating user-friendliness, experimental freedom and integration in its products. Three systems have been developed at Delmic: the cathodoluminescence detector SPARC, correlative light and electron microscopy platform SECOM and Delphi, and a fully integrated fluorescence and scanning electron microscope. They are offering the customers superior performance, accuracy in acquiring data, compatibility with various scanning electron microscopes, and flexibility needed for the research (Delmic, 2009).

By developing a new sample transfer system for the correlative light and electron microscopy platform SECOM, customers of Delmic will benefit from a better sample imaging yield and a better user experience while operating integrationally in pre-existing systems.

1.5. Methodology

The design process of this projects strictly follows the Verification and Validation model (also called V model) and the fast feeding forward method (FFWD). The detailed design is based on proposing the project objective, system requirements, risk analysis. The solution space is iterated with integration, verification, validation, and is completely documented.

This project was designed by focusing on solving the relevant issues and dilemmas found within the current system. Critical analysis of current system setbacks and disadvantages led to a theoretical construction of an ideal system. Combining the elements that would make up an ideal system with customer requirements and avoiding stereotyping of current technologies, allowed for the generation of a solution space that could be checked with the

[10]Image courtesy: Leica VCT500 by Leica Microsystems, 2019 https://www.leica-microsystems.com/products/sample-preparation-for-electron-microscopy/p/leica-em-vct500/

detailed system requirements. The process endues a great amount of creativity, free-thinking, and innovation to come to a solution that is restricted by the very same requirements that are set for its creation.

2

Project objective and research questions

The above-mentioned current workflow is not ideal in fulfilling the best sample transfer performance. Basically, the objective of this project is to systematically analyze the workflow and generate a better sample transfer workflow of CLEM.

2.1. Project Objective

The project aims to create a new workflow that better connects the sample transfer chain between the vitrobot, the FIB/SEM, and the TEM, to prevent samples from all kinds of damages, improve the imaging results, the yield, and the user experience.

My colleague, Bas Bikker, oversees optimizing the AutoGrid and the plunge freezing process, which may optimize the thermal/mechanical behaviors of the original AutoGrid or integrate certain mini sensors to it to have the samples better monitored.

My work in the system is to create a more contamination-free, temperature-controlled cryo-sample transfer solution for the CLEM workflow which starts from plunge freezing the grids and ends with feeding the sample into the targeted TEM chamber.

My colleague, Shubhonil Chatterjee is designing a robotic arm sitting inside the FIB/SEM chamber to take over the samples from the transfer device and place them onto the cryo stage.

The work distribution is shown in figure 2.1.

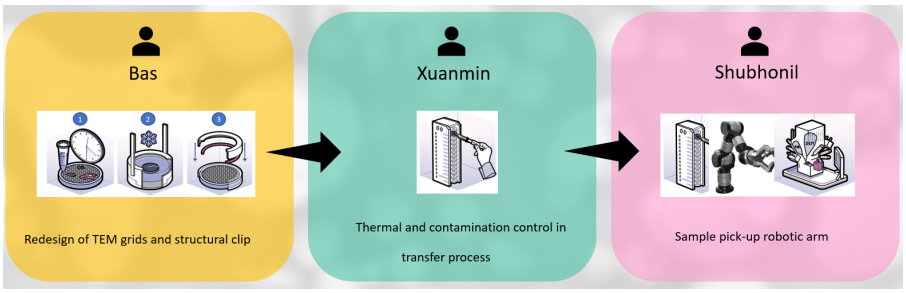

Figure 2.1: Overview of interface

On the base of the ideal workflow, the main challenges of my part are formulated as follows:

- Improve the temperature, contamination control.
- Improve and integrate the transfer devices/interfaces for both FIB/SEM and TEM.
- Improve the transfer throughput and efficiency.

2.2. Research question

To create a logical construction in approaching the objective, a number of research questions are proposed, which includes the literature research and the developing process, to identify the necessity, possibility, and solution to create a better solution. These questions include a main question and several subquestions.

The content and results of the literature research are attached in the appendix A.

2.2.1. Main research question

What is the cheapest, easiest, most damage-free workflow for CLEM system?

2.2.2. Sub questions

- What are the reasons for developing sample transfer systems?
- What is the current market state of such systems?
- What functions will this system fulfill?
- What are the boundary conditions and application environment of this system?
- What does the system infrastructure look like?
- What is the future vision and development orientation of the system?

2.2.3. Reasoning for the research choice

Answering the first question helps to build a solid background in the current workflow and related technologies, generate the problem statements and create the project objective. The answer to the market state leads to a benchmarking and a full case study of the industry solutions. The boundary definitions and system infrastructures give a clear guideline and large room of play for the requirements and solutions. Thinking of the future version will offer a chance of checking for improvements especially in the automation possibilities.

Answering these questions will lead the literature research to the right direction and further contribute to the overall design of the sample transfer system. The forward-looking research and design will guarantee a faster, cheaper, less contaminated product with better performance and long-lasting market life.

3

Problem statements

3.1. Problem statements

3.1.1. Problems

Even though strict rules are applied in the sample transfer workflow, contamination, sample heating and other problems which influence imaging results still happen in the current workflow. After a careful study of each step of this workflow, the protection gaps and current specs that can be improved are categorized and listed below:

1. Time consumption: FIB/SEM sample-loading is repeated six times to obtain 12 samples.
2. Contamination: AutoGrids are transferred through air every time when switching loading boxes.
3. Contamination: rough vacuum in the transfer unit.
4. Contamination: AutoGrids travel through vacuum imaging chambers unprotected.
5. Devitrification: no active cooling in transfer unit.
6. Devitrification: AutoGrids are heated by FIB/SEM imaging.
7. Damage: mount and clip AutoGrids.
8. Damage: handle AutoGrids with tweezer.
9. Misplacement: human error can happen in placing AutoGrids in shuttle and in cassette, may disrupt the order.
10. Damage: frequently taking samples in and out of the LN2 may cause fracture of the ice due to the temperature fluctuation.

As mentioned, the strict temperature requirements are attributed to the important physical features that amorphous ice can achieve in bio-materials and the harsh conditions required by it. Also, the forms of ice resulted from unwanted transition of amorphous ice are regarded as cryo deposits or contaminants. These contaminants absorb, scatter, and cause unwanted interference[36].

The sample heating that will start the devitrification of the amorphous ice and the contamination can directly influence the imaging yield and results. The slow workflow exacerbates the contamination and heating. Mechanical compacts and temperature change fracture the fragile sample. All these factors result in a ratio of unusable samples of around 90% in the current sample transfer workflow.

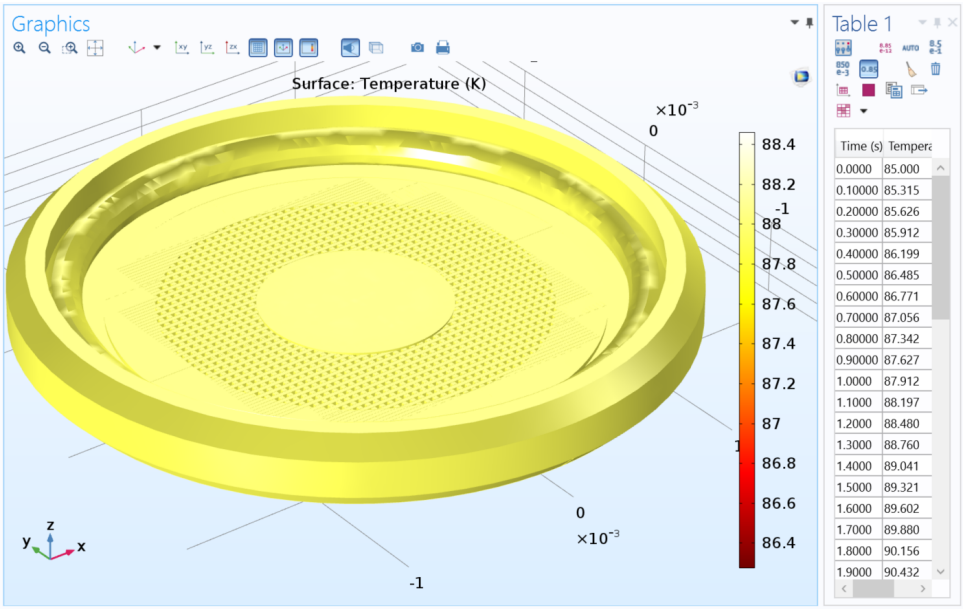

Figure 3.1: The thermal simulation results of AutoGrids exposed in the air

3.1.2. Problem identification by thermal analysis

The sample heating during the transfer between the loading boxes and within the transfer unit are simulated in COMSOL. According to the workflow, the samples are mainly exposed in the following conditions: the first model simulates the process when transferring AutoGrids between loading boxes without protection. The second model simulates the process when two AutoGrids are placed on the shuttle and the shuttle is held in the middle of the transfer unit in N2 environment before pumping. The third model is like the second model, except that the shuttle is in a vacuum tube of 10^{-3}mbar in the transfer unit. The last model simulates the time that the shuttle can keep samples from devitrification within the high-vacuum imaging chamber of FIB/SEM.

- `AutoGrid exposed in air with normal pressure`
  Due to the heavy computational requirements of directly determining the radiation over the full-scale model of the AutoGrids, a copper plate of the same size (same surface area), replaces the AutoGrid in the modeling. This plate then receives the radiative heat flux from the lab walls represented by a block. The COMSOL module used in this simulation is the 'surface to surface radiation'. The same amount of flux and the gaseous heat conduction are then added up and jointly applied to the full-scale model as the boundary heat flux condition to simulate the temperature rise of the AutoGrid.

  The surface emissivity and the thermal conduction are set temperature dependent. The initial temperatures of the AutoGrid and the Walls are -196.15°C and 26.85°C. The time span of this simulation is 1 second, as the process is very fast.

  According to Eq.(A.1) and Eq.(A.3), the numerical gaseous conduction heat load to the AutoGrid is $\dot{q}_{air} = 7.269 \times 10^{-4} W$, the radiation heat load is $\dot{q} = 6.863 \times 10^{-3} W$.

  The time-dependent simulation results of the radiation heat load in the first few seconds have an average of $6.725 \times 10^{-3} W$, which is very close to the numerical result. When applying the gaseous heat load and the radiation heat load to the model, the temperature rise of the AutoGrid surface in the first second is $2.912°C$.

- `Two AutoGrids in a shuttle in the transfer unit, normal pressure, N2 environment`
  In this model, the shuttle is simplified as a 2cm×1.6cm × 0.8cm block. The transfer unit is modeled as a cylinder that has a diameter of 0.1m and a height of 0.08m.

Figure 3.2: The thermal analysis results

Subject	Environment	Numerical results		COMSOL simulation results	
		Gaseous conduction (W)	Radiation (W)	Radiation (W)	Temperature rise (°C)
AutoGrid	Air, normal pressure	7.269×10^{-3}	6.863×10^{-3}	6.725×10^{-3}	-188.150~-185.238°Cafter 1s
AutoGrid on shuttle	N2, normal pressure	1.810×10^{-1}	4.393×10^{-1}	4.195×10^{-1}	-196.150~-188.057°Cafter 60s
AutoGrid on shuttle	in tube $1 \times 10^{-3} mbar$	1.810×10^{-1}	/	1.877×10^{-1}	-188.057~-185.552°Cafter 60s
AutoGrid on shuttle	1×10^{-6} mbar	1.022×10^{-5}	/	3.952×10^{-1}	-185.552~-165°C after 331s

The numerical results of gaseous conduction heat load of the shuttle is 1.81×10^{-1}W, the radiation heat load of the shuttle is 4.393×10^{-1}W.

The COMSOL radiation simulation is set to have a time span of one minute, the average heat load is 4.195×10^{-1}W. The temperature rise of the AutoGrid surface after 1 minute is $8.093°C$.

- Two AutoGrids in a shuttle in the vacuum tube of the transfer unit, 1×10^{-3}mbar, N2

  The vacuum tube within the transfer unit is simulated as a cylinder of 3cm in diameter, 5cm in height and 3mm in thickness.

  The numerical results of the shuttle's gaseous conduction heat load is 1.810×10^{-1}W. The numerical results of radiation heat load of the shuttle is not reliable due to the surface complexity in this configuration.

  The COMSOL radiation simulation is again set to have a time span of 1 minute, the average heat load in these 60 seconds is 1.877×10^{-1}W. The temperature rise of the AutoGrid surface after 60 seconds is $2.505°C$.

- Two AutoGrids in the shuttle in the targeted vacuum chamber, 10^{-6}mbar

  This simulation has only two differences with the second simulation: the pressure and the gaseous conduction regime caused by the pressure drop.

  The numerical results of the shuttle's gaseous conduction heat load is 1.022×10^{-5}W. The radiation heat load of the shuttle is again not reliable due to the surface complexity in this configuration.

  The COMSOL radiation simulation indicates that the heat load is at least 3.952×10^{-1}W. The temperature of the AutoGrid surface will stay below -165°C within 331 seconds.

The results of the simulations show that the process of taking the grids out of the loading bath can cause temperature fluctuation of the cryo sample. This can possibly cause fractures of the bio-materials and even crystallization of the amorphous ice and influence the imaging results.

It is also shown that the shuttle has effective thermal shielding against sample heating, but the shielding power is limited due to the exposure of the sample surface when sitting on the shuttle and the limited thermal mass provided by the shuttle. In the pumping process of the transfer unit that can last from 30 seconds to one minute, the temperatures of the samples will have a rise of around 10.598°C (the computation of the heat convection current is neglected, therefore the results presented are the worst case scenario).

The last simulation suggests that theoretically the shuttle can protect the samples from devitrification within a high vacuum chamber for around 5.5 minutes with its best performance. Therefore the time for transfer should be kept well within this limit to make sure that the samples do not get damaged. During this period, the transfer process includes detaching the transfer unit from the station, reattaching it to the airlock of FIB/SEM, pumping the airlock, opening and closing the valves and inserting the shuttle to the cryo stage.

4

Requirement risk identification

The problem statements addresses the gaps between the current state and the ideal state[33]. Despite looking for all the problems in the current workflow, the discussion of the ideal workflow that fulfills all the customer requirements is also of great importance. Rating the solutions that leads to the ideal protection and evaluate whether they are feasible are the key to building a successful product.

4.1. Customer requirements

The slow and complex workflow is caused by the fact that the sample preparation procedures of FIB/SEM imaging and TEM imaging are bluntly combined. For research facilities, CLEM imaging is expensive not only for the instruments, but the low efficiency of transferring samples in between FIB/SEM and TEM. The journey for an individual sample is long and cumbersome. A smart combination of two transfer workflows with less manual operation involved would be ideal.

Under this circumstance, customers want a new product or system that can provide a better workflow:

- The new system/product should increase the yield of the CLEM imaging.
- The new system/product should provide a quick and easy workflow for sample transfer from plunge freezing to FIB/SEM to TEM.
- The workflow should be as automated as possible that needs less human handling.
- The new system matches with the interface of the FIB/SEM chamber and the Autoloader of Titan TEM as well as the cassette for Autoloader.

4.2. Ideal workflow

The ideal workflow that fulfills the key tasks of the transfer, is proposed without considering possibilities and difficulties of realizing or the price-performance ratio. This helps in evaluating and keeping the most essential component and function of the workflow, generating good ideas, and a broad solution space.

Based on the customer requirement, an ideal workflow aims for reducing human operation, increasing throughput can be proposed. This workflow can avoid contamination, heating and other sample damage and in the end, contribute to a better yield of CLEM imaging.

The ideal workflow would be:

1. After the sample preparation, which is pipetting the sample to grids and plunge freezing them with a vitrobot, the grids are easily and safely clipped to AutoGrids.
2. A transfer device takes over the AutoGrids

3. The transfer device sends the AutoGrids to the FIB/SEM imaging chamber.
4. The AutoGrids are send to the cryo stage of the FIB/SEM imaging chamber and imaged.
5. The AutoGrids are sent back to the device and wait for next imaging.
6. The device transfers the AutoGrids to the Autoloader of the TEM.
7. TEM imaging.

4.3. System requirements and risk matrix

For system requirements, see appendix B. For risk matrix, see appendix C.

5

Design

A solution space has been proposed based on the system requirements. Sound reasoning of whether these solutions are feasible or useful to be applied to the new workflow is given to generate the final solutions.

The final design and the considerations over it are introduced in the last section. A Delmicup, a plunging bath, a vacuum box and a cold finger have been designed along with a detailed new workflow to fulfill the transfer. All the off-the-shelf products integrated or needed for the functioning of the system are chosen from the current market according to their specifications and registered in the appendix C.

5.1. Solution space

5.1.1. Throughput increasing solution

A solution space to increase the throughput is proposed initially to increase the number of AutoGrids transferred each time. A possible solution would be to put more AutoGrid slots on the shuttle. However, it should be noted that the shuttle is small and increasing its size may exceed the motion range of the cryo stage in FIB/SEM to move the ROI (region of interest), to the point of focus. A better solution could be directly using the cassette to receive and transfer 12 AutoGrids to the FIB/SEM, and to integrate a robot arm into the imaging chamber to unload and take the AutoGrids to the cryo stage one by one. The design of this robot arm is the scope of my colleague Shubhonil Chatterjee.

5.1.2. Anti contamination solution

In the CLEM workflow, the distances between the vitrobot, FIB/SEM and TEM can be significant and the reachability of these instruments varies. Therefore a portable long-distance integrated transfer device or a long-distance transfer station with a portable transfer device that can travel a short range are the two feasible transfer solutions to send AutoGrids to the targeted instruments. An anti-contamination solution space is generated over these two general directions. Multiple ideas can be of value and many can be combined to contribute to building a clean transfer workflow. The proposed solutions are listed below.

- Vacuum transfer.
- Glove box transfer.
- Cryogen transfer.
- Shielding.
- Reduce transfer time/step/device and optimize transfer device.
- Avoid direct manual operation.

- Anti-contaminator.

The benefits of reducing contaminants by vacuum is too important to be ignored as the partial pressure of water drops heavily when the pressure is lowered to 10^{-6}mbar according to chapter A.3. The system should have a vacuum transfer device that can be attached to the vacuum chamber of FIB/SEM to fulfill the transfer. The transfer device needs to be docked to an airlock at the FIB/SEM for the vacuum transfer.

The vacuum generation of the transfer device has many options: integrate a mini high-vacuum pumping system to the transfer device so that this device itself can be used for long distance vacuum transfer; Dock the transfer device to a pump station/box which is connected to a pumping system; attach the transfer device directly with the tube of a pumping system.

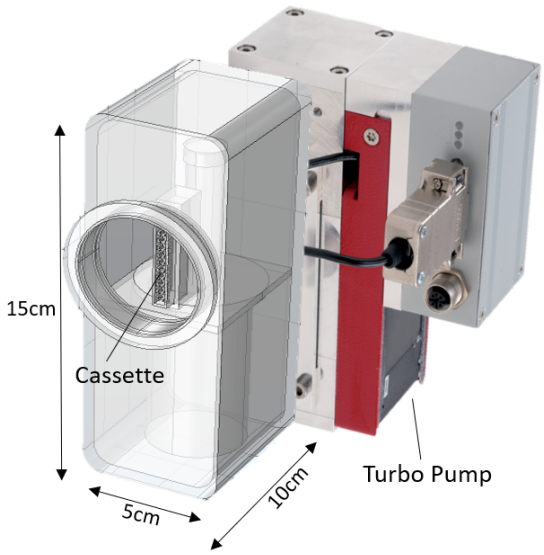

Figure 5.1: Conceptual design of an actively cooled and pumped transfer box, with the turbo pumping system from Pfeiffer[1]

The first idea was initially adopted (see figure 5.1), by integrating the Pfeiffer TPH-055 Turbo Pump to the transfer device. However, the problems of vibrations and the large footprint/weight of the pump weaken the performance and portability of the device.

The two later solutions have the station/box move a long distance and let the transfer device fulfill the last-meter transfer. Yet, attaching the transfer device with a tube for pumping is not ideal either, because the frequent moving of the transfer device might loosen the tube connection and cause leakage and other safety issues.

Designing a vacuum pumping box/station can reduce the footprint and weight, and increase the safety and stability of the transfer device. Also, the pumping from atmosphere to high vacuum in general needs a pump station which consists of a rough pump and a high vacuum pump.

A vacuum glovebox on the pump station can be used to create a comparably clean environment to protect all the transfer processes when the samples are not within vacuum or cryogen environment. Two workflows were proposed to implement the glovebox workflow (see figure 5.2). The workflow in a) uses a wobble stick to clip the grids, load them to the cassette and put the cassette to the vacuum transfer device. The workflow b) uses vacuum compatible gloves to do the operations. Both workflows need the operator to manually put the ethane bath with frozen grids into the box, and contamination can be introduced into the glovebox in the process. An idea of using a newly developed plunge freeze device with a much smaller footprint and height within the glovebox was proposed (see figure 5.2 (c)). But this solution is not preferred either as this device from Linkam is still in the prototype phase and

[1] Image credit: 55l/s turbo pump TPH-055 by Pfeiffer, https://www.pfeiffer-vacuum.com/en/

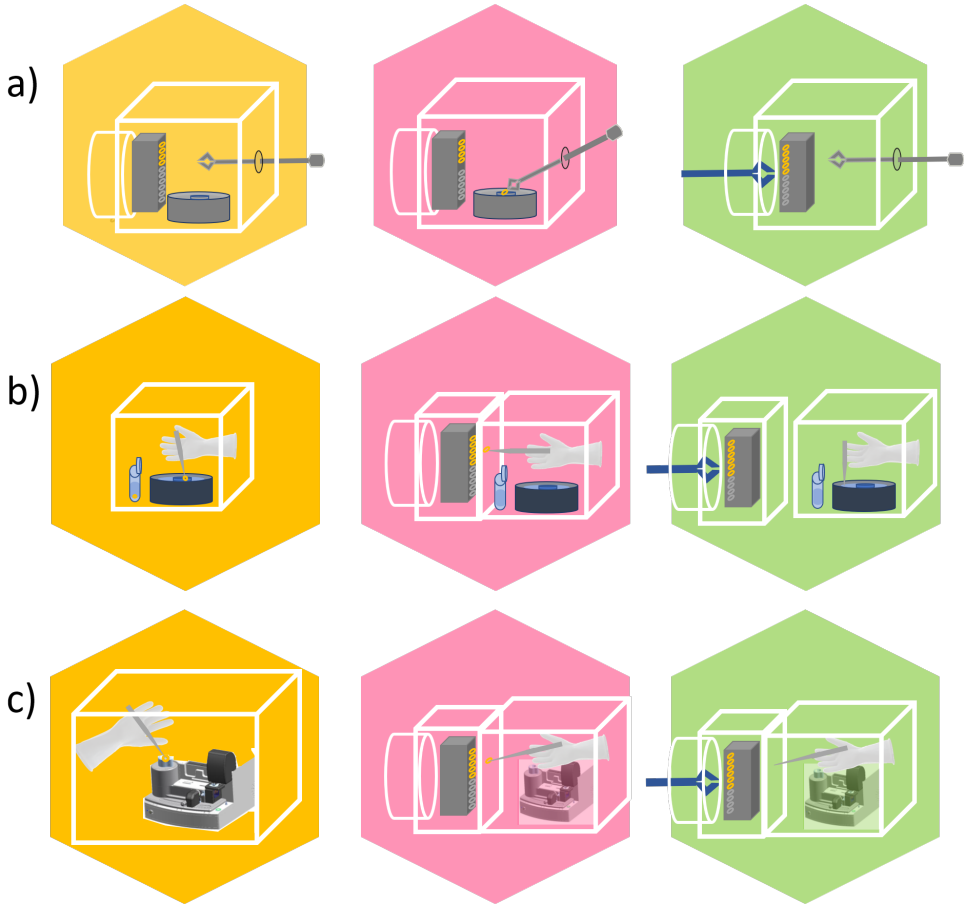

Figure 5.2: Anti contamination solutions[2]

not yet available in the market and the device is very unlikely to be vacuum compatible. Special considerations should be taken to separate the device from the vacuum condition if this idea is adopted. Besides, operating a wobble stick precisely in a) to pick up the grids might be difficult and vacuum gloveboxes in general cannot easily reach high vacuum. Therefore, using a glovebox does not seem to be an trustworthy standalone solution to have grids safely transferred inside.

Then the feasibility of the transfer within cryogen is considered: though industrial cryogens still have moisture, transferring the AutoGrids within cryogen has a smaller chance of contamination compared to high vacuum transfer. This is also a much smaller chance than transfers within atmosphere or hydrocarbon environment.

Combining the cryogen and vacuum protection and protecting the samples during the transition period between cryogen and vacuum can be used to cover the whole process of sample preparation. The AutoGrids can be plunged, clipped, transferred to the cassette inside the cryogen environment, and then taken to vacuum transfer.

Shielding the AutoGrids or the cassette can exactly be used to cover the transition process. A cold shield in vacuum can efficiently block or divert the particles away from the sample surfaces, especially when the cryogen is no longer immersing the AutoGrids and the pump has not yet lowered the water composition in the chamber down to optimum. Many ways of shielding can be implemented: shielding the AutoGrids individually, shielding the cassette with a box, or attaching a door to the cassette (since the cassette itself has the shape of a box). The pros and cons of the different shielding techniques mentioned above are discussed in detail later in the section of choice of cooling solutions because a good shield helps not

[2]Image courtesy: Linkam cryo plunger by Linkam Scientific http://www.linkam.co.uk/linkam-blog/2017/8/18/introducing-the-prototype-of-the-linkam-plunger

only in anti-contamination, but also heating prevention.

As for optimizing the transfer devices and the workflow, the process of transferring AutoGrids between different loading boxes can be avoided since these loading boxes are all creating a LN2-cooling operating environment. The main reason of transferring samples between them is the unsystematic loading box design when combining two different workflows together. In redesigning the loading boxes and integrating different functions, the unprotected steps can be avoided and the time of transfer and radiation/contamination exposure can be decreased. This means integrating the ethane bath, the loading box for the clipping station, the loading box for the transfer unit, and the loading box for the cassette. Also, the transfer unit and the Nanocup can be integrated for transferring samples to the targeted imaging instruments.

To realize the above integration, first, a bath with cryogen where AutoGrids can be plunge frozen, clipped and directly transferred to the carrier is ideal. To make the most of the function of the irreplaceable vitrobot, the up-down motion of the plunge arm can be used to insert AutoGrids to the cassette simply by placing the cassette below the plunge arm with its slots facing upwards and reaching the arm deeper down to insert the grid to the slot of the cassette after plunge freezing. The arrangement of the plunge bath and the vacuum box can be side by side or in upper & lower structure: either the cassette is soaked directly in the deep plunging bath and is later pushed to the vacuum box horizontally through a connection, or a vertically placed cryogenic valve is used to separate the upper cryogen bath and the lower vacuum box where the cassette is placed. When thinking twice about these two solutions, the second solution has a large amount of cryogen consumption in every plunging when the gate valve is opened to let out the grid. The first solution, on the other hand, requires less operating of cryogenic valves and less frequency of cryogen refilling. The height of a cryogenic valve might also not accommodate well within the space beneath the vitrobot when placed vertically.

When applying the first solution, the clipping process should not be neglected. As the clipping motion is linear, a mechanism for auto-clipping can be designed to have two arms approach from both sides of the grid horizontally while the grid is held vertically by the plunge arm and sandwich the grid with the AutoGrid ring and C ring by a linear motion of both of these arms. The arms can be fed with multiple AutoGrid rings & C rings and can push one of each out for clipping in every plunging cycle.

The last anti-contamination technique is to use an anti-contaminator. In the benchmarking in the previous chapter, a cryo cold finger or a mini pump is used in sample transfer devices to act as the anti-contaminator, because they both can divert contaminants away from the sample. As a vacuum box, a transfer device and a shield will be designed in the new workflow, the shield can be used as the cold finger. The necessity of integrating other anti-contaminators can be decided under experimental results of the sample contamination of the new workflow in the future work.

5.1.3. Temperature control solution

As a cryogen bath for plunge freezing, a vacuum box for pumping and a transfer device for transferring are preliminarily proposed in the anti-contamination solution space, the discussion of the solution space for cooling will be based on the optimization and integration on these components.

To obtain better temperature control, the following solutions are proposed:

- Reduce the time of transfer, optimize unprotected transfer steps.
- Passively soak the samples in cryogen
- Shield the AutoGrids/cassette
- Reduce the radiation by cooling the chamber walls
- Actively cool down the AutoGrids

Plunging the grids directly to the cassette in cryogen and transferring 12 AutoGrids a time in the cassette have already avoided the multiple unprotected transfers between the

four loading boxes and two transfer devices in the old workflow and saved a lot of time in sample preparation process.

Many cryogens have been tested on their plunging behavior and ethane was chosen as the plunge freezing cryogen in the old workflow. A plunging bath needs to have a structure to have the ethane in the inner chamber cooled by LN2 (at -196.15°C) in the outer chamber to liquefy the ethane gas. But ethane also suffered frequently from being frozen completely into solid[67] as the liquid range of Ethane is -183.25 to -88.55°C. This is not tolerable in the proposed deep plunging bath equipped with an auto-clipping mechanism and the cassette. According to William F. Tivol in his article 'An Improved Cryogen for Plunge Freezing[67],' the mixture of ethane and propane can be a better cryogen to remain liquid when even directly contacting with LN2 while maintaining the ability to form vitreous ice in grids. The concentration of moisture and the price of industrial-level ethane and Et/Pr mixture are therefore compared to find out the feasibility to replace ethane with Et/Pr mixture: the water concentration in both liquids are around 2-3 ppm, the price of Et/Pr mixture is 0.39€/L, even slightly cheaper than that of ethane at 0.48€/L. Therefore, in this project, Et/Pr mixture will be replacing ethane for plunge freezing to avoid solidification of the cryogen.

To quick-transfer the cassette from the plunging bath to the vacuum box, taking out the cassette from the plunge bath and manually place it to the vacuum chamber can be an option, it can also be connecting the plunging bath and the vacuum box with a cryogenic valve and transfer the cassette in between. When the cassette is ready for transfer, the cryogenic valve is opened and the cassette is pushed to the vacuum box with a linear motor, a magnetic coupling or a feedthrough rod. Taking the cassette out of the plunging bath can cause contamination and heating to the AutoGrids in the cassette while using a cryogenic valve simplifies the workflow, reduces human contact/contamination and is easier for automation in the future work.

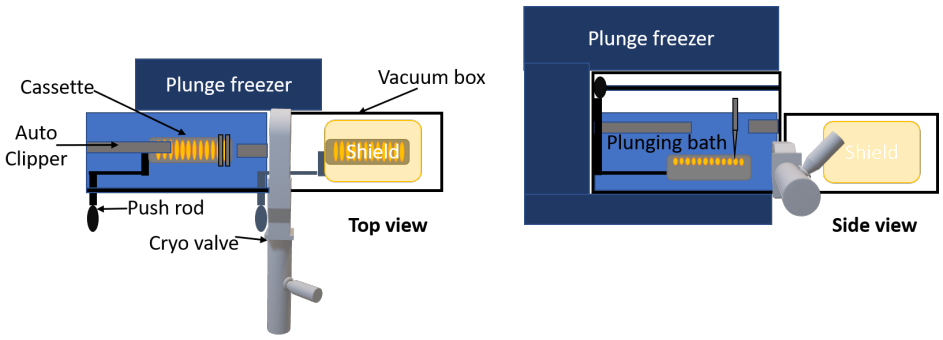

Figure 5.3: Concept design of the plunging bath and vacuum box

So far, the concept design of the plunging bath and the vacuum box has the arrangement shown in figure 5.3. Based on the thermal analysis results in chapter three, the AutoGrids will suffer from heating when being exposed to the room-temperature vacuum box, during the pumping or uncooled transfer, a good shield is needed to slow down the heating and contamination. However, if shielding the AutoGrids individually, a mechanism or a manual step to take off the shield should be added. Besides, the shield might be too small to have sufficient thermal mass to protect sample in the pumping process which could last more than 5 minutes. Attaching a door to the cassette is also not an ideal solution, since the exact inner dimensions of the cassette are patented but not yet released and the Autoloader mechanism that handles the cassette is not 100% clear, the modification of the cassette might cause the Autoloader to malfunction. Building a metal block of shield for the cassette can be the best solution, since this block of shield can not only shield the cassette from radiation but also prevent particles from entering its opening. Copper with a large thermal conductivity can be a good material to build such a shield to act as a large thermal mass and slow down the heating of the AutoGrids. When attached with a cooler, the shield can even be a cold finger that wraps around the cassette and cools it down actively, the concept is shown in the first picture of figure 5.4.

Cooling the wall of a cryostat is a general application to reduce radiation heat load of the objects inside the chamber. Multi-layers, a vacuum layer, an additional opaque layer or a water/cryogen jacket over the chamber wall can help to lower the temperature of the wall. But as the transfer chamber needs to be portable, moving a cooling jacket with hoses attached to it frequently might be unreliable or even dangerous especially when cryogen is running through. Besides, the radiation from the chamber wall can be compensated easily by providing a stronger cooling solution. A muti-layer of Metal or aluminum-coated Mylar™ might be used to cover the transfer chamber if the experimental results suggest the necessity in the future work.

As the samples will eventually be transferred to a vacuum chamber where cryogen will not be maintained, besides the FIB/SEM imaging process can last longer than 12 hours, cooling samples only by soaking them in cryogen is not enough. An active cooling solution is necessary at least when the AutoGrids are waiting at the airlock of the FIB/SEM. When the cryogenic valve is opened, certain amount of Et/Pr mixture will flow into the vacuum chamber, a draining process might be needed depends on whether the pump can pump away all the cryogen within time allowed.

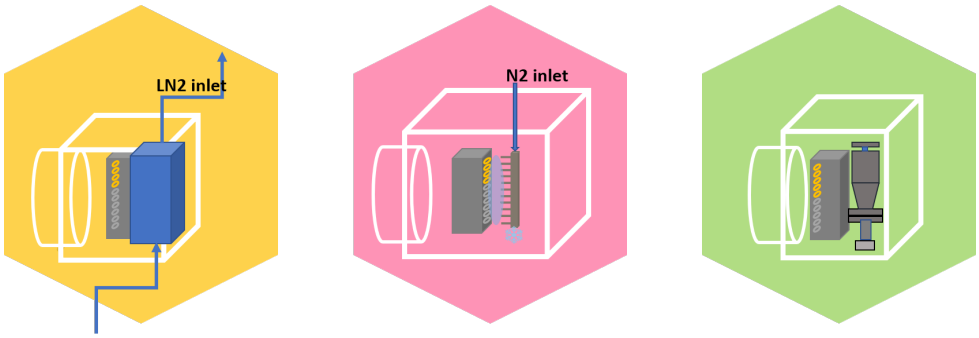

Figure 5.4: Cooling solution

Three active cooling ideas are presented in figure 5.4 to provide cooling for the AutoGrids: solution one is to attach a cold finger (a copper block, may as well be the shield) to the cassette, and the finger is attached with a electric-cooler or hoses through which the cryogen is circulated. Solution two is to have a jet of cold N2 blown into the cassette. But as the cooling is mostly needed in vacuum operations, this solution is not feasible. Solution three is to integrate a thermal electric cooler within the transfer chamber. The thermal electric cooler comes with the problems of vibrations and noise, besides, the weight of such a cooler can easily reach 5kg, along with an undesirable footprint for a transfer device aims for portability and the tube connecting the electric cryo cooler and the cold finger has a limited length. Eventually, a cold finger with cryogen circulating for cooling is chosen as the best cooling solution as it generates limited vibrations. A more detailed considerations will be discussed later in the concept realization design.

5.1.4. Towards the overall transfer

Three main components: the plunging bath, the vacuum box, and the transfer cup are fixed for the system. The connections and different transfer proposals are to be discussed to complete the transfer flow: the plunging bath sits right below the plunging arm of the vitrobot, the auto-clipper works within the cryogen and has its arms aiming at the grid surfaces. The cassette is placed at the bottom of the plunging bath with its slots facing the plunging arm and can be pushed horizontally to receive up to 12 plunged AutoGrids. Further in this direction, the cassette can go on being pushed through and out of a cryogenic valve which is connecting the plunging bath with the vacuum box. The shield, due to its large diameter, is better accommodated outside the plunging bath as the opening of the cryogenic valve is limited (cryogenic valves with a larger opening have larger size and weights that are not compatible with the limited space below the vitrobot). Both the plunging bath and the shield should be cooled, hence a LN2 bath should surround the two boxes. When the Et/Pr mixture flows into

the vacuum box while opening the cryogenic valve for transfer, the cassette is soaked within the liquid to continue the protection.

As the Autoloader takes the cassette out vertically from the Nanocup, and rotating to reorient the cassette within the device is not easy due to the small inner space of the device, the cassette should stand vertically in the transfer device (the transfer device is preferably in a cylindrical shape to have good mechanical behaviors and ease of manipulation). The design space for the transfer of the cassette from the vacuum box to the transfer device is therefore limited too.

The allocation of the transfer device when attached with the vacuum box determines the transfer motion. There are two allocation schemes of the transfer device: attaching the transfer device vertically at the top of the vacuum box, with its opening held right above the shield, and attaching the transfer device horizontally in line with the cassette-pushing path where the shield is also aligned.

The workflow of the first scheme is shown in figure 5.5: Plunge freeze, clip and insert 12 grids to the cassette in the left plunging bath, open the cryogenic valve, let the cryogen flow into the vacuum box, push the cassette to the right box where it is aligned with and inserted to the cavity at the left side of the shield. Lock the cassette with the shield and rotate the shield to have the cassette standing vertically with the cavity of the shield facing downwards to allow the Autoloader to take away the cassette. Drain the cryogen and start the pumping. Rise up the shield with the cassette to lock them inside the transfer device. Then the transfer device is ready to be detached and transferred to the FIB/SEM or TEM.

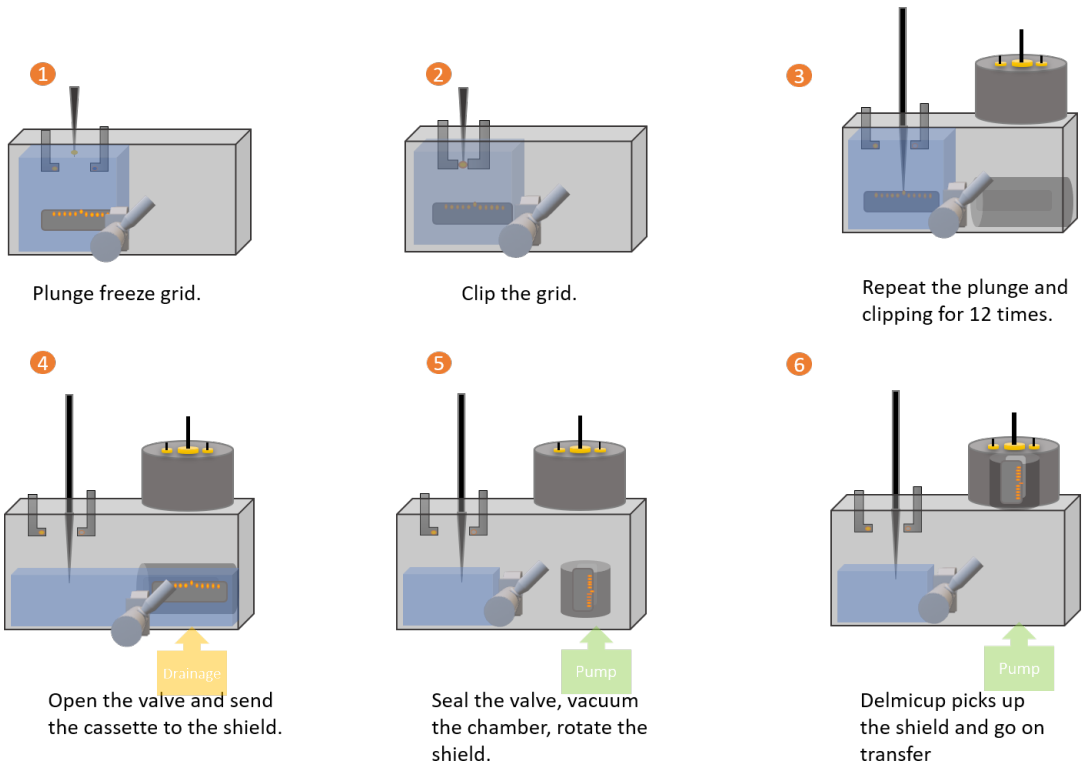

Figure 5.5: Vertical transfer cup

The tricky part of this scheme is to rotate the shield and lift it up to the transfer device above. A number of rotating methods are shown in figure 5.6: shift the center of gravity of the shield when inserting the cassette and let it fall, using an electro-magnetic lock or a elecro-strike lock at the other end of the shield, place the center of gravity of the shield outside the rim of the stage and release the lock when rotating. A long feedthrough or a linear motor can be used to lift the shield, but this causes problems too, as a long rod attached at the end of the transfer device will prevent the device from attaching to the Autoloader. Designing

a mechanism to lift the shield up with a linear motor is not ideal either because the motor should be placed outside of the vacuum box.

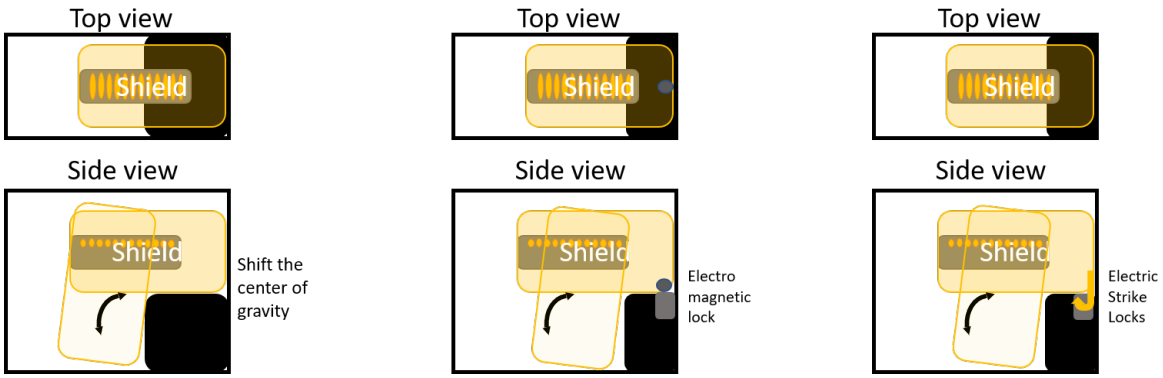

Figure 5.6: Proposals for shield rotation

These problems can be bypassed by adopting the second scheme: when the transfer box is placed on the path where the cassette is pushed, by placing the center of the transfer device on the same level with the cassette and the shield, a linear pushing motion of the cassette can transfer it to the shield and further transfer them together to the center of the transfer device. The pushing mechanism can be realized easily with a cryo feedthrough rod, a linear motor or a magnetically coupled rail.

The second scheme is more intuitive and simpler for manipulation, the automation of the motion is also easier in the future work.

5.2. Components

The system is designed strictly following the customer requirements and system requirements to fulfill the easy, safe, cheap, quick transfer goal. The integrated device is made of three main parts: the plunging bath, the vacuum box, and the transfer device 'Delmicup'.

Sitting right beneath the vitrobot, the system starts with the plunging bath equipped with a magnetic coupled feedthrough, see figure 5.7. The plunging bath has an inner chamber (the blue chamber in the figure) filled with Et/Pr liquid for plunge freezing and is surrounded by an outer chamber filled with LN2 to keep the Et/Pr liquid and all the inner devices at required cryo temperature. The feedthrough rod is used to push and position the cassette precisely to receive AutoGrids from the vitrobot and transfer them to the vacuum box and the Delmicup.

The vacuum box is designed to generate the vacuum. Since the cassette is pushed straightly to the vacuum box, the shield sits with its cavity pointing right towards the cassette and receives the cassette into its cavity when further pushing the feedthrough rod. As the shield and cassette both need to be cooled, the vacuum box is also designed to be a double-chambered box with a LN2-cooling outer chamber to cool down the shield and cassette sitting within the vacuum chamber. A vacuum compatible cryogenic valve connects and seals the vacuum chamber when pumping, the vent valve is integrated to relieve the pressure.

On the other end of the vacuum box, the Delmicup can be docked to receive the cassette and the shield. When detached, it can keep its vacuum to transfer the shield because it is equipped with a high vacuum gate valve. Also, a lock-lock mechanism and a rotary feedthrough are used to lock the shield with the Delmicup and seal the opening of the shield cavity.

The dimension of the designed components is registered in the appendix B.

5.2.1. Plunging bath

The plunging bath is a sample preparation station made from copper and filled with cryogen. It fits well with the space beneath the tweezer of the vitrobot.

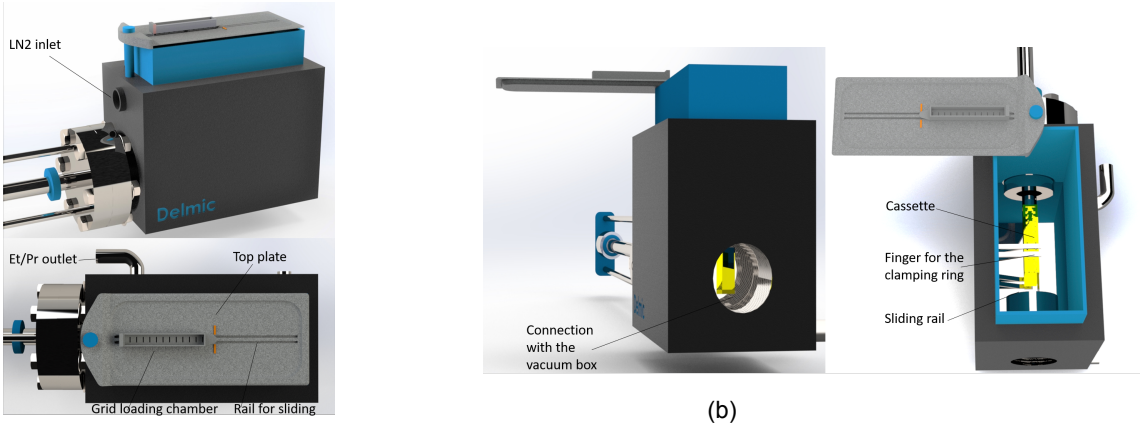

Figure 5.7: The plunging bath

It fulfills a number of functions in the old workflow which include solution preparation/sample culturing, replacing the grids on the tweezer of the vitrobot, transferring the frozen grids to the clipping station which is situated in a different LN2 box, clipping the grids with AutoGrids and transferring the AutoGrids to another loading station for slush pumping.

This bath avoids the transfer between three different LN2 loading baths and can take advantage of the up-down motion of the plunge tweezer of the vitrobot to pick-up, insert and release grids into the cassette. This can replace the tweezer/grid replacing operation by human and largely increase throughput. A horizontal finger is used to fasten and unfasten the clamping ring of the tweezer to grip or release the grid from the tweezer. The moveable cassette sits right beneath the tweezer and can be pushed forward by the feedthrough rod according to a reference scale to precisely receive 12 AutoGrids from the tweezer in each slot. The frozen samples are soaked in Et/Pr mixture in the inner chamber and the inner chamber is cooled with LN2 in the outer chamber. The samples are thereby protected from particle contamination and heating in the preparation and transfer process.

Components

The plunging bath is designed to sit beneath the vitrobot and is composed of the following parts:

- `A rotatable grid plate with slideable grid loading chamber`
  Like the cassette, the grid loading chamber can be loaded with 12 empty grids or grids with bio-sample. It can be filled with medium for the cultivation and can be detached and stored in cultivators easily.

  The grid plate has a rail with a reference scale to support the grid loading chamber and enable its precise sliding. It also acts as a rotatable lid of the plunging bath to prevent particle contamination and cryogen evaporation.

- `A plunging chamber`
  The plunging bath is a double-chambered copper box that can be filled with 1.6L Et/Pr liquid in the inner chamber and 2.6L LN2 in the cooling chamber. The inner plunging chamber is designed with a rail at its bottom to smoothly slide the cassette to the next chamber, two fingers are designed to fasten/unfasten the clamping ring of the tweezer. The auto-clipper will be hanging 5cm below the cryogen. The wall is strong enough structurally while having good thermal conduction for the heat exchange between the Et/Pr and LN2.

- `A cooling chamber`
  The cooling chamber surrounds the plunging bath and is attached to the LN2 inlet and

outlet that leads to the vacuum box cooling chamber. The box is also attached with the magnetic feedthrough and the cryogenic valve on each side.

Functions

- Grid preparation: the grid loading chamber slides on the rotatable grid plate. When the sample preparation starts, a grid loading chamber with either 12 empty grids or grids with bio-materials cultivated in media is placed on the grid plate. The plunge tweezer is attached to the vitrobot and the vitrobot is started to lower the tweezer. The fingers reach ahead while the tweezer is going down and the clamping ring of the tweezer is unfastened. Retreat the fingers. Push the grid chamber further ahead and aim each grid beneath the tweezer precisely according to the reference scale on the grid plate. Go on lowering down the tweezer to reach the grid. Reach ahead with the finger again and fasten the tweezer while it is moving upwards, retreat the fingers once the tweezer is fastened and the grid is ready to be pipetted with bio-sample or get blotted in case of cultivated grids.

  Then the grid is ready to be plunge frozen rapidly to 2cm below the cryogen level within the plunging bath.

- Clipping: after plunge frozen, the grids are further lowered to the clipping station. An auto-clipper comes from both sides of the grid and clip the grid with the AutoGrid ring and the C ring.

- Transferring: the AutoGrid is now ready to be inserted to the cassette simply by lowering the tweezer further more. The cassette can be pushed following the reference scale on the magnetic feedthrough to have the right slot aiming at the tweezer.

- Repetition: repeat the previous steps 12 times to prepare 12 AutoGrids and load them into the cassette. Now the cassette is ready to be transferred to the next device.

5.2.2. Vacuum box

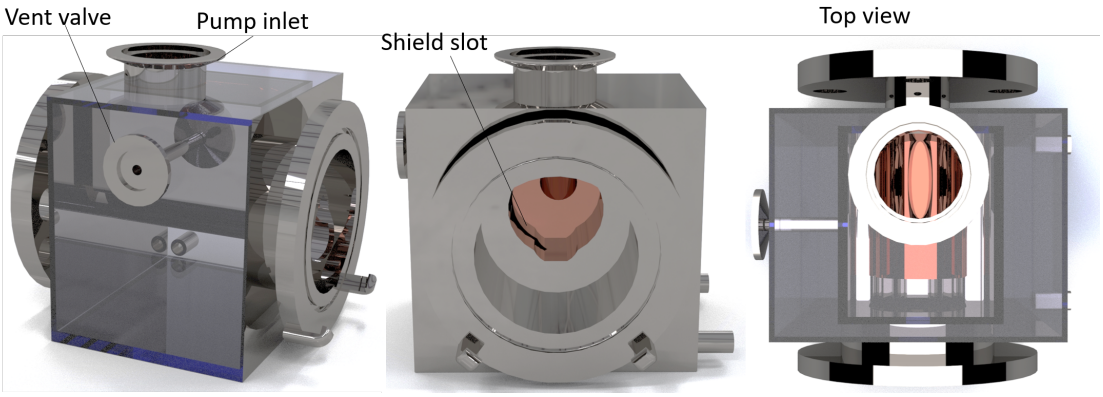

Figure 5.8: The vacuum box

The stainless-steel vacuum box is connected to the ethane bath with a cryogenic valve to receive the cassette loaded with the AutoGrids. A shield made from copper is designed to be loaded in the vacuum chamber with its cavity facing towards the cryogenic valve opening to receive the cassette. The Delmicup will be docked at the other side of the vacuum box to receive the shield and the cassette. The vacuum chamber is connected to a pumping system and can be drained and vacuumed up to 10^{-6}mbar; a vent valve connected with LN2 dewar can vent the chamber with N2. The vacuum chamber is surrounded by the cooling chamber which is connected with the LN2 outlet of the plunging bath.

Compared to the old workflow, the new vacuum box and its sealing is designed to bring the transfer vacuum to 10^{-6}mbar. It takes over the following steps in the old workflow: the AutoGrids is transferred to the pumping box, two AutoGrids are placed into the shuttle under

LN2, the shuttle is then picked up with the feedthrough rod and the pump box is pumped by the slushy pump. The introduction of a cold shield will also better protect the cassette and AutoGrids from contamination and create a large thermal mass to keep samples from being heated too quickly.

The shield sits on the bottom plate of the vacuum chamber where it can be cooled by the LN2 in the cooling chamber underneath. The inner chamber will be purged at the beginning of every transfer circle and will be kept in either vacuum or Et/Pr gas mixture to avoid particle contamination. The Et/Pr liquid that comes in with the cassette when opening the cryogenic valve will be drained before pumping.

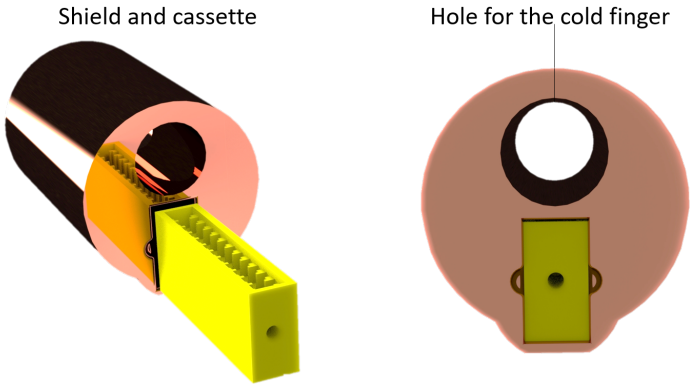

Figure 5.9: The shield and cassette

Components

The vacuum box is composed of:

- `A vacuum chamber`
  The vacuum chamber is connected to the cryogenic valve and the gate valve of the Delmicup to act as the relay station for the cassette to reach the shield and get into vacuum condition. The bottom plate of the chamber has a well adapting shape with the bottom of the shield to have a good thermal contact to cool down the shield with the LN2 below the bottom plate within the cooling chamber.

- `A LN2 chamber`
  Like the plunging bath, the vacuum box also has a double chamber structure to have the shield cooled by LN2. The LN2 inlet is connected to the LN2 chamber of the ethane bath.

- `A vent valve`
  A vent valve is attached to the vacuum box to balance the inner and outer pressure of the vacuum box before detaching the Delmicup from the vacuum box. The vent valve is connected with a LN2 source and will therefore not introduce contamination when venting.

- `The LN2 inlet/outlet`
  The LN2 chambers of the ethane bath and the vacuum box are connected with a LN2 hose, and eventually lead to the LN2 dewar.

Functions

- Preparation: the vacuum chamber can create a clean environment to be able to receive the cassette and the shield by purging the chamber with N2 to drive away the air with moisture and other particles. Then LN2 is added to the cooling box which can cool down the shield which will later add to the thermal mass of the cassette to keep it cool during the transfer. Then the copper shield is placed (after pre-treatment like ultrasonic bath

washing, high pressure washing to clean its surfaces) into the vacuum chamber from the opening where the Delmicup will be attached to. The side with the cassette cavity should be faced to the direction of the plunging bath to receive the cassette. Then the Delmicup is attached (with its gate valve closed) to the vacuum box.

- Cassette loading: when the Delmicup is docked, the cryogenic valve is ready to be opened to receive the cassette from the plunging bath. Open the cryogenic valve, let the liquid in the plunging bath flow into the vacuum chamber. The liquid level will be higher than the cryogenic valve. Then use the magnetic feedthrough to push the cassette through the cryogenic valve, the cassette will be inserted right into the cavity of the shield. Drain the cryogen and open the gate valve. Go on pushing the feedthrough rod to push the shield and cassette together to the Delmicup. Rotate the locking mechanism of the Delmicup to seal the cavity of the shield and lock it. Retreat the feedthrough and close the cryogenic valve.
- Vacuum generation: turn on the pump and wait until the pressure drops to 10^{-6}mbar and close the gate valve of the Delmicup.
- Venting: the pressure of the vacuum chamber remains low; it should be vented with N2 to reach atmosphere pressure to be able to detach with the Delmicup. Turn on the vent valve which is connected to a LN2 flask and slowly vent the chamber to atmospheric pressure. Now the Delmicup is ready to be detached and transferred.

5.2.3. Delmicup

Delmicup is a high vacuum transfer device made from stainless steel and aims for transferring the cassette with AutoGrids from the vacuum box to the airlock of the FIB/SEM and to the Autoloader of the TEM while passively and actively cooling down the samples.

In the old workflow, a Quorum sample transfer unit is used to fulfill similar functions, two AutoGrids in a shuttle are transferred each time and are kept in a pressure of around 10^{-3}mbar. The samples are constantly heated by radiation from the wall and conduction from a feedthrough rod.

The Delmicup, on the other hand, transfers 12 samples with the cassette each time. It shields the samples with a block of copper to protect them from contamination and heating. It can also actively cool the samples with a cold finger while providing a better sealing and can transfer samples with high vacuum.

Components

The components of the Delmicup are:

- A stainless-steel cup: the main part of the Delmicup is the cup body that keeps the cassette in vacuum. The cup is a cylinder of 10cm in diameter, 19cm in height, with a wall thickness of 4mm. The size and weight are small so that the operator can detach and move it to the next device with ease.
- A hollow, cold finger: at the bottom of the cup, a protruding hollow cylinder with a stage is designed to go through and hitch the shield by its hole. It can couple and lock the shield with a push-push mechanism. The hollow cylinder has good thermal conduction with the shield and the cooler finger to achieve good heat exchange during cooling.
- A rotary feedthrough lock: the locking mechanism is made by integrating a copper plate to the tip of a rotary feedthrough to cover the cavity of the shield and to protect the cassette from heat radiation and contamination. This mechanism is also attached at the bottom of the cup.
- A connecting base: the connecting base is designed to sandwich an insertable gate valve with the cup and create a tight connection with the vacuum box, it has a pin on its connection surface to lock the cup from rotation with reference to the vacuum box.
- A gate valve: the gate valve is sandwiched between the cup and the connection base to seal the Delmicup in high vacuum.

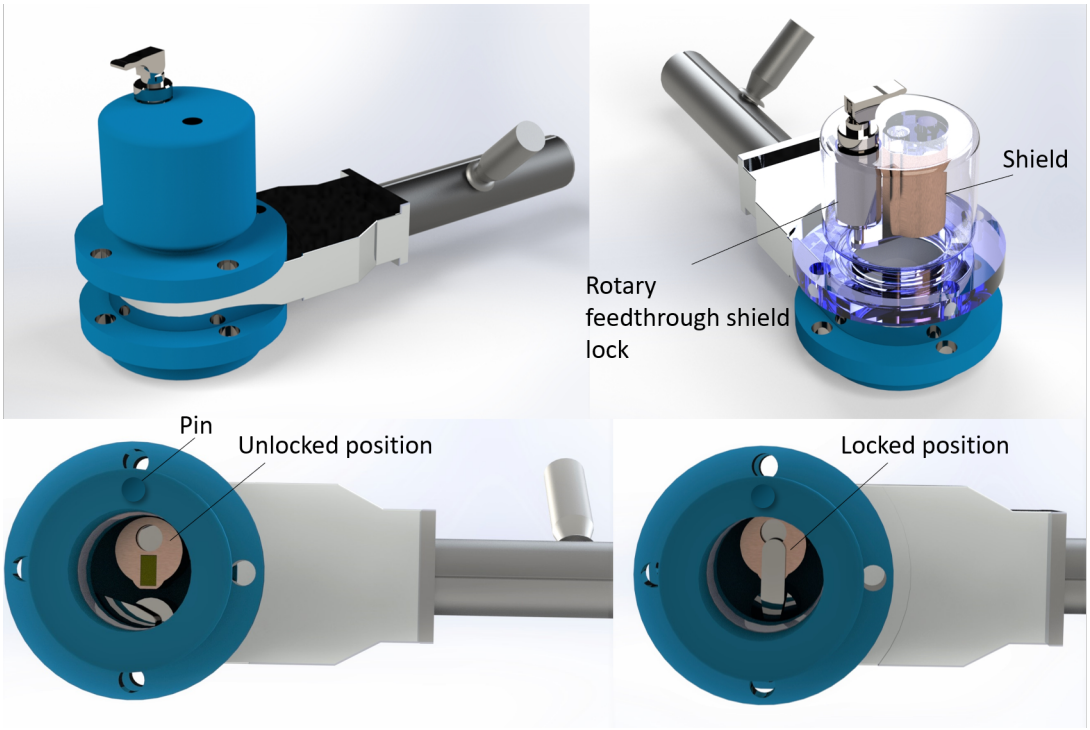

Figure 5.10: Delmicup

Functions

- Receiving the cassette: the Delmicup receives the cassette from the vacuum box. It can lock the shield and the cassette tightly and cover the opening of the shield. The cup can tolerate the high vacuum and the gate valve can seal and preserve the inner pressure of the cup.

- Transferring: the latch design enables the Delmicup to quickly attach and detach with its docking devices. After detaching from the vacuum box, the Delmicup can be moved freely to the next lab to have the cassette and samples transferred and imaged.

- Cooling: a cold finger can be attached to the Delmicup to cool down the shield and the cassette during FIB/SEM imaging process, the cooling can last up to 24 hours.

5.2.4. Cold head

The cold head is designed to be inserted into the hollow cylinder that reaches into the Delmicup and thermally connect with the shield to actively cool the cassette while the Delmicup is waiting at the airlock of the FIB/SEM. Imaging one sample can take around 2 hours and the whole imaging process can last up to 24 hours.

The shield is only able to passively keep the samples from devitrifying for limited time, while the active cooling can keep the samples intact for more than 24 hours. The copper, cold finger is designed with an inner tube circulated with LN2 and is connected with a LN2 pumping system. The finger does not feed through the vacuum cup but has a good thermal conduction between the long finger and the shield.

5.2.5. Engineering fit and connections

The tolerances for the holes and shafts in this design are listed in the table below according to ISO 286-2[5]:

Figure 5.11: Tolerances of the holes and shafts according to ISO 286-2

Hole	Shaft	Diameter	Category	Fit grade	Hole limits (10^{-6})	Shaft limits (10^{-6})
Cup hole 1	Rotary feedthrough	25mm	Location	H7/h6	+25 0	0 -16
Cup hole 2	Cold finger	13mm	Easy running	H9/e9	+53 0	-40 -53
Shield hole	Shaft in cup	16mm	Close running	H8/f7	+33 0	-20 -41
Shield cavity	Cassette	18.4mm	Easy running	H9/e9	+52 0	-40 -53

5.2.6. Off-the-shelf products

The off-the-shelf products used in this system are the pumping system (includes sensors and controllers), the cryogenic valve, the gate valve, the vent valve, the cryogen pump and the feedthroughs. Their detailed specifications are listed in appendix C.

Pump

The HiCube 30 Eco turbo pumping station by Pfeiffer Vacuum GmbH is used as the pumping system in this setup, it includes a turbo vacuum pump as the high vacuum pump and an MVP 015-2 as the back pump. The ultimate pressure this system can reach is $1\times10^{-7}mbar$, the pumping speed for N2 is 22L/s. The pump is connected to the vacuum box with DN 40 ISO-KF flanges.

Valves

- Vent valve: the vent valve controls the flow of N2 into the vacuum to increase the inner pressure of the vacuum box to atmospheric level for opening. The vent valve in this system is manufactured by Swagelok. The connection to the system is NW-16.
- Cryogenic valve: the cryogenic valve in this system is the C31W series cryogenic valve by Habonim. It can withstand high vacuum condition while being able to perform cryogenic shutoff. Its leakage is smaller than 1×10^{-8} Pam^3/s. The inlet has been modified into a pipe connection from the original flange according to ISO Specification 7/1 for the fluid-tight seal of the threads, to shorten the foot print of the connection[20]. The flange in the outlet is DN25 with bolts M10×4.

Table 5.1: Tapered thread

Pipe Size (inches)	Threads per Inch	Lead (mm)	Outside Diameter (mm)	Pitch Diameter (mm)	Minor Diameter (mm)
7/8	14	1.81	30.201	29.039	27.877

- Gate valve: this design adopts the Series 081 vacuum gate valve by VAT Group AG. Its leak rate is less than 1×10^{-10} Pa m^3s^{-1}.

Cryogen

The liquid ethane/propane mixture is used for creating vitreous ice in the grids and keep them cool while they are being transferred to the vacuum box and the Delmicup. The LN2 is used to cool the Et/Pr liquid in the plunging bath and the shield in the vacuum box. N2 is also circulated in the cold finger to actively cool the Delmicup. The pedal boosting pump is manufactured by MRCLAB and is able to pump LN2 to the chamber at 8L/min. LN2 is pumped to the outer chamber of the plunging bath and the vacuum box. The Et/Pr liquid is poured into the inner chamber of the plunging bath after the LN2 stops boiling.

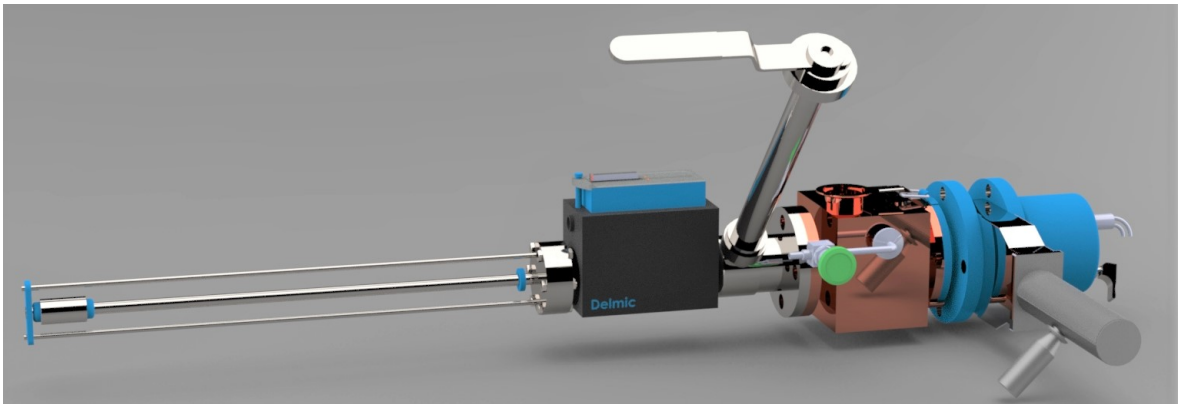

Figure 5.12: The assembly

5.3. Workflow

The new workflow is proposed as follows:

- Cleaning: clean all the devices and tools that are needed for the workflow. Bake the Delmicup, shield, cassette and the vacuum box at 150°C for 10 hours.
- Assembling: connect the plunging bath and the vacuum box with the cryogenic valve, connect the pump, vent valve, LN2 hose to the system. Rotate and cover the plunging bath with the grid plate. Close the cryogenic valve and close the gate valve of the Delmicup. Place the system under the vitrobot.
- Cryogen: start the LN2 pump, purge the vacuum box with N2. Wait until the LN2 stops boiling. After the chambers are cooled, rotate and open the grid plate, pour 1.6L Et/Pr liquid to the plunging bath. Insert the shield to the vacuum box and attach the Delmicup to the vacuum box, stop purging.
- Grid loading: place 12 grids to the grid loading chamber (in case of cultivating the bio-material directly in the grid loading chamber: pipette bio-materials to the grids and pour in the media, cultivate them until they are ready to be imaged). Push the grid loading chamber according to the reference scale to aim the right grid beneath the tweezer. Allow the tweezer to lower and reach the grid, push the fingers to fasten the clamping ring while the tweezer rises and retreat the fingers afterwards. Rotate the grid plate 90° clockwise.
- Plunge freezing: set the humidity and blotting force/time for the vitrobot, blot the grid and plunge it into the plunging bath at a depth of 2cm under the liquid.
- Clipping: go on lowering down the grid with the tweezer, the clipping mechanism then clips the grid.
- Loading: further lower the tweezer to load the AutoGrid into the cassette and repeat the steps from grid loading to loading the AutoGrids to the cassette 12 times until the cassette is fully loaded with AutoGrids.
- Transfer to the vacuum box: open the cryogenic valve, push the cassette to the vacuum chamber with the feedthrough rod until the cassette is fully fed into the shield. Now the Et/Pr liquid also half fills the vacuum box. Start the N2 purging and drain the Et/Pr liquid. Open the gate valve and push the cassette with the shield to the Delmicup, push it harder when it reaches the push-push lock to lock it there. Rotate the rotary feedthrough to seal the opening of the shield. Then pull back the feedthrough rod and close the cryogenic valve. Stop venting. The process is shown in figure 5.14.

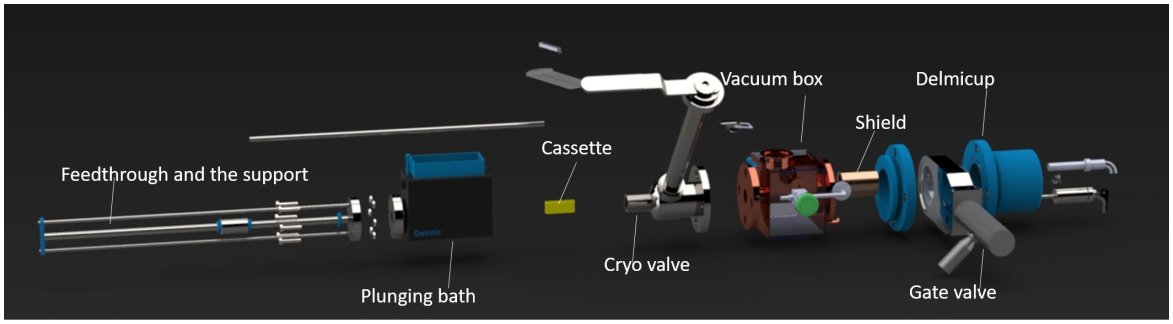

Figure 5.13: The exploded view

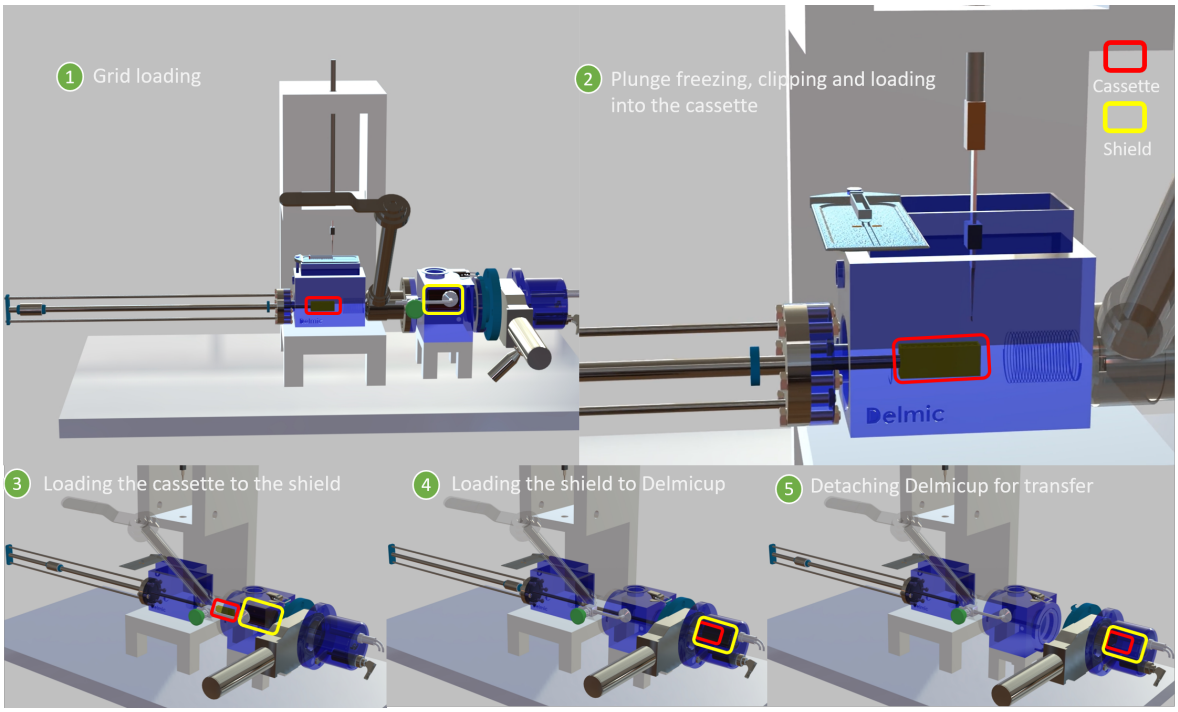

Figure 5.14: Transfer process

- Pumping: start the vacuum pump and pump the vacuum box and Delmicup to high vacuum, close the gate valve. Open the vent valve of the vacuum box and vent the box to atmospheric pressure with N2. Detach the Delmicup and transfer it to the airlock of the FIB/SEM. Connect and lock the two devices with the latches. Insert the cold finger to the Delmicup and actively cool it down.
- Imaging: pump the airlock to high vacuum, open the gate valves of the Delmicup and the imaging chamber. The robot arm takes away the cassette and individually move the AutoGrids to imaging stage. After all samples are imaged, the cassette with the samples is pushed back to the Delmicup by the robot arm. Rotate the rotary feedthrough and close the two gate valves. Vent the airlock to atmospheric pressure and detach the Delmicup.
- Transferring: transfer and dock the Delmicup back to the vacuum box. Push the station to the TEM lab. Vacuum the vacuum chamber and open the gate valve. Vent the Delmicup and vacuum bath with N2. Close the gate valve and detach the Delmicup.
- TEM imaging: transfer the Delmicup to the TEM, connect the Delmicup with the Autoloader and open the gate valve. The Auto loader will then take away the cassette and

image the samples in TEM.

5.4. Cost

Figure 5.15: Overall cost of the system

Item	Manufacturer	Price
Rotary feedthrough	Elastomer-sealed Rotary/Linear Feedthrough DS	€ 420.00
Feedthrough	Ferrovac MD40	€ 2,090.00
Pump system	HiCube ECO Dry Pumping Station	€ 6,668.00
LN2 pumping system	Small cryo pump	€ 300.00
Cryogenic valve	Habonim cryogenics valve	€ 600.00
Gate valve	VAT insertable Gate Valve	€ 1,000.00
Vent valve	Swagelok vent valve	€ 309.40
Manufacturing		€ 3,500.00
Total		€ 14,887.40

6

Results & Conclusions

6.1. Summary of results

6.1.1. Vacuum calculation

The vacuum box and the Delmicup are pumped by the Pfeiffer Hicube Eco vacuum station. The pump speed and other important parameters of the system are calculated as follows:

According to Eq.(A.10)- Eq.(A.12), the conductance of the duct (0.5m in length, 0.028m in diameter) is $9.994\times10^{-5}m^3/s$, the maximum pump speed is $1.339\times10^{-3}m^3/s$.

The gas leakage within the chamber consists of the degassing from the stainless steel walls and leaks in the connections of the cryogenic valve, the gate valve and the feedthrough. The outgassing rate of stainless steel after baking at 150°C for 10 hours is $3\times10^{-13}Pa\,l/s/cm^2$. Therefor the total gas load is $Q_1 = Q_{Stainlesssteel} + Q_{gatevalve} + Q_{cryogenicvalve} + Q_{feedthrough} = A_{stainlesssteel}q_{stainlesssteel} + 6\times10^{-10}Pa\,m^3/s + 1\times10^{-6}Pa\,m^3/s + 1\times10^{-11}Pa\,m^3/s = 1.785074\times10^{-5}Pa\,m^3/s$.

The ultimate pressure this chamber can reach is 8.038×10^{-6}Pa. The minimum time needed to pump down the vacuum chamber (with a volume of $8.304\times10^{-4}m^3$) is 8.308s.

6.1.2. Mechanical calculation

The COMSOL simulations of the Delmicup and the vacuum box are carried out to find out the mechanical strength of the designs. According to chapter A.3, the vacuum chamber shall have its stress generated anywhere at its body less than half of the yield strength of the material. The yield strength of stainless steel 304 is 205MPa.

The simulation of mechanical stress of the Delmicup in COMSOL simplified the shapes of the shield and the rotary feedthrough loaded on the cup to two cylinders. The deformation is calculated by setting the model to be linear elastic material. The bottom of the Delmicup is set as the fixed constraint, the pressure generated by vacuum is simulated by putting the pressure as the boundary load to the cup surface. The gravity of the cup is set to be vertical to the center line of the cup cylinder as the cup is in lying position when transferring the samples. The maximum Von Mises stress of the cup is 27MPa, much smaller than the limited value, the simulation results are shown in figure 6.1.

The simulation of the vacuum box is also simplified as the adapting shape of the bottom of the inner chamber is not structurally determining the support. A flat plate is used to replace the bottom. Linear elastic material is again set in the solid mechanics module. The gravity of the shield is set to be a boundary load of 10N to the bottom of the inner chamber. The vacuum pressure is set by applying a boundary pressure load of 10^5Pa to the inner chamber. The ultimate Von Mises stress of the chamber is 98.9MPa, the simulation results can be seen in figure 6.2.

6.1.3. Thermal analysis

AutoGrids in the new workflow are transferred in five main conditions: the preparation process in cryogen; the draining process in the vacuum box (-196.15°C, filled with Et/Pr gas

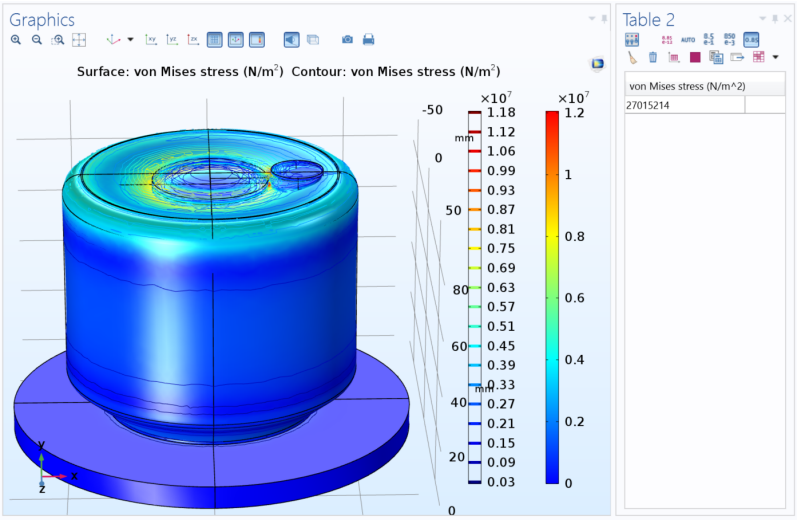

Figure 6.1: Von Mises stress of the Delmicup

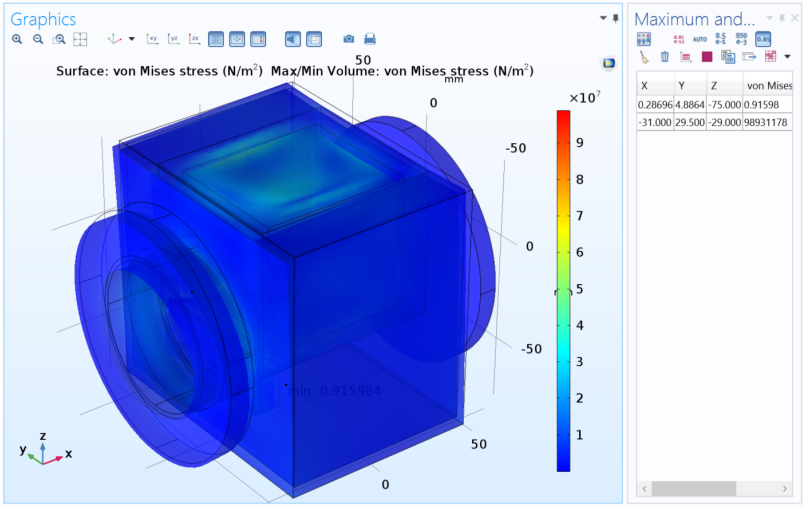

Figure 6.2: Von Mises stress of the vacuum box

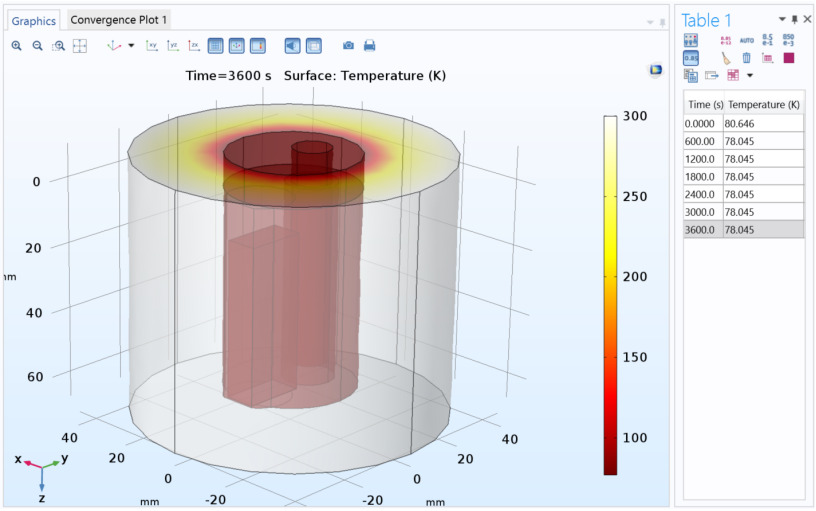

Figure 6.3: The thermal simulation results of the shield in the Delmicup

where the samples are shielded by the shield); the pumping process of the Delmicup (filled with Et/Pr gas where the samples are shielded by the shield); the high vacuum transfer process within the Delmicup and the actively cooled sample imaging process.

The thermal analysis therefore focuses on these five conditions and tries to find out how much the temperatures of the samples rise in each of these scenarios.

Preparation process in cryogen

The samples are safe from heating after being plunge-frozen to the beginning of the draining process. The temperature of the samples will remain at -196.15°C during this process.

Cryogen draining process

In this process, the cassette with samples and the shield are held in the vacuum chamber within the vacuum box. The vacuum chamber is constantly cooled by the LN2 beneath, it should hence remain at -196.15°C and create no radiation heat load over the shield. The environment is filled with Et/Pr gas, these molecules also absorb a small amount of heat while being pumped away.

Pre-pumping process

After the cryogen is drained, the shield is pushed to the Delmicup. The feedthrough rod is pulled out, the cryogenic valve and the vent valve are closed. Then the pump starts to pump down the pressure. The cassette and the shield are not cooled with cryogen anymore and hence start to receive irradiation from the Delmicup. This process takes around 15 seconds.

The numerical results of gaseous conduction heat load on the shield in this condition according to Eq.(A.4) is 2.450W, the radiation heat load is 3.791W. The COMSOL simulation on the radiation suggests the heat load of the shield is 3.588W. When added with the gaseous conduction heat load, the temperature rise of the cassette after 15s is 0.751°C.

High vacuum transfer process

When the pressure of the chambers reaches 10^{-6}mbar, the Delmicup is ready to close the gate valve and detach with the vacuum box. Then it can be taken to the FIB/SEM and attach to the airlock, this process takes around of 60 seconds.

The gaseous conduction is $\dot{q}_{gas} = 9.383\times10^{-5}$W, the radiation heat load starts with 3.791W, similar to the last case.

The COMSOL simulation on the radiation heat load is 3.587W. The temperature rise of the sample surface is 0.595°C after 60 seconds. In this situation, the ultimate time that the cup can keep samples from devitrification (the temperature of samples remains below -165°C), is 1156 seconds, which is around twenty minutes.

Active cooling process

During the process which starts from attaching the Delmicup to the imaging chamber to the robot arm successfully taking away and sending back the AutoGrids for imaging, the cold finger provides active cooling for the Delmicup all the time.

When simulating this case in COMSOL, a constant temperature of liquid nitrogen of -196.15°C is set at the interface of the cold finger and the cup. The cassette can be kept beneath -195.11°C by the cold finger.

The heat load of radiation and gaseous conduction will be further decreased slightly due to the cooling down of the cup body.

6.1.4. Results

The vacuum calculation suggests the pump down time and the ultimate pressure of the system. Ideally the pump can vacuum the chamber in a few seconds and the ultimate pressure is lower than that required by the system that can guarantee the partial pressure of water is low enough.

The mechanical analysis shows that the wall thickness, structure of the Delmicup, and the vacuum box are strong enough to withstand the high vacuum transfer process.

The thermal modeling investigates the thermal protection ability of the Delmicup over the AutoGrids during the transfer process. It quantifies the improvement of control on sample

Figure 6.4: Simulation results of the temperature of the cassette

Process	Cassette	Shield	Environment	Numerical results		COMSOL simulation results	
	Time			Gaseous conduction (W)	Radiation (W)	Radiation (W)	Temperature rise (°C)
Preparation	10min	\	Cryogen 77°C	\	\	\	\
Draining	3min	\	Cryogen 77°C	\	\	\	\
Pre-pumping	15s	Shielded within the cup	N2, normal pressure	2.450	3.791	3.588	-196.15~-195.40°C
High vacuum	1156s	Shielded within the cup	N2, 1×10^{-6}mbar	9.353×10^{-5}	3.791	3.587	-195.40~-165.15°C
Active cooling	24h	Shielded within the cup	N2, 1×10^{-6}mbar	9.353×10^{-5}	\	\	-165.15~-195.11°C

temperatures of the new workflow over that of the old workflow. The time dependent study under the 'heat transfer with surface to surface radiation' module suggests that the system can well protect the AutoGrids during the pumping and transfer between the vacuum box and the airlock of the FIB/SEM, also between the vacuum box and the Autoloader of the TEM.

The thermal modeling of the cassette with the shield within the actively cooled Delmicup suggests that the cooling power of the cold finger is sufficient to keep the AutoGrids at the required temperature. The time dependent study under the heat transfer module gives a reference to the to-be-achieved constant sample temperature of -195.11°C.

Due to limited computing capability and the lack of the detailed information of the shuttle, transfer unit and the cassette, the models in COMSOL are simplified. They are still valid versions of the original models that assume more critical conditions and generate rather conservative results as a reference.

In conclusion, the new workflow is safe and fast enough, it can transfer and protect the AutoGrids by actively and passively maintaining the temperature of the AutoGrids under -165°C at all times.

6.2. Conclusions

An integrated sample transfer system, which protects the samples from heating and contamination in the transfer process and is compatible with the interfaces of CLEM devices, has been designed to conquer the problem of low yield in sample imaging due to the problematic current sample transfer workflow.

These problems in the current CLEM workflow lie in the damage suffered by the delicate cryo samples which are caused by heating and contamination during the process of being transferred from the sample preparation device to the imaging chambers of the Focused Ion Beam Scanning Electron Microscopes (FIB/SEM) and Transmission Electron Microscopes (TEM).

The design of the new system to solve these problems is based on a thorough literary investigation on related topics and simulations to better understand the essence of the problems. The proposal of the research questions aims at creating a logical construction in solving the problems, which includes the research and the developing process, to identify the necessity, possibility and solution to create a better sample transfer workflow of CLEM. The relations between the project construction and these questions are:

- What are the reasons for developing new sample transfer systems?
  Answering this question helps in building a solid background in the current workflow and related technology, generating the problem statements and creating the project objective.

- What is the current market state of such systems?
  A bench marking of the sample transfer systems in the market focused on the vacuum transfer devices, blood sample storage devices, room-temperature EM sample transfer devices and the current cryo CLEM transfer devices works as a full case study of the industry solutions and suggests the potential of an integration in functionalities and gives a clear image of the ideal workflow.

- What functions will this system fulfill? What does the system infrastructure look like? What are the boundary conditions and application environment of this system?
  The boundary definition and system infrastructure give a clear guideline and large room of play for the requirements and solutions.
- What is the future vision and developing orientation of the system?
  Thinking of the future version offers a chance of checking for room of improvements especially the automation possibilities of the workflow in the future.
- Main question: what is the cheapest, easiest, most damage-free workflow for cryo sample transfer systems?

The answer to the main question leads to the final design of the new workflow, which consists of four main components to realize the transfer: a plunging bath for cryo loading and clipping of the grids that is directly attached to the vitrobot to utilize the up-down motion of its tweezer; a transfer cup to transfer the samples in high vacuum while passively/actively shielding and cooling them; a vacuum box that connects the plunge bath, the cup and the pump create vacuum conditions; a cooling rod that can be attached to the Delmicup and actively cool the samples.

The system takes over the samples from the preparation process within the vitrobot and can guarantee their safe transfer by using Delmicup. It can send them to be imaged through the airlock of FIB/SEM and then to the Autoloader of the TEM with minimum sample damage.

Compared to the old workflow which transfers samples in rough vacuum condition, the high vacuum Delmicup provides a much more stable and protected environment. Based on simulation results, the cup along with the shield can keep the samples from devitrification for a long time without active cooling, which is more than sufficient for transferring the Delmicup to FIB/SEM or to the TEM. This will enable the researcher to take breaks in between and provide tolerance to slight delays. While waiting at the airlock of the FIB/SEM, the cooling rod can take over the cooling, thereby controlling the temperature of the samples during the entire process.

The system is highly integrated to rely less on human operation and devices so that it reduces contamination, heating and errors induced by human handling and transfer between devices. Since the cassette is introduced early to carry and transfer 12 samples a time, the up-down motion of the vitrobot is effectively used to replace slow human handling in sample insertion. The push rod is designed to fulfill most motions between chambers under safe conditions, the throughput and efficiency is therefore largely increased. All the steps within the workflow are carefully designed to be minimum yet essential to eliminate the chance of sample contamination and heating. The amount of LN2 and ethane/propane mixture used in this system is considerably less than required by the old workflow and can be circulated, allowing the current workflow to be more environmentally friendly.

The Verification and Validation model (also called V model) and fast feed forward method are used to iterate and improve the design. The verification is largely based on the simulation results of the temperature preservation and the inspection of the system requirements.

The final design demonstrates its ability to keep samples safe during the whole workflow. The overall system is integrated, fast, more contamination-free, more stable in temperature and with a much higher throughput. With the new workflow, the yield of the transfer is expected to be increased from 10% to 90%.

7

Discussion & future work

7.1. Discussion

The new system is proposed with careful considerations, detailed simulations of the existing problems, and sound reasoning in choosing the best solution within the solution space generated. All the steps of the final solution are optimized and all the gaps without active controlling have been backed with simulations. The new system has apparent time, environment and throughput improvement over the old workflow, while guaranteeing the sufficient control of the AutoGrids during the entire transfer workflow. The workflow is a systematic solution to the sample transfer problem.

Side by side comparisons on the improvements of the new workflow over the old one are mapped with the problem statement and listed as follows:

1. Time consuming: in the old workflow, the FIB/SEM sample-loading is repeated 6 times.

   In the new workflow, 12 samples are prepared and transferred together. The repetition of the tweezer replacing, AutoGrids replacing and transferring between loading boxes as well as 6 times of pumping and venting are avoided.

2. Contamination: in the old workflow, AutoGrids are transferred through air every time when switching loading boxes.

   In the new workflow, mostly the AutoGrids are either in the cryogen environment (for around 7min), or in high vacuum conditions (for less than 5min) and shielded with the cassette and the shield. The process of pumping the vacuum box is operated in an Et/Pr gas environment and the AutoGrids are shielded.

3. Contamination: rough vacuum in the old transfer unit.

   The new workflow provides high vacuum transfer of 10^{-6}mbar.

4. Devitrification: no active cooling in the transfer unit.

   In the Delmicup, the cold finger can actively cool the cassette.

5. Damage: the old workflow involves a large amount of tweezer handling of the AutoGrids.

   The new workflow avoids tweezer operations after the plunging by cassette transferring, which avoids many damages caused by improper handling.

6. Misplacement: in the old workflow, human error can happen in placing AutoGrids in shuttle and in cassette, the order might be disrupted, for example.

   In the new workflow, the AutoGrids and grids are prepared in a row, mistakes are less likely to happen.

7. Damage: in the old workflow, frequently taking samples in and out of the LN2 may cause fracture of the ice due to the temperature fluctuation.

   The new workflow has only one time of taking AutoGrids out from cryogen.

7.2. Recommendations and future work

There are many research topics arising from the development process of this project and some of them remain unsolved:

Due to the limit in time and equipment, a lot of experiments, adaptations and automation opportunities have been left for the future work. Manufacturing the components according to high standards as POC (proof of concept models), for experiments is expected to take 8 weeks, excluding delivery time.

7.2.1. Components not yet realized

In the plunging bath, the cryogen might absorb heat from the grid plate and cool it down. The media inside the grid loading chamber might get frozen, even when there are only empty grids in the loading chamber, cooled grids have higher risk of particle contamination. Potentially some heating elements can be added to the plate in the future to heat up the plate.

The development of the auto-clipper is left as future work. It is an indispensable component in the new workflow, but the time required is out of scope since it needs many trials and errors for development. Some suggestions and guidelines are hereby proposed to help with the future work: this system holds the grid vertically with a tweezer therefore the clipping can be actuated vertically from both sides of the grid. One side is approached with a clip ring holder and the other side the AutoGrid holder. Together they push against each other and sandwich the grid to get the clipping done.

The difficult parts lie in the area where the tip of the tweezer is gripping the grid that blocks the sandwich motion and the continuity in feeding new C rings and AutoGrid rings to the holder. For example, the previous problem can be solved by redesigning the AutoGrids and leave a small groove at its periphery, the clip ring itself has a C shape and therefore does not need modification. Then the mechanism shall be able to correct the orientation of the C ring and AutoGrid ring to aim the grooves at the tip of the tweezer. This can be solved, for example, by gravity.

7.2.2. Automation of the system

The sliding of the grid loading box to aim the grid to be picked up right below the tweezer can be actuated with a linear motor. The rotation of the grid plate can be actuated by a rotary motor.

The fastening and unfastening of the clamping ring of the tweezer can be actuated since it is only a linear motion for the finger and a linear motor can be used.

As the workflow aims to be a cheap solution and the automation of these two steps is not strictly necessary, this part is also left as the future work.

7.2.3. Experiments on imaging result improvements

Figure 7.1: Metrics of success

Process	Rate of ice thickness growth (nm/min)	Time needed (min)	Total growth (nm)
Plunge freeze (Initial thickness)	/	/	20
Sample preparation	0.2	10	2
Pre-pumping	0.4	4	1.6
Vacuum transfer	1	3	3
FIB/SEM imaging	0.2	600	120
Transfer to TEM	0.2	120	24
Venting	0.5	10	5
Total			175.6

The metrics of success of the device are to create better images of Cryo samples and in-

crease the yield of the transfer. The imaging results are determined directly by the crystalline ice thickness on the sample, the less crystalline ice forms on the sample surface, the better the imaging results will be. An experiment on the ice thickness growth on each step of the old and new workflow and the comparison of imaging results of the two workflows can help to quantify the improvements of the new workflow.

However, the ice thickness detection on AutoGrids is complex enough to launch another research project. My fellow classmate, master student Alok Bharadwaj, is indeed working on a related project: water thickness detection on AutoGrids. His work will very likely to contribute to the future detection work of the ice thickness growth of the proposed system.

To verify

- The ice growth rate in different phase of the current workflow.
- The ice growth rate of the new workflow in the vacuum loading phase, FIB/SEM imaging phase, the transfer process.
- The imaging results improvements comparison.

Materials and equipment

FIB/SEM, LN2 dewar, heat exchanger, cold finger, AutoGrids, cassette, shield, pump station interface, ice thickness detector.

Data collections instruments and methods

- Double laser interferometry.
- Integration of the energy loss spectrum.
- Scattering outside the objective aperture.
- The most well-defined method is to collect a tomographic tilt series of the desired area, calculate a tomogram, and determine the local ice thickness across the reconstructed area, more time consuming.
- Tilting the sample to 30 degrees, milling a small hole through the ice, tilting to -30 degrees, and taking an image.
- Log-ratio method (Malis et al. 1998).
- FIB/SEM can measure it directly.

Procedures for conducting the experiment

Old workflow: Measure ice thickness growth in sample preparation & transfer & imaging with Quorum PP3006T transfer system.

New workflow: Measure ice thickness growth with Delmicup preparation workflow.

Compare the results of these two experiments.

7.2.4. Experiments on thermal-protection improvements

To verify

- The cooling down/heating up time of cassette, AutoGrids and shield.
- The thermal insulation of shield and Delmicup, the heat up time of AutoGrids when insulated by the shield and the Delmicup.
- The cooling effect of the cold finger, the thermal conduction of the structure.

Materials and equipment

Delmicup (with a temperature sensing feedthrough at its bottom) and shield, cassette, AutoGrids, LN2, Lakeshore DT-670E-BR.

Data collections instruments and methods

The data output of the temperature sensor placed inside the cassette.

Procedures for conducting the experiment

- Manufacture the shield, cold head, Delmicup and build the setup.
- Freeze the AutoGrids, cassette and the shield.
- Measure the temperature rise of the AutoGrids & AutoGrids within cassette & AutoGrids within cassette and shield over time.
- Measure the temperature change of the AutoGrids when being actively cooled by the cold finger, run the system for 24h non-stop.
- Decide whether more powerful cooling/shielding is needed. Iterate the experiments.

Appendix

The appendix includes the research topics (appendix A), the dimensions of the designed components (appendix B), the off-the-shelf products registration (appendix C), and the requirement risk identification (appendix D).

Appendix A includes the content of the literature research carried out in the beginning of this project, which covers the related topics that help to identify the necessity, possibility, and the solution space to create the final design.

Appendix B and C register the dimensions of the designed components and the specifications of the off-the-shelf products used in this system. They can offer a clear image of the size, footprint, and the details of the design. The off-the-shelf products in this system are chosen according to the system requirements and are available in the current market. Customers can choose or replace them with other products by using the specifications of this registration as a reference.

The detailed system requirements and risk matrix in appendix D work as the system design guidance and the standards of system verification and iteration.

A

Research topics

A.1. Cryogenics technology

The development of Cryo-CLEM is closely related to the cryogenics technology. The cryo sample properties, the refrigeration and cryo preservation techniques are essential topics to start with when designing cryo transfer systems.

Cryogenics technology deals with the refrigeration process and material properties at a temperature lower than 150K[34]. In the cryo-CLEM workflow, freezing samples with liquid nitrogen, ethane or mixture of ethane and propane changes the physical properties of the bio-materials. These liquid compounds used in CLEM are called cryogens. Cryogens are made of stable and simple molecules that only physically react with samples in most of the cases. When choosing a cryogen, density, specific heat, thermal conductivity, boiling points, critical points, and triple points are important parameters to be considered[56]. Liquid air, propane, LN2, Freon, liquid helium, liquid ethane, the mixture of ethane and propane and many other coolants have be experimented on their plunge cooling behavior since the early light microscopy exploring year in 1930's[56]. While ethane and later the mixture of ethane and propane were chosen as the plunge-freeze cryogen due to the fact that they cool down the sample much faster than others. Besides, their large thermal conductivity and close contact with the object freeze it effectively rather than forming a boiling vapor layer that separates the coolant with the sample like LN2.

These cryogens need to be condensed and maintained in LN2 which has a lower boiling point of -196°C[56]. LN2 is also used for cryo samples storage in order to provide long-term cooling at constant temperature. In some cases a pump is attached to the LN2 dewar for LN2 or N2 gas circulation. It is also normal to use a heat exchanger between the dewar and the system to be cooled so that the system can keep working with infrequent refills of cryogen. When it comes to precise temperature control, a cryo-cooler with temperature sensing feedback control would be a good replacement. To get an idea on the possible temperature controlling solutions for this project, a study on cryo cooler is listed below.

- `Cryo-cooler`
  The cryo coolers carry away the heat of the cooling objects actively by energy conversion to fulfill rapid refrigeration. Active coolers can provide more efficient, stable and faster refrigeration in EM applications. Most cryo coolers use a compressor and refrigerant such as a refrigerator to continuously fulfill thermodynamic circles (the cycle of conversion between heat and kinetic energy), four main types of cryo coolers following this principle include Stirling cooler, Gifford McMahon Cooler, pulse tube cooler and Joule-Thompson cooler. There is also the Peltier cooler that takes advantage of the heat flux between a junction of two different types of materials to transfer heat from one of its side to the other side to generate continuous cooling. The advantages and disadvantages of different types of coolers are listed in the table A.1 below.

  These coolers can bring temperature from 26.85°C to a few K with ease. When choosing the right cooling device for the project, the performance data, the cooling power, effi-

ciency, price, vibrations and influences on the system for the candidate coolers are all to be considered. Other considerations need to be taken are that if the cooler is to operate close to a CLEM device, it should create minimum vibration and parasitic influences to the system while working, otherwise, the cooler should only be working when the devices might get influenced are not functioning.

Table A.1: Advantages/disadvantages of different types of cooler technology[1]

Cooler	Temperature	Heat lift	Advantages	Disadvantages
Radiator	80 K	0.5 W	Reliable, low vibration, long lifetime	Complicates orbit
Cryogen	4 K	0.05 W	Stable, low vibration	Short lifetime, out-gassing
Stirling – 1 stage	80 K	0.8 W	Efficient, heritage	Vibrations
Stirling – 2 stage	20 K	0.06 W	Intermediate temp	Under development
Pulse tube	80 K	0.8 W	Lower vibrations	Lower efficiency than Stirling
Peltier	170 K	1 W	Lightweight	High temp, low efficiency
Joule-Thompson	4 K	0.01 W	Low vibrations	Requires hybrid design
Sorption	10 K	0.1 W	Low vibrations	Under development
Rev. Brayton	65 K	8 W	High capacity	Complex
ADR	0.05 K	0.01 mW	Only way to reach these temps.	Large magnetic field

- `Temperature sensor`
  Temperature sensors are important components in a temperature control system. By converting the temperature into electrical signals, temperature sensors can help the cryo system remain below the desired set point.

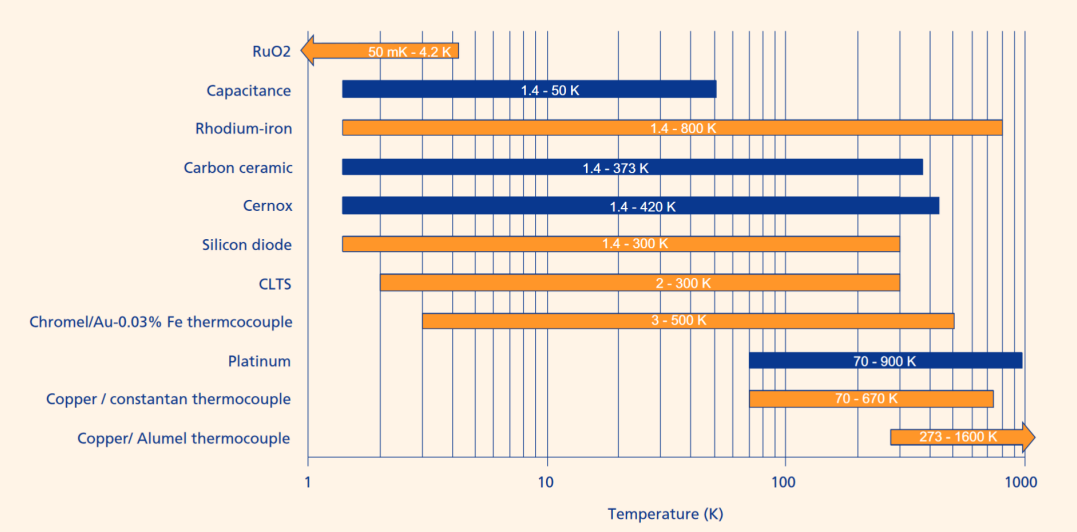

Figure A.1: Ranges of different temperature sensors[2]

  As the temperature range of the cryo-CLEM system starts from the constant temperature of LN2 of -196.15°C to room temperature, which is 27°C. Thermal couples, platinum sensors, CLTS, silicone diodes, Cernox, carbon ceramic sonsors and rhodium iron sensors can all cover the range. When choosing the temperature sensor for the transfer system, the dimension, sensitivity at cryo temperatures, reproducibility, tolerance of radiation, vacuum or magnetic field, self heating capabilities are to be considered.

- `Thermal isolation technique`
  To keep the temperature of the cryo sample stable and below the transition point effi-

[1] Table courtesy: Department of Engineering Science, University of Oxford in the online article "Cryocoolers for space applications ", `http://www2.eng.ox.ac.uk/cryogenics/research/cryocoolers-for-space-applications`

[2] Image courtesy: thermometry by Oxford Instruments,`https://www.oxinst.com/`

ciently and economically, a smart design of the system is needed to have good thermal isolation of the sample. When the cryogenic load is minimized, less cooling power is required when transferring samples.

To reduce thermal conduction load, reducing the conduction load of the structural support and connections, reducing the gaseous conduction of the samples by creating vacuum condition, and using multi-layer insulation to slow down the heat transfer are general considerations in the current systems.

To reduce radiation heat load, carefully considering the system configuration to exert minimum radiation load on the samples, shielding the sample with a large thermal mass to reduce radiation and temperature lift when exposed to a heat source or lowering the temperature of the outer chamber have been adopted in many industry applications[54].

- `Thermal Analysis`

Numerical analysis

The heat transfer computation is combined with the COMSOL simulation in this study. Samples undergo radiation heat transfer, conduction through gases and solids with the ambient and the transfer unit in the old workflow. In the new workflow, the shielded samples can have radiation heat transfer with the chamber wall in the non-vacuum and high vacuum regime.

The numerical calculation functions are listed below:

The heat conduction through a small element of a solid bar or tube is given as

$$\dot{q}_{cond} = \lambda\,(T)\,A dT/dx, \tag{A.1}$$

A is the area of the cross section and λ is the thermal conductivity of the material. When the cross section of the material is nearly uniform, this equation can be simplified as

$$\dot{q}_{cond} = (A/L)\,\bar{\lambda}\Delta\,(T)\,. \tag{A.2}$$

The computation of gaseous conduction can help predict the gaseous conduction heat load when the samples are transferred in environments like air or other gases. The gaseous conduction behaviors and calculations are divided into two different regimes: the hydrodynamic regime and the molecular regime. They are defined by the pressure range. The transition of the two regimes happens when the mean free path of the gas reaches the distance of the cold and the warm surface[17].

In the hydrodynamic regime, the gas heat conduction $\dot{q}_{gas}$ between two surfaces is estimated with the following equation:

$$\dot{q}_{gas} = \bar{\lambda} A \Delta T/d, \tag{A.3}$$

where $\bar{\lambda}$ is the mean value of the thermal conductivity of the gas between the two temperature boundaries as the thermal conductivity is time dependent, d is the distance and A is the surface area. This value is independent of pressure and is a low value due to the negligence of the convection currents[17].

In the molecular regime, the gas conduction of two concentric cylindrical surfaces is no longer related with the distance, so the $\dot{q}_{gas}$ is expressed as:

$$\dot{q}_{gas} = k a_0 P A_1 \Delta T[watts], \tag{A.4}$$

k is a constant given by White and Meeson in their book 'Experimental Techniques in Low-Temperature Physics[71]' , P is the pressure in the space and a_0 is the dimensionless number which is related to the accommodation coefficients of the inner and the outer surfaces and approximately equals 0.33 for common geometries of parallel plates[17].

The radiative heat transfer in the old and new systems is the biggest contributor to heat load on the samples. The net heat exchange between two surfaces generated from the Stefan-Boltzmann equation is:

$$\dot{q}_{rad} = \sigma E A \left(T_2^4 - T_1^4\right), \tag{A.5}$$

where σ is $5.67\times10^{-8} W/\left(m^2 K^4\right)$, E is a factor related to the surface emissivity of the two surfaces, whether their reflection type is specular or diffuse. For cylinders like the transfer unit in this project, the type of reflection does not matter, the value of E is given by:

$$E = \varepsilon_1 \varepsilon_2 / \left(\varepsilon_1 + \varepsilon_2 - \varepsilon_1 \varepsilon_2\right), \tag{A.6}$$

for specular reflection,

$$E = \varepsilon_2 / [\varepsilon_2 + (A_1/A_2)\,(\varepsilon_1 - \varepsilon_1 \varepsilon_2)], \tag{A.7}$$

for diffuse reflection.
A_1 and A_2 are the areas of the enclosed surface and the outer surface. ε_1 and ε_2 are the surface emissivities.

A.1.1. Simulation

The research on thermal simulation with COMSOL is carried out[38][53] to find out how fast the AutoGrids are heated, the necessity of integrating a shield or an active cooler to the transfer system, the heat load and cooling power needed for the cooling solution, and to make a clear comparison of the current transfer workflow and the proposed workflow.

COMSOL Multiphysics is a powerful finite elements analysis software for multiphysics simulation. It helps to create accurate models, and the testing of the temperature control capacity of the transfer system with COMSOL is of valuable reference importance in the verification and iteration process of the design phase.

The simulation will focus on the thermal simulation of samples in different conditions according to the current transfer workflow and the proposed workflow. The different pressure, handling tools, transfer device and humidity are all influencing the heating rate of the sample[44].

A.2. Anti-contamination technology

Airborne molecular contaminants are regarded as one of the biggest problems in fields such as electronic processing, semiconductor manufacturing, electron microscopy, and precision mechanisms especially when vacuum or ultra clean environments are involved.

- `Influence of Contamination`
  In electronic processing, contaminants are shorting adjacent lines, causing open circuits and shorting conducting layers[13][49][48]; In the semiconductor industry, contaminants can cause hazing of reticles and wafers, corrosion and unwanted doping[47]. In electron microscopy, the contaminants absorb as well as scatter electrons and may cause unwanted interference in imaging.

- `Contamination type and source`
  What kind of particle is considered a contaminant varies by field. In semiconductor facilities, water, aqueous acids, sulfur compounds, organic, oxidic and metallic particles, dust, O_2, CO, CO_2, C, hydrocarbons and even H_2 can be harmful to the system. In UHV or HV plants like a Quadrupole Ion Trap Mass Spectrometer[70], lubricant, silicone molecules, mineral oil and organic matters can all influence the sensitivity and performances of the device greatly[27]. When it comes to electron microscopes, many studies found that the main contaminants in the vacuum EM chambers are water vapor, vacuum grease, gaskets, organic molecules, grid materials, hydrocarbon molecules, pump oil, and adsorbed molecules like H_2, N_2, O_2 and CO[21].

Water vapor, according to Jesse Michael Labello in his article 'Water Ice Films in Cryogenic Vacuum Chambers', is by far the most prevalent species[36] in cryogenics vacuum chambers. The research on water contamination in vacuum condition has a rather long history. It has been 62 years since researchers started measuring the outgassing rate. The modeling of adsorption and desorption phenomena on technical and model surfaces has a history of 52 years, while the surface science measurement study started 37 years ago[16].

In general, contamination is introduced by three aspects in EM technologies: the operating process, equipment used, and imaging process. In the operating process, human operators are a major contamination source. For example, a breath can damage a cryo sample, a finger print takes a very long time for the pump to pump out and vibrations in operation can generate small flakes and deposit on vacuum surfaces. Equipment wise, traditional pumps that rely on pump oil and are not equipped with oil filters can suffer from back-streaming of oil to the vacuum chamber. Vacuum chamber walls, devices, and tools, when not baked or cleaned properly, constantly release particles to vacuum. Actually, all warm surfaces within vacuum chambers are contamination sources. Also, O-rings, used as a vacuum seal, have a leak rate of around 10^{-9}Pa l $s^{-1}cm^2$ and are the main cause of water permeation from ambient to vacuum chambers[72]. In sample imaging, the absorbed organic molecules of the sample, the electron source/ion source are all reacting with the samples and can cause large amount of unwanted particles[28][41].

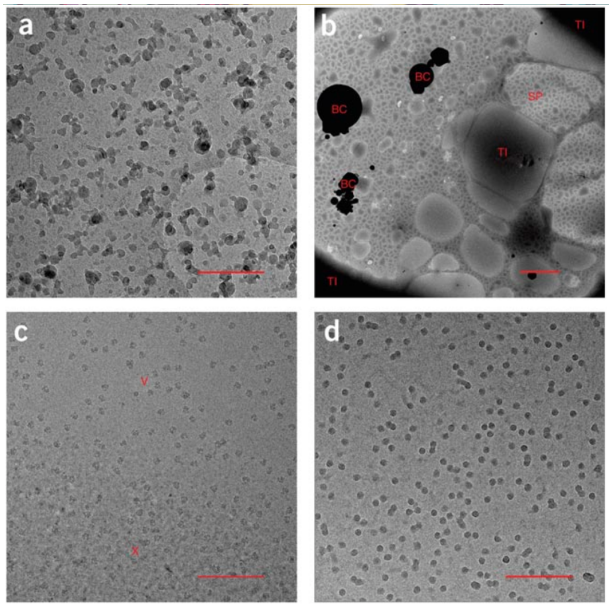

Figure A.2: Imaging results
(a) Ethane contamination, (b) Low-magnification cryo-EM image of a bad grid, (c) Vitreous and crystalline ice (d), Freeze-dried particles[3]

The contaminated imaging results are shown in figure A.2[24].

- Contamination sensor
  Many attempts have been made to monitor, prevent or reduce contamination: at ASML, for example, thermal desorption-gas Chromatography, mass spectrometric techniques, photoionization detection technique, line photo-ionization detector, chemiluminescent detector, gas chromatograph coupled to mass spectrometer are listed in the paper 'Contamination monitoring and control on ASML MS-VII 157-nm exposure tool[49]' to detect

[3]Image credit: Grassucci, Robert and Taylor, Derek and Frank, Joachim in their article 'Preparation of macromolecular complexes for cryo-electron microscopy', 2007

contamination in the system. When the water is the prevalent contaminants, interferometers, atomic force microscopes are used to detect the ice thickness to indicate the contamination.

- `Overview of anti-contamination technique`
  Anti-contamination solutions of CLEM can be implemented in five general directions

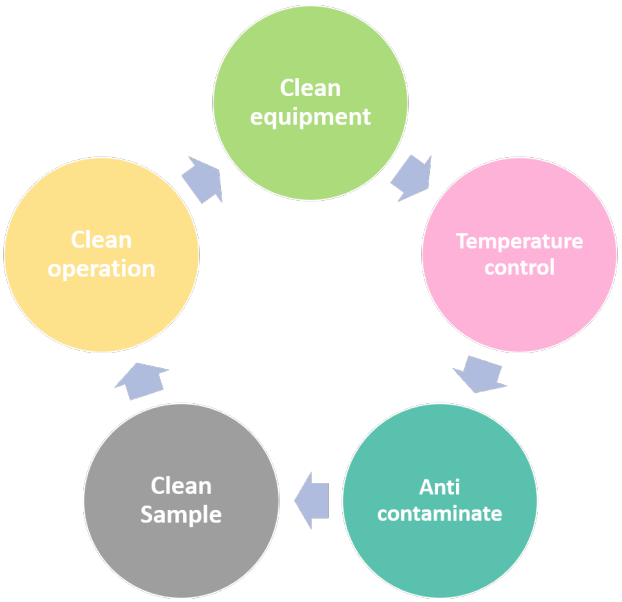

Figure A.3: Anti contamination solutions in EM

(see figure A.2): clean equipment, clean operation, clean sample, good temperature control and anti-contamination device. They can be easily mapped with the contamination source in EM technologies mentioned above. Clean equipment can be realized by pre cleaning the vacuum equipment with plasma, baking, purging with clean gas or fluid source, and clean storage.

As for clean operation, it can be slow venting/pumping[63][10][64], clean handling following operation instructions. To keep samples clean, charging or ion sputtering can help prevent a portion of particles from being attracted by the sample. Good temperature control will also prevent transition of amorphous ice into cubic ice or hexagonal ice that causes contamination of imaging.

Anti-contamination devices can be a separate reaction chamber or devices within the chamber like Plasma trapping devices, gas purifiers, air purifiers to get rid of the targeted contaminants. Specifically for cryogenic applications, a pump or a cold trap can also be used divert the particle flow away from the samples.

Anti contamination solutions in industry also show many possibilities.

The semiconductor industry uses high efficiency particulate air filter, on-board purge control units equipped with gas purifiers, tacky rollers and high voltage cleaning, laser ablation[6] and ion sputtering to keep the production of wafers clean. In some UHV plants, water cooled baffles or adapter baffles[31], N2 traps, reaction chambers, and cold wall reactors are used to generate clean environments. In EM applications, cold traps like two cold blades around the sample, cryo shields, washing the sample with methanol or ethanol overnight, heating the sample (also can be understood as secondary sublimation) and computational denoising methods[26], post processing to reconstruct the tomograms have been facilitated to get rid of contamination and improve the sample quality[32].

A.3. Vacuum technology

One of the most efficient way of reducing contamination is vacuum. In Vacuum transfer and imaging, the number of particles per cubic centimeter in the environment is reduced from 10^{19} (in atmospheric pressure), to 10^{10} when the pressure drops from atmosphere to 10^{-6}mbar which is defined as high vacuum. In the high vacuum regime, the partial pressure of water molecules, the most important contaminants for cryo samples, drops to a minimum level and helps to prevent sample damages. Two essential parameters of high vacuum regime should be mentioned: the mean free path of particles (the average distance that a particle can travel between two successive collisions with other particles[22]), is around 10 to 100 meters, and the Knudsen number (the ratio of the mean free path to the flow channel diameter can be used to describe types of flow[22]) is around 10^4 to 10^5. The gas flow with Knudsen number larger than 0.5 is defined as molecular flow regime, where many behaviors changes due to the disappearance of molecular interactions.

- Pumping water molecules in high vacuum

  The water molecules in a vacuum chamber come in three different sources: some molecules are filling the volume and the others are adsorbed in the wall surfaces and other objects, the rest is the molecules permeated from vacuum connections like O rings. When the pressure of a chamber is pumped down from atmosphere, three stages are exhibited (see table A.4):

Figure A.4: Pumping zones and their properties[4]

Zones	Major gas removed	Residual gas	H_2O	Source
Volume zone (Atm - 10^{-3}mbar)	Non-condensable gas filling the chamber is being removed.	Residual gas is still dominated by the volume gas filling the chamber	At 20^{-3} mbar, water vapor that has been adsorbed on the chamber's internal surfaces begins to slowly desorb	Non-condensable gas filling the chamber
Drydown Zone (10^{-3} – 10^{-6} mbar)	Air gases are vanishing, dry down desorbed H_2O.	H_2O (75%-85%) , 10^{-3} mbar H_2O, CO , 10^{-6} mbar	Water vapor makes up at least 98% of the total pressure.	H2O desorbed from internal surfaces, diffusion from hygroscopic materials.
Hydrogen zone (10^{-6} mbar - lower)	Remove H_2 mostly	H_20, CO, N_2, H_2	Little	Permeation, desorption

Pump down the chamber from atmosphere first involves with the volume zone, then the dry down zone and the hydrogen zone. In the volume zone, the pressure drops from atmosphere to 10^{-3}mbar, the non-condensable gas that fills the chamber are pumped away first, the partial pressure of water drops fast along with other particles in the volume. When the pressure reaches around 10^{-3}mbar, the drydown zone starts, most particles are dying down, water adsorbed in the walls start to desorb and water molecules become the main particles in the chamber, taking up around 98% of the remaining gas. When the pressure goes lower than 10^{-6}mbar, H2 becomes the main particle in the chamber as little water remains, these remaining water molecules are mainly permeated from connections like O rings and some come from constant desorption or diffusion[12].

- High Vacuum Pump

  A vacuum pump generates vacuum by removing the particles from the targeted chamber. There are three main types of vacuum pumps that work under different principles, all of which have different pumping effects: the momentum transfer pumps, the entrapment pumps, and the positive displacement pumps. Momentum transfer pumps such as turbo molecular pumps use high speed jets of dense fluid or high speed rotating

[4]Table courtesy: Phil Danielson in his article 'Pumping Specific Gases in High Vacuum', Normandale community college, http://www.normandale.edu/departments/stem-and-education/vacuum-and-thin-film-technology/vacuum-lab/articles/pumping-specific-gases-in-high-vacuum

blades to knock gas molecules out of the chamber to reach vacuum; The entrapment pumps like ion getter pumps capture gas particles from the chamber, they usually work as a second stage pump and start to reach lower pressure after the rough pump reduce the pressure to a certain level; Positive displacement pumps include mechanical pumps, rotary pumps and scroll pumps. They use a mechanism that repeatedly expands a cavity, allowing gases to flow in and exhaust them after sealing them off.

Not all the pumps can pump down and cover the whole pressure range from standard atmosphere to 10^{-6}mbar. The ion getters are designed for reaching 10^{-11}mbar, but it gets saturated easily when operating outside high vacuum conditions. Turbo molecular pumps too, operate at the range of 10^{-2} to 10^{-8}mbar. These two types of pumps therefore need rough pumps to pre-vacuum the chamber.

- `Vacuum gauge`
  To realize the control of vacuum pressure, vacuum gauges are used to feed back the pressure readout. Most vacuum gauges cannot measure the whole pressure range from atmosphere to high vacuum. For example, the hot-cathode ion gauge measures the pressure from 10^{-4} to 10^{-9}mbar. The cold cathode gauge has a measurement range of 10^{-2} to 10^{-14}mbar. Residual gas analyzers have a detection range between 10^{-4} and 10^{-14}mbar. The Pirani gauge measures pressure between 0.5 mbar to 10^{-4}mbar. Since none of these vacuum gauges above cover the whole range, a combination of multiple gauges can help cover the overall pumping process.

- `Vacuum chamber`
  The vacuum chamber design defines the boundary conditions of the sample protection device (inner and outer envelopes, operational constraints, etc.), it involves choosing the material, designing the parts, manufacturing and assembling these parts together and testing the structural strength[25]. Improper chamber design may result in gas leak, collapse, buckling, or even serious operating accidents.

  The chamber carries the cryo devices and samples, and it undergoes high vacuum pressure. Good material selection based on its creep data, fatigue limit, and fracture toughness should be considered carefully[25]. The most common materials used for vacuum chambers are austenitic stainless steels (316LN, 316L, 304L), aluminum alloys (5000 and 6000 series) and copper (OFHC, Glidcop)[25]. Also, since the radiation coming from the warm chamber to the cold surface of the sample will cause heating, special treatments of the inner wall may help with degassing and sample heating.

  Structurally, the stress generated by the loads everywhere of the chamber should remain in the elastic range. The safety factor applied to any buckling value must be at least 2.0 for outer jackets according to EN 13458-2, 3.0 by pressure vessel codes CODAP[25] The von Mises stress is kept to less than about half the material's yield strength. For stainless steel, the yield strength is 205MPa, for copper, it is 40MPa.

  An observation window might be needed if the loadlock and chamber are designed in a way that the cassette insertion is not visible and adds up the difficulty of cassette locking. The best shape for resisting external pressure is spherical dome, but due to the difficulty of manufacturing, a flat circular window is often the best option.

- `Valve and airlock`
  Valves are essential parts in a vacuum chamber to connect and isolate the whole transfer workflow and enable the transfer of the sample and the cassette. An airlock is made of two valves, a pre-chamber and a vacuum pump. When transferring a vacuum chamber, the chamber door is attached with one end of the airlock then the pre chamber is pumped down to the same pressure. When three chambers all have the same pressure the transfer is ready after the opening of the second valve.

  In the market, there is an airlock that is specially designed for cryo EM sample transfer: the Coolok developed by Quorum. It controls the separation automatically and can actively cool down the sample in the mean time.

- Pumping speed and ultimate pressure

The vacuum pumping speed and the ultimate pressure are important parameters for the designed pumping system. The pump and the vacuum chamber have a connection duct between them, which slightly lowers the pump speed of the vacuum chamber. The pressure drop in the duct for molecular flow is[17],

$$P_1 - P_2 = C^{-1}Q, \tag{A.8}$$

Q is the gas flow, C is the conductance of the duct, P_1 and P_2 are the pressures of the chamber and the pump. In laminar flow, the conductivity of a pipe is,

$$C_{pipe,lam} = \frac{\pi d^4}{256\eta l}(P_1 + P_2), \tag{A.9}$$

where d is the diameter of the duct, η is the dynamic viscosity of the gas and l is the length of the duct.

In the molecular regime, the conductivity is expressed as follows,

$$C_{pipe,mol} = C_{orifice,mol}P_{pipe,mol}, \tag{A.10}$$

where the $C_{orifice,mol}$ is the orifice conductivity, which is equal to,

$$C_{orifice,mol} = A\frac{\bar{c}}{4} = A\sqrt{\frac{kT}{2\pi m_0}}, \tag{A.11}$$

where k is the Boltzmann Constant, $1.381 \times 10^{-23} m^2 kgs^{-2}K^{-1}$. m_0, the mass of a N2 molecule is equal to $4.6511628\times10^{-23} kg$. The $P_{pipe,mol}$ is the mean probability, the following equation applies to the mean probability of the long round pipes,

$$P_{pipe,mol} = 4d/3l, \tag{A.12}$$

Then the $C_{pipe,mol}$ can be expressed as $A\sqrt{\frac{kT}{2\pi m_0}}4d/3l$[23].

With the conductance, we have the equation describing the chamber pumping speed:

$$\mathrm{S_{chamber}}=\mathrm{S_{pump}}[\mathrm{C}/(\mathrm{S_{pump}}+\mathrm{C})]=\mathrm{S_{pump}}/[1+(\mathrm{S_{pump}}/\mathrm{C})] < \mathrm{S_{pump}} \tag{A.13}$$

The maximum molecular flow rate can be generated from kinematic theory[17],

$$\mathrm{Q_{max}}= \mathrm{P}(\mathrm{k_B}T/2\pi m)^{1/2}A, \tag{A.14}$$

The maximum pumping speed is therefore expressed as[17],

$$S_{chamber,\max}=\mathrm{Q_{max}}/p = (\mathrm{k_B}T/2\pi m)^{1/2}A, \tag{A.15}$$

The ultimate pressure that a vacuum chamber[17] can reach is,

$$P_{ult}=\mathrm{Q_1}/S_{chamber}, \tag{A.16}$$

where Q_1 is the gas influx of leaks and permeation.

B

Dimensions

Figure B.1: Dimension of the Delmicup

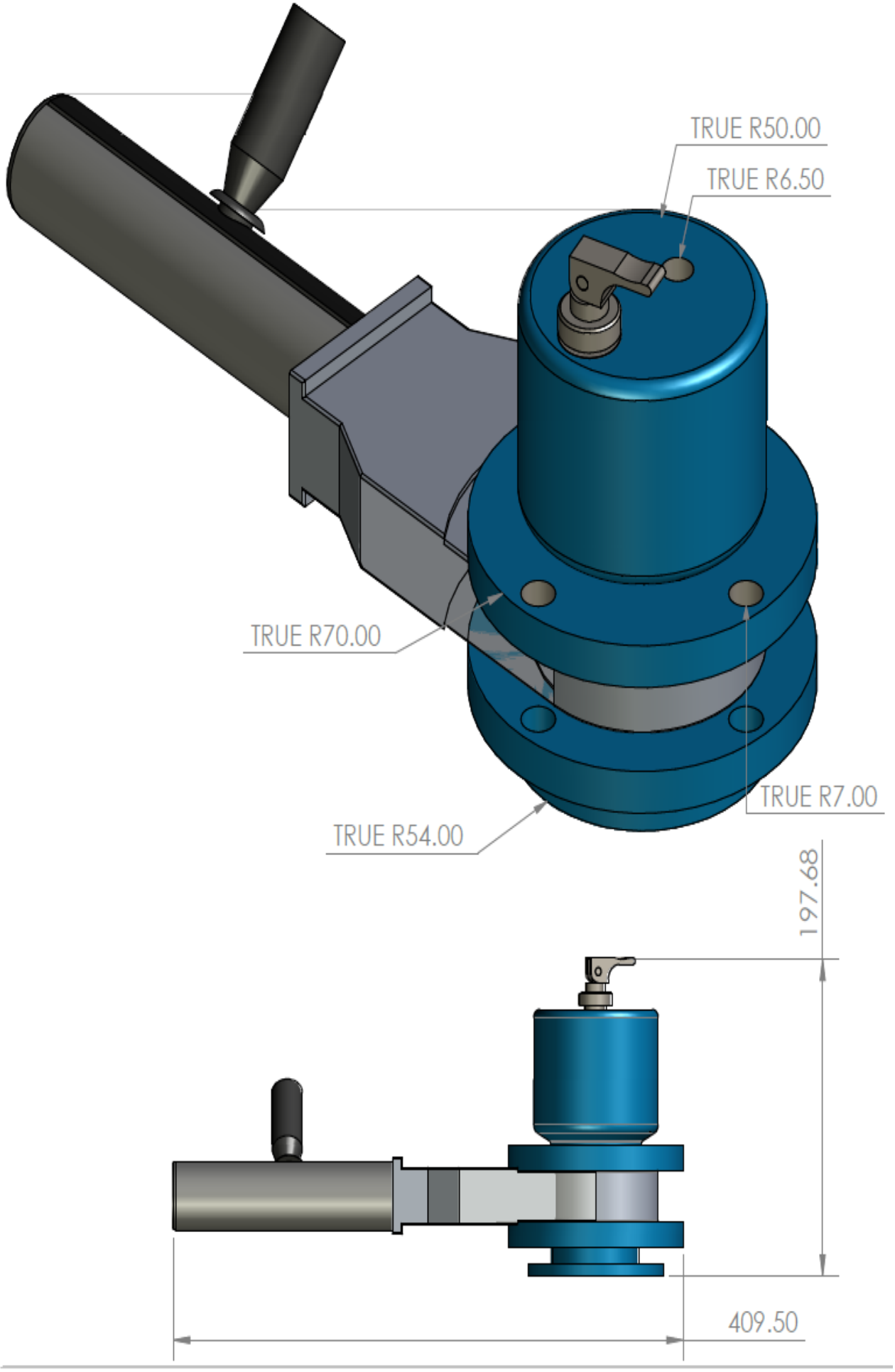

Figure B.2: Dimension of the plunging bath

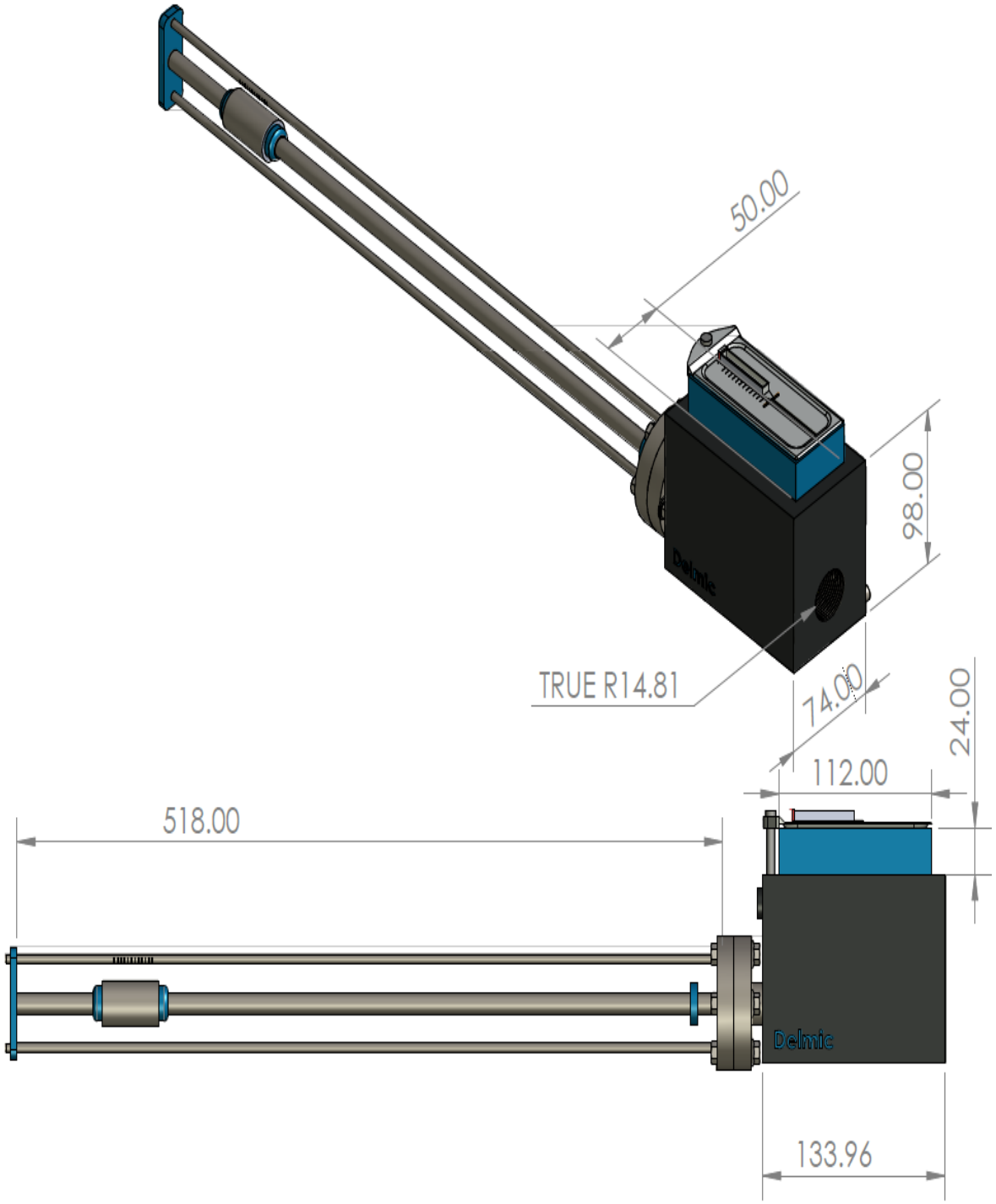

Figure B.3: Dimension of the vacuum box

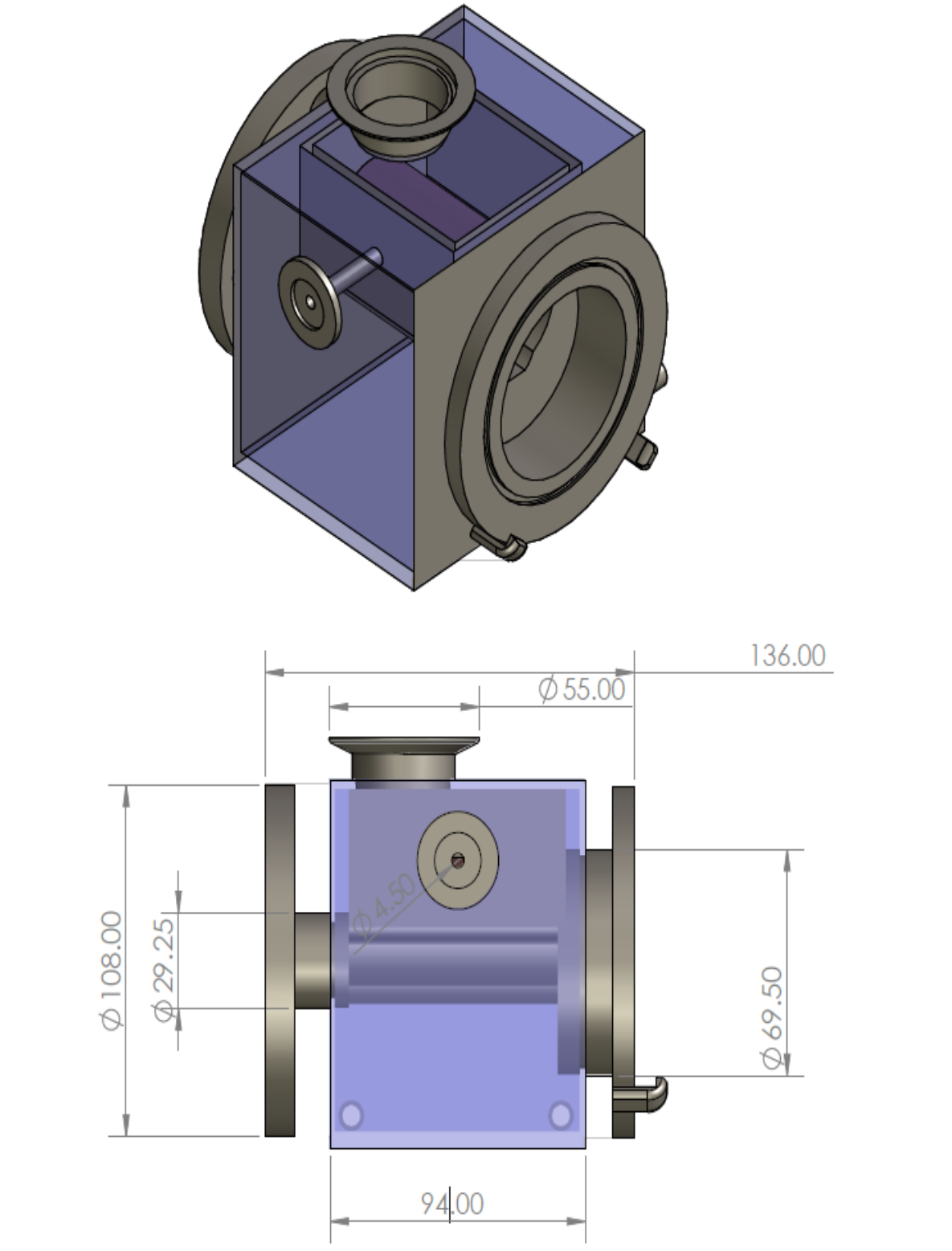

Figure B.4: Dimension of the assembly

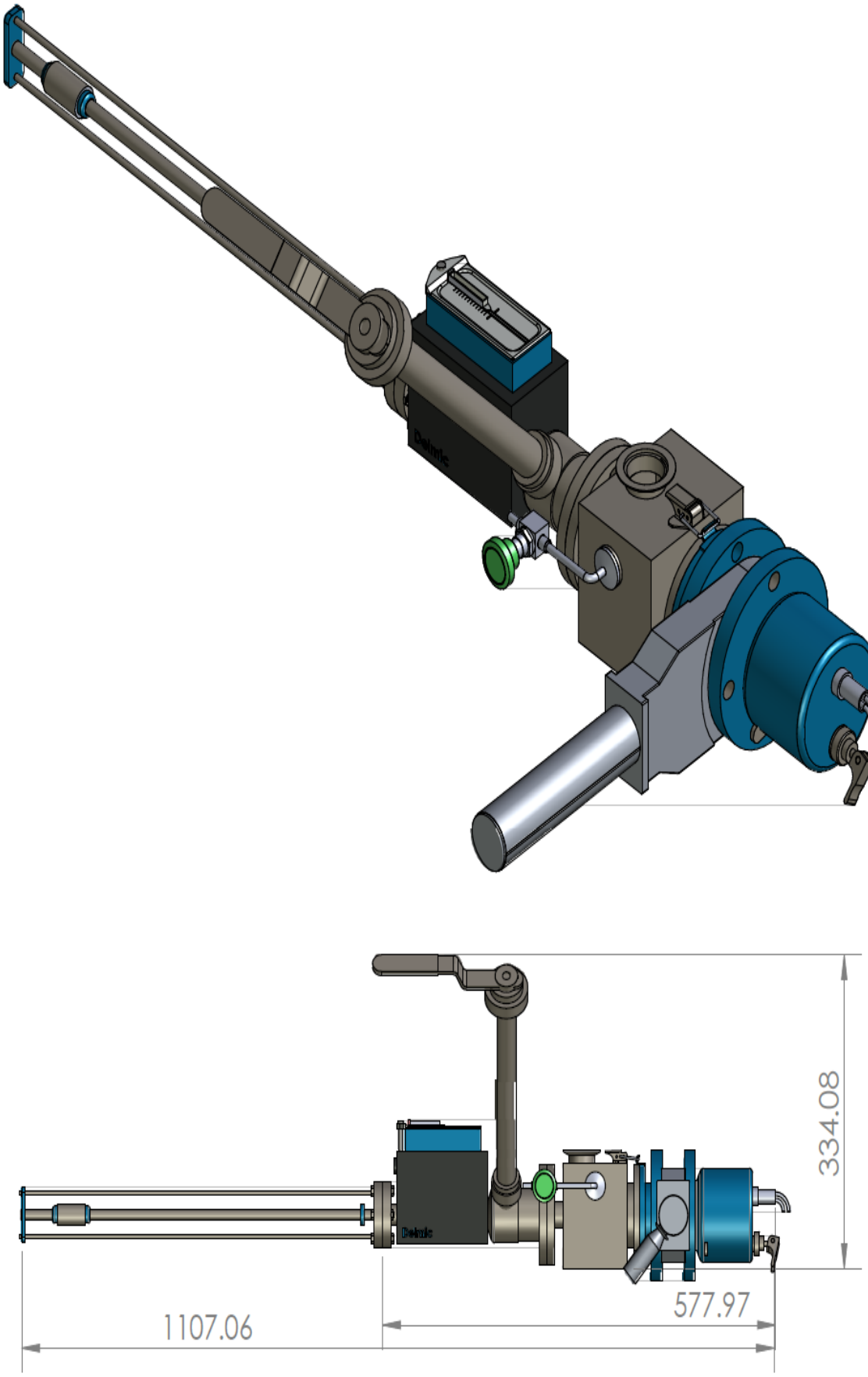

C

Off-the-shelf product registration

1. DS 040 A, Elastomer-Sealed Rotary/linear Feedthrough
   Specification:
   - Bakeout temperature: 110°C
   - Feedthrough: FPM shaft seals
   - Load capacity: torsion 20 Nm
   - Load capacity: radial at max. displacement 30 N
   - Material: housing aluminum; shaft: stainless steel
   - Nominal diameter: DN 40 ISO-KF
   - Operating temperature: max. 50°C
   - Pressure range: 1×10^{-8}mbar to ambient pressure
   - Seal: FKM
   - Shaft connection: M6× 10/ϕ 12 mm
   - Stroke: 150 mm
   - Weight: 0.8 kg
2. Ferrovac MD40 Linear Rotary Feedthrough
   Specification:
   - Linear travel: 400mm
   - Retracted shaft length: 30mm
   - Mounting flange: DN40CF
   - Linear force: 30N
   - Torque: 0.5Nm
   - Bakeout temperature: 150°C max.
   - Pressure range : 1×10^{-11}mbar to 1000mbar
   - Fully UHV compatible materials
3. MVP 015-2, HiCube 30 Eco pumping system
   Specification:
   - Backing pump: MVP 015-2
   - Cooling method: standard Air
   - Flange (in): DN 40 ISO-KF
   - Flange (out): Silencer, G 1/8”

- Mains requirement: 110 - 240 V AC, 50/60 Hz
- Power consumption: max. 170 W
- Pumping speed backing pump at 50 Hz: 1 m^3/h
- Pumping speed for N2: 22 l/s
- Sound pressure level: ≤ 50 dB(A)
- Turbopump: HiPace 30
- Ultimate pressure: < 1 $\times 10^{-7}$mbar
- Weight: 11.7 kg

4. `Pedal Auto-Boosting Liquid Nitrogen Pump ZYB-8`
   Specification:
   - Letting liquid pressure: 0.04 Mpa
   - Letting liquid velocity: 8 L/min
   - Liquid nitrogen consuming rate: < < 2.5%
   - Pedal frequency: 60 times/min
   - Weight: 7.51kg
5. `Habonim cryogenic valve C31C/C31W series Standard port`
   Specification:
   - Size: DN15
   - Pressure range: ANSI Class 150 | Vacuum 10^{-6}mbar to 20000 mbar
   - Body leakage: ≤ 1^{-8}Pam^3/s
   - Seal leakage: ≤ 1^{-8}Pam^3/s
6. `Series 081, Insertable gate valve, VAT`
   Specification:
   - Sealing technology: VATLOCK-System
   - Sealing Gate: FKM
   - Sealing Bonnet: FKM
   - Leak rate body: 1^{-9}mbar l/s
   - Leak rate seat: 1^{-9}mbar l/s
   - Nominal inside diameters (ID) in mm: 63
   - Material: Aluminum
   - Pressure range: 1^{-7}mbar to 1.6 bar (abs)
   - Differential pressure at opening: 30 mbar
   - Temperature:(Maximum values: depending on operating conditions and sealing materials) Valve Body ≤ 120°C
   - Weight: 2.2 kg
7. `N-Vision Optics NVAC-124, N2 purging kit`
   Specification:
   - Tank volume: 20 cubic feet
   - Dimensions: 63 ×51 ×23 cm
   - Weight (tank Empty): 15 kg

D

System requirements

Cryo transfer system requirements specifications

Revision History

Date	Who	Change
11/1/2019	X He	Initial version
8/2/2019	X He	First modification
23/2/2019	X He	Second modification
25/4/2019	X He	Third modification

Definitions

ID	Item	Definition	link
DEF01	Cryo transfer system	Standalone system combining	

Customer requirements

#	Requirement	Value	Unit	Justification	Verification measurement
General					
1	The user shall be able to easily operate with the system without assistance after simple training.			Lower the threshold and time cost of cryo research.	By design.
2	The system shall create a fast workflow with minimal actionable steps.				By design.
3	The transfer system shall keep the AutoGrids at a temperature lower than [value][unit].	108.0	K	To prevent samples from devitrification or fracturing.	Measure the T of the AutoGrid and it should be within the limit.
4	The system shall provide a vacuum level of [value][unit] in the main transfer device.	10^(-6)	mbar	To minimize the water and other particle contained in the transfer device and keep samples more contamination-free	Use vacuum gauge to measure the vacuum level within the transfer device.
5	The cassette shall not be exposed to non-vacuum/non-LN2 condition longer than [value][unit].	5.0	s	To avoid particle contamination during transfer/loading/unloading.	By design of the workflow.
6	All components of the transfer system that are completely or partially inside the vacuum chamber shall be made of vacuum compatible materials as listed in [value].	RD02		Prevent contamination of sample in vacuum system.	By design.
7	All operations of the workflow when the cassette is not in vacuum shall be carried out in protected environment.			To avoid particle contamination during transfer/loading/unloading.	By design of the workflow.
8	Any device that is directly connected with the targeted chamber shall not generate magnetic field larger than [value][unit].	1.0	T	To avoid influencing the magnetic field while imaging.	Measure the magnetic field.
9	Any device that is directly connected with the targeted chamber shall not generate vibration larger than [value][unit].			To avoid influence of performance of targeted chamber.	Measure the vibration generated by he cooler.
10	The system shall allow more slots for batch processing of AutoGrids and related tools.			To be able to prepare more samples at a time.	By design.
11	The system shall transfer the cassette with AutoGrids instead of individual AutoGrids.			To be able to integrate devices and increase throughput.	By design.
12	All devices of the system shall be supporting the whole workflow to operate for at least [value][unit] .	24.0	hr	To make sure the system keeps samples safe during the whole workflow.	
Delmicup					
13	The Delmicup shall have a dimension that allows space for the cassette, the shield and other necessary accessories.			To allow cooling, preparation of AutoGrids and accessories.	By design.
14	The Delmicup shall be able to be transferred to the targeted chamber which is at least [value][unit] away from the station.	10.0	m	To allow the Demicup travel from loading station to the FIB/SEM and TEM.	By design.
15	The Demicup shall be able to reach the same environment (pressure & temperature) required by the targeted imaging chambers.			To be able to connect with the targeted environment.	Measure the pressure and temperature within the Delmicup in steady state, they should be <108K and 10^-6mbar within hours.
16	The Delmicup shall have a weight lower than [value][unit].	5.0	kg	To guarantee the portability of the device, easily liftable for female researchers.	Weight the Demicup and it shall be less than 5kg.
17	The time for connecting Delmicup and station shall be within [value][unit].	5.0	sec	To ensure quick transfer	Measure the T needed for connection.
18	The Delmicup shall have a easy mechanism to connect with the shield that can be operated without assistance of extra tools or help, the time for connecting and locking shall be within [value][unit].	3.0	sec	To reduce contamination due to long time of loading and guarantee easy operation.	Measure the time needed for loading cassette and lock it into Delmicup, it should be less than required.

19	Th Delmicup together with the shield shall be able to keep the AutoGrids from devitrification for at least [value][unit].	2.0	hr.	To keep samples cooled during non-actively-cooled transfer between pumping statin to FIB/SEM.	Measure the dT, T of the cassette without cooling and it should be lower than required after two hours.
20	The Delmicup shall be integrated with cooling device and cool the samples during sample imaging.			To prevent samples from devitrification or fracturing.	The cooling solution should be detachable from the Delmicup and have good thermal connection with it.
21	The Delmicup shall have a least vacuum level of [value] [unit] during loading and transfer.	10^(-6)	mbar	To minimize particle contamination on the sample.	Measure vacuum pressure and mass spec of prototype.
22	The Delmicup shall have tight seal against leakage. The leaking rate shall be lower than [value] [unit].	1E-08	Torr l/cm^2 s	To reduce contamination in time gap.	Measure vacuum pressure and mass spec of prototype.
23	The Delmicup shall have a vacuum-tight connection to the docking station.			For vacuum transfer of the AutoGrids to the FIB/SEM.	By design.
24	The Delmicup shall be able to connect with the interface of Autoloader or have an adaptor to connect with the Autoloader.			For vacuum transfer of the AutoGrids to the TEM.	By design.
25	The orientation and depth of the cassette sitting within the Delmicup shall be the same as how the cassette is sitting in the Nanocup.			To allow the unloading of cassette by the Autoloader.	By design.
26	The Delmicup shall be able to reach same environmental condition as the targeted imaging chamber.			For transferring AutoGrids between devices	By design.
Sample preparation station (The plunging bath and the vacuum box)					
27	The station shall have space for clipping, loading, sample preparation, and temperature/contamination control devices and accessories.			To fulfill the integration of functions.	By design.
28	The LN2 loading station shall be able to cool down all the tools needed for cryo operation.			To fulfill the integration of functions of the loading boxes	By design
29	The station shall have space for all the cryo operations.			To provide space for all the cooling devices needed.	Every device shall be visible for operation and placed at handy places.
30	The AutoGrids shall always be cooled except when transferred with shield and the time shall not be longer than [value][unit].	1.0	hr.	To keep samples cooled during non-actively-cooled transfer between pumping statin to FIB/SEM.	By design.
31	The materials the station uses shall withstand the cryogenic temperature of [value][unit].	77.0	K	To avoid fracture and increase durability.	By design.
32	The vacuum box shall be equipped with a pumping system that can reach [value] [unit].	10^(-6)	mbar	To keep the particle density within vacuum at a tolerable level.	Measure vacuum pressure and mass spec of prototype.
33	The vacuum box shall be strong enough to bear the force generated by the external pressure.			To mechanically undertake the vacuum pressure.	By design.
34	The LN2 loading station shall have enough slots for batch processing of AutoGrids and related tools.			To be able to integrate devices and increase throughput.	By design.
Cold finger					
35	The cold head of the cooling device shall allow a motion from the vacuum box to the docking station of a distance [value][unit].	1.0	m	To allow the Demicup travel from loading station to the targeted chamber	By design.
36	The cooling system shall keep the sample at a temperature lower than [value][unit].	108.0	K	Sample has to remain fully vitrified	Measure dT, T from cryo cooler base to sample.
37	The cooling system shall be able to actively cool the [value].	Delmicup		To keep the cassette cooled during the imaging process.	Measure dT, T of the AutoGrids during 10h Delmicup cooling.
38	The cooling system shall be able to operate for at least [value][unit] after cooling down without refill or reconditioning.	10.0	hr.	Maximum time of sample loading and unloading to the cryo stage.	Perform up-time tests (5x)
39	The mounting of the cold head of the cooler shall be easy and shall not generate impact larger than [value] [unit] on the targeted system.			To avoid influence of performance of targeted chamber.	Measure the vibration generated by mounting cooler.
Shield					
40	The shield shall have a weight lower than [value][unit].	1.0	kg	For portability	Weight the shield and it should be less than 1 kg.
41	The shield shall have easy connection with the cassette that can be operated without assistance and the time needed shall not excess [value][unit].	3	sec	To enable quick & clean transfer	By design.
42	The shield shall keep the samples under [value][unit] when the cassette is not actively cooled by cooler or LN2.	108.0	K	To prevent devitrification during transfer that is not covered by active cooling.	Measure the dT, T of the AutoGrids in the cassette after 2 h without cooling, it should be lower than required.
43	The shield shall have a door that can shield the cassette after loading the cassette in position.			To prevent cassette from contamination in the Delmicup.	By design.
44	The cassette shall be able to connect & lock with the shield with the original pin mechanism.			To shield the cassette quickly and effectively.	By design.

E

Risk register

		Categories	Value	Probabilit	Impact	Certainty	Status
		Technical	1	<10%	0.05	<10%	Open
		Project	2	11-30%	0.1	11-30%	progress
		External	3	30-50%	0.2	30-50%	on hold
			4	51-70%	0.4	51-70%	closed
			5	>70%	0.8	>70%	
Keyword	**Description**	**Category**	**Probal**	**Impact**	**Certain**	**risk-factor**	**action**
Cold link	The cold link connects the N2 and the heat sink (shield). The force, surface area and shape all influence the heat transfer efficiency. We might not have very good thermal efficiency.	Technical	2	1	2	4.00	Check the engineering fits of the shield and the cassette and the cold finger with the cup body, make sure they have good thermal contact with each other.
Clamping mechanism	The force and contact points of the clamping mechanism in the Nanocup are unclear. It doesn't have good thermal conduction. We need to find out the force we need to clamp cassette tightly so that the thermal connection is good while the Autoloader can still take it out.	Technical /external	1	2	3	6.00	Cool down the cassette by wrapping it with the shield and cool down the shield with tight thermal contact.
Cold head	The cold head attaching to the Delmicup have the possibility of being damaged due to frequent transfer, we migh need to design a detachable cold head for the cooler.		1	4	3	12.00	Make the cold finger detachable and only use it when the transfer device is docked.
Shield	The shield shall have a externally controlled door that closes after inserting the cassette. But the feed through might introduce contamination.	Technical	3	1	2	6.00	Use feedthrough with less leakage and reduce the transfer time.
Vacuum gauge	Long term calibration is needed.	External	2	1	2	6.00	Choose stable gauges.
Valves	Leakage	External	4	1	2	8.00	Use metal seal rings and reduce time.
Competitors	While working on this project one of the competitors could bring out a new product which competes with the or has an impact on the workflow.	External	2	4	1	8.00	Design a cheap, reliable and versatile system.
Position	The locking mechanism of the cassette within the Delmicup should be losen to allow Autoloader and robot armto unload it. But firm grip is also needed for thermal conduction. A clever design is needed here.	Technical	2	3	1	6.00	Build a locking mechanism that can be easily controlled externally

List of Figures

Bibliography

[1] M. van Nugteren M.Schwertner D. Stacey R.I. Koning A. Kamp, H. Vader. Automated cryo-plunging for clem and cryo-fluorescence, 2018. URL http://www.focusonmicroscopy.org/2017/PDF/1367_Schwertner.pdf.

[2] C. A. Angell. Formation of glasses from liquids and biopolymers. *Science*, 267(5206): 1924–1935, mar 1995. doi: 10.1126/science.267.5206.1924.

[3] Robyn Aston, Kim Sewell, Travis Klein, Gwen Lawrie, and Lisbeth Grøndahl. Evaluation of the impact of freezing preparation techniques on the characterisation of alginate hydrogels by cryo-SEM. *European Polymer Journal*, 82:1–15, sep 2016. doi: 10.1016/j.eurpolymj.2016.06.025.

[4] Robyn Aston, Kim Sewell, Travis Klein, Gwen Lawrie, and Lisbeth Grøndahl. Evaluation of the impact of freezing preparation techniques on the characterisation of alginate hydrogels by cryo-SEM. *European Polymer Journal*, 82:1–15, sep 2016. doi: 10.1016/j.eurpolymj.2016.06.025.

[5] Roy Beardmore. ISO system of limits and fits, hole and shaft tolerances to iso 286-2. Online, January 2017. URL http://www.roymech.co.uk/Useful_Tables/ISO_Tolerances/ISO_LIMITS.htm.

[6] S. Becker, A. Pereira, P. Bouchut, F. Geffraye, and C. Anglade. Laser-induced contamination of silica coatings in vacuum. In Gregory J. Exarhos, Arthur H. Guenther, Keith L. Lewis, Detlev Ristau, M. J. Soileau, and Christopher J. Stolz, editors, *Laser-Induced Damage in Optical Materials: 2006*. SPIE, oct 2006. doi: 10.1117/12.696042.

[7] Isabell Begemann and Milos Galic. Correlative light electron microscopy: Connecting synaptic structure and function. *Frontiers in Synaptic Neuroscience*, 8, aug 2016. doi: 10.3389/fnsyn.2016.00028.

[8] Ariane Briegel, Songye Chen, Abraham J. Koster, Jürgen M. Plitzko, Cindi L. Schwartz, and Grant J. Jensen. Correlated light and electron cryo-microscopy. In *Methods in Enzymology*, pages 317–341. Elsevier, 2010. doi: 10.1016/s0076-6879(10)81013-4.

[9] E. F. Burton and W. F. Oliver. The crystal structure of ice at low temperatures. *Proceedings of the Royal Society A: Mathematical, Physical and Engineering Sciences*, 153(878): 166–172, dec 1935. doi: 10.1098/rspa.1935.0229.

[10] Degang Chen and Susan Hackwood. Vacuum particle generation and the nucleation phenomena during pumpdown. *Journal of Vacuum Science & Technology A: Vacuum, Surfaces, and Films*, 8(2):933–940, mar 1990. doi: 10.1116/1.576899.

[11] Jae-Hee Chung and Ho Min Kim. The nobel prize in chemistry 2017: High-resolution cryo-electron microscopy. *Applied Microscopy*, 47(4):218–222, dec 2017. doi: 10.9729/am.2017.47.4.218.

[12] Phil Danielson. Pumping specific gases in high vacuum. Online, 2019. URL http://www.normandale.edu/departments/stem-and-education/vacuum-and-thin-film-technology/vacuum-lab/articles/pumping-specific-gases-in-high-vacuum.

[13] A. J. de Jong, J. C. J. van der Donck, T. Huijser, O. Kievit, R. Koops, N. B. Koster, F. T. Molkenboer, and A. M. M. G. Theulings. Contamination control: removing

small particles from increasingly large wafers. In Alexander Starikov, editor, *Metrology, Inspection, and Process Control for Microlithography XXVI*. SPIE, mar 2012. doi: 10.1117/12.916366.

[14] Jacques Dubochet. On the development of electron cryo-microscopy (nobel lecture). *Angewandte Chemie International Edition*, 57(34):10842–10846, jul 2018. doi: 10.1002/anie.201804280.

[15] Jacques Dubochet, Marc Adrian, Jiin-Ju Chang, Jean-Claude Homo, Jean Lepault, Alasdair W. McDowall, and Patrick Schultz. Cryo-electron microscopy of vitrified specimens. *Quarterly Reviews of Biophysics*, 21(02):129, may 1988. doi: 10.1017/s0033583500004297.

[16] H. F. Dylla. The problem of water in vacuum systems, 2006. URL https://cas.web.cern.ch/sites/cas.web.cern.ch/files/lectures/platjadaro-2006/dylla-2.pdf.

[17] Jack Ekin. *Experimental Techniques for Low-Temperature Measurements*. Oxford University Press, oct 2006. doi: 10.1093/acprof:oso/9780198570547.001.0001.

[18] EMS. Cryo-sem & cryo-fib/sem preparation techniques & applications, 2017. URL https://www.emsdiasum.com/microscopy/products/brochures/2015/EMS_CryoSEM_Brochure2015.pdf.

[19] EMS. Quantifoil® holey carbon films, electron microscopy sciences, 2018. URL https://us.vwr.com/store/product/12360609/quantifoil-holey-carbon-films-electron-microscopy-sciences.

[20] Tools Engineering ToolBox Resources, Basic Information for Engineering, and Design of Technical Applications! Iso 7 - pipe threads where pressure-tight joints are made on the threads. Online, 2004. URL https://www.engineeringtoolbox.com/iso-threads-d_752.html.

[21] Jose-Jesus Fernandez, Ulrike Laugks, Miroslava Schaffer, Felix J.B. Bäuerlein, Maryam Khoshouei, Wolfgang Baumeister, and Vladan Lucic. Removing contamination-induced reconstruction artifacts from cryo-electron tomograms. *Biophysical Journal*, 110(4):850–859, feb 2016. doi: 10.1016/j.bpj.2015.10.043.

[22] Pfeiffer Vacuum GmbH. Introduction to vacuum technology. Online resource, 2019. URL https://www.pfeiffer-vacuum.com/en/know-how/introduction-to-vacuum-technology/fundamentals/molecular-number-density/.

[23] Pfeiffer Vacuum GmbH. Pfeiffer. Online, 2019. URL https://www.pfeiffer-vacuum.com/en/know-how/introduction-to-vacuum-technology/fundamentals/conductance/.

[24] Robert Grassucci, Derek Taylor, and Joachim Frank. Preparation of macromolecular complexes for cryo-electron microscopy. *Nature protocols*, 2:3239–46, 02 2007. doi: 10.1038/nprot.2007.452.

[25] C. Hauviller, CERN, Geneva, and Switzerland. Design rules for vacuum chambers. *Online*, 1999. URL http://edge.rit.edu/edge/P14651/public/Miscellaneous/Design%20rules%20for%20vacuum%20chambers.pdf.

[26] R. Henderson. Avoiding the pitfalls of single particle cryo-electron microscopy: Einstein from noise. *Proceedings of the National Academy of Sciences*, 110(45):18037–18041, oct 2013. doi: 10.1073/pnas.1314449110.

[27] L. Holland, L. Laurenson, and C. Priestland. Contamination in ultra-high vacuum plant. *Review of Scientific Instruments*, 34(4):377–382, apr 1963. doi: 10.1063/1.1718370.

[28] Jeromy Hollenshead and Leonard Klebanoff. Modeling radiation-induced carbon contamination of extreme ultraviolet optics. *Journal of Vacuum Science & Technology B: Microelectronics and Nanometer Structures*, 24(1):64, 2006. doi: 10.1116/1.2140005.

[29] M J Kääb, Robert Richards, P Walther, Iolo Gwynn, and Hubert Nötzli. A comparison of four preparation methods for the morphological study of articular cartilage for scanning electron microscopy. *Scanning microscopy*, 13:61–70, 01 1999.

[30] Rainer Kaufmann, Pascale Schellenberger, Elena Seiradake, Ian M. Dobbie, E. Yvonne Jones, Ilan Davis, Christoph Hagen, and Kay Grünewald. Super-resolution microscopy using standard fluorescent proteins in intact cells under cryo-conditions. *Nano Letters*, 14(7):4171–4175, jun 2014. doi: 10.1021/nl501870p.

[31] Jung Hyeun Kim, Christof Asbach, Se-Jin Yook, Heinz Fissan, Kevin J. Orvek, Arun Ramamoorthy, Pei-Yang Yan, and David Y. H. Pui. Protection schemes for critical surface in vacuum environments. *Journal of Vacuum Science & Technology A: Vacuum, Surfaces, and Films*, 23(5):1319–1324, sep 2005. doi: 10.1116/1.1978890.

[32] Tomio KUBO, Yoshihiro SATOH, and Yoshio SAITO. Outgassing rate measurement of the electrical cables and the elastomer/plastomer materials. *SHINKU*, 41(3):217–221, 1998. doi: 10.3131/jvsj.41.217.

[33] Max Kush. The statement problem. *Quality Progress*, June 2015.

[34] Myer Kutz, editor. *Mechanical Engineers' Handbook*. John Wiley & Sons, Inc., nov 2005. doi: 10.1002/0471777471.

[35] Jesse Michael Labello. *Water ice film in cryogenic vacuum chambers*. PhD thesis, University of Tennessee, 2011. URL `http://trace.tennessee.edu/utk_graddiss/1201`.

[36] Jesse Michael Labello. *Water Ice Films in Cryogenic Vacuum Chambers*. Doctoral dissertations, University of Tennessee, Knoxville, jlabello@utsi.edu, December 2011. URL `http://trace.tennessee.edu/utk_graddiss/1201`.

[37] European Molecular Biology Laboratory. Sample preparation - embl, 2018. URL `https://www.embl.de/services/core_facilities/em/services/sample_prep`.

[38] Octave Levenspiel. *Engineering flow and heat exchange, third edition*. Springer US, 01 2004. doi: 10.1007/978-1-4899-7454-9.

[39] Shuoguo Li, Gang Ji, Yang Shi, Lasse Hyldgaard Klausen, Tongxin Niu, Shengliu Wang, Xiaojun Huang, Wei Ding, Xiang Zhang, Mingdong Dong, Wei Xu, and Fei Sun. High-vacuum optical platform for cryo-CLEM (HOPE): A new solution for non-integrated multiscale correlative light and electron microscopy. *Journal of Structural Biology*, 201(1): 63–75, jan 2018. doi: 10.1016/j.jsb.2017.11.002.

[40] David T. Limmer and David Chandler. Theory of amorphous ices. *Proceedings of the National Academy of Sciences*, 111(26):9413–9418, may 2014. doi: 10.1073/pnas.1407277111.

[41] Xiulan Ling and Shenghu Liu. Laser-induced thermal damage simulations of optical coatings due to intercoupling of defect and organic contamination. *IEEE Photonics Journal*, 10(4):1–7, aug 2018. doi: 10.1109/jphot.2018.2848619.

[42] Thomas Loerting1 and Nicolas Giovambattista2. Amorphous ices: experiments and numerical simulations. In *JOURNAL OF PHYSICS: CONDENSED MATTER*, Department of Chemical Engineering, Princeton University, Princeton, NJ 08544, USA, November 2006. Institute of Physical Chemistry/Institute of General, Inorganic and Theoretical Chemistry, University of Innsbruck, Innrain 52a, A-6020 Innsbruck, Austria 2 Department of Chemical Engineering, Princeton University, Princeton, NJ 08544, USA. doi: 10.1088/0953-8984/18/50/R01. URL `stacks.iop.org/JPhysCM/18/R919`.

[43] JEOL Ltd. Introducing the alto series (cryo systems), 2011. URL https://www.jeol.co.jp/en/.

[44] A. F. Mills. *Basic Heat and Mass Transfer: Pearson New International Edition*. Pearson Education Limited, 2013. ISBN 1292042486. URL https://www.ebook.de/de/product/33627737/a_f_mills_basic_heat_and_mass_transfer_pearson_new_international_edition.html.

[45] O. Mishima, L. D. Calvert, and E. Whalley. An apparently first-order transition between two amorphous phases of ice induced by pressure. *Nature*, 314(6006):76–78, mar 1985. doi: 10.1038/314076a0.

[46] Antonis Nanakoudis. Sem and tem: what's the difference?, 2018. URL "https://blog.phenom-world.com/sem-tem-difference".

[47] John F. O'Hanlon and Harold G. Parks. Impact of vacuum equipment contamination on semiconductor yield. *Journal of Vacuum Science & Technology A: Vacuum, Surfaces, and Films*, 10(4):1863–1868, jul 1992. doi: 10.1116/1.577760.

[48] John F. O'Hanlon and Harold G. Parks. Impact of vacuum equipment contamination on semiconductor yield. *Journal of Vacuum Science & Technology A: Vacuum, Surfaces, and Films*, 10(4):1863–1868, jul 1992. doi: 10.1116/1.577760.

[49] Uzodinma Okoroanyanwu, Roel Gronheid, Jan Coenen, Jan Hermans, and Kurt G. Ronse. Contamination monitoring and control on ASML MS-VII 157-nm exposure tool. In Bruce W. Smith, editor, *Optical Microlithography XVII*. SPIE, may 2004. doi: 10.1117/12.536440.

[50] Jon Orloff. Fundamental limits to imaging resolution for focused ion beams. *Journal of Vacuum Science & Technology B: Microelectronics and Nanometer Structures*, 14(6):3759, nov 1996. doi: 10.1116/1.588663.

[51] Tim Palucka. Overview of electron microscopy, 2002. URL https://authors.library.caltech.edu/5456/1/hrst.mit.edu/hrs/materials/public/ElecMicr.htm.

[52] Acta Radiologica. Theoretical and technical considerations. *SAGE Publications*, Original Series, Volume 39(103 Suppl):15–22, may 1953. doi: 10.1177/0284185153039s10303.

[53] Michiel Klep Randy van Eck and Jos van Schijndel. Surface to surface radiation benchmarks * eindhoven university of technology *corresponding author: P.o.box 513 eindhoven, netherlands, a.w.m.schijndel@tue.nl. 2016.

[54] Jr. Ronald G. Ross. Refrigeration systems for achieving cryogenic temperatures. In *Refrigeration Systems for Achieving Cryogenic Temperatures*, Pasadena, CA 91109, 2016. Jet Propulsion Laboratory,California Institute of Technology, California Institute of Technology.

[55] H. Gunther Rudenberg and Paul G. Rudenberg. Origin and background of the invention of the electron microscope. In *Advances in Imaging and Electron Physics*, pages 207–286. Elsevier, 2010. doi: 10.1016/s1076-5670(10)60006-7.

[56] K.P. Ryan. Cryofixation of tissues for electron microscopy: A review of plunge cooling methods. *Scanning Microscopy*, 6:715–743, 09 1992.

[57] Miroslava Schaffer, Benjamin Engel, Tim Laugks, Julia Mahamid, J□rgen Plitzko, and Wolfgang Baumeister. Cryo-focused ion beam sample preparation for imaging vitreous cells by cryo-electron tomography. *BIO-PROTOCOL*, 5(17), 2015. doi: 10.21769/bioprotoc.1575.

[58] Martin Schorb and John A.G. Briggs. Correlated cryo-fluorescence and cryo-electron microscopy with high spatial precision and improved sensitivity. *Ultramicroscopy*, 143:24–32, aug 2014. doi: 10.1016/j.ultramic.2013.10.015.

[59] Electron Microscopy Sciences. Cryo instruments and supplies, 2018. URL https://www.tedpella.com.

[60] Thermo Fisher Scientific. An introduction to electron microscopy focused ion beam systems and dualbeam™ systems, 2019. URL "https://www.fei.com/introduction-to-electron-microscopy/fib/".

[61] Shimoni and Muller. On optimizing high-pressure freezing: from heat transfer theory to a new microbiopsy device. *Journal of Microscopy*, 192(3):236–247, dec 1998. doi: 10.1046/j.1365-2818.1998.00389.x.

[62] N. R. Silvester, S. Marchese-Ragona, and D. N. Johnston. The relative efficiency of various fluids in the rapid freezing of protozoa. *Journal of Microscopy*, 128(2):175–186, nov 1982. doi: 10.1111/j.1365-2818.1982.tb00449.x.

[63] G. Strasser, H. P. Bader, and M. E. Bader. Reduction of particle contamination by controlled venting and pumping of vacuum loadlocks. *Journal of Vacuum Science & Technology A: Vacuum, Surfaces, and Films*, 8(6):4092–4097, nov 1990. doi: 10.1116/1.576445.

[64] G. Strasser, H. P. Bader, and M. E. Bader. Reduction of particle contamination by controlled venting and pumping of vacuum loadlocks. *Journal of Vacuum Science & Technology A: Vacuum, Surfaces, and Films*, 8(6):4092–4097, nov 1990. doi: 10.1116/1.576445.

[65] Sebastian Tacke, Vladislav Krzyzanek, Harald Nüsse, Roger Albert Wepf, Jürgen Klingauf, and Rudolf Reichelt. A versatile high-vacuum cryo-transfer system for cryo-microscopy and analytics. *Biophysical Journal*, 110(4):758–765, feb 2016. doi: 10.1016/j.bpj.2016.01.024.

[66] Louise Helene Søgaard Jensen Ben van den Brandt Arnaud Comment Anders Meibom Tian Cheng, Florent Plane. A new passive system for contamination-free long and effect of wavefront and distortion bypropagation through inhomogeneous and layer to the directivity and of ultrasonic. In *IOP Conference Series: Materials Science and Engineering*, 2018. doi: 10.1088/1757-899X/278/1/012123.

[67] William F. Tivol, Ariane Briegel, and Grant J. Jensen. An improved cryogen for plunge freezing. *Microscopy and Microanalysis*, 14(5):375–379, sep 2008. doi: 10.1017/s1431927608080781.

[68] Linda F. van Driel, Jack A. Valentijn, Karine M. Valentijn, Roman I. Koning, and Abraham J. Koster. Tools for correlative cryo-fluorescence microscopy and cryo-electron tomography applied to whole mitochondria in human endothelial cells. *European Journal of Cell Biology*, 88(11):669–684, nov 2009. doi: 10.1016/j.ejcb.2009.07.002.

[69] Marie Vancová, Nataliia Rudenko, Jiří Vaněček, Maryna Golovchenko, Martin Strnad, Ryan O. M. Rego, Lucie Tichá, Libor Grubhoffer, and Jana Nebesářová. Pleomorphism and viability of the lyme disease pathogen borrelia burgdorferi exposed to physiological stress conditions: A correlative cryo-fluorescence and cryo-scanning electron microscopy study. *Frontiers in Microbiology*, 8, apr 2017. doi: 10.3389/fmicb.2017.00596.

[70] Kent M. Verge and George R. Agnes. Plasticizer contamination from vacuum system o-rings in a quadrupole ion trap mass spectrometer. In *Plasticizer Contamination from Vacuum System O-rings in a Quadrupole Ion Trap Mass Spectrometer*. Department of Chemistry, Simon Fraser University, Burnaby, British Columbia, Canada, American Society for Mass Spectrometry, 2002.

[71] Guy Kendall White and L. Marton. Experimental techniques in low-temperature physics. *Physics Today*, 13(3):52–52, mar 1960. doi: 10.1063/1.3056873.

[72] Nagamitsu Yoshimura. Water vapor permeation through viton o ring seals. *Journal of Vacuum Science & Technology A: Vacuum, Surfaces, and Films*, 7(1):110–112, jan 1989. doi: 10.1116/1.575756.